DOKUZ EYLÜL UNIVERSITY

GRADUATE SCHOOL OF NATURAL AND APPLIED

SCIENCES

DESIGN AND ANALYSIS OF PROJECTED CAPACITIVE METHODS FOR TOUCH SENSING

by

Ferat AKKOÇ

August, 2011

İZMİR

DESIGN AND ANALYSIS OF PROJECTED CAPACITIVE METHODS FOR TOUCH SENSING

A Thesis Submitted to the
Graduate School of Natural and Applied Sciences of Dokuz Eylül University
In Partial Fulfillment of the Requirements for the Degree of Master of Science
in Electrical and Electronics Engineering Program

by
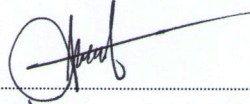**Ferat AKKOÇ**

August, 2011
İZMİR

M. Sc THESIS EXAMINATION RESULT FORM

We have read the thesis entitled **"DESIGN AND ANALYSIS OF PROJECTED CAPACITIVE METHODS FOR TOUCH SENSING"** completed by **FERAT AKKOÇ** under supervision of **ASST. PROF. DR. ÖZGE ŞAHİN** and we certify that in our opinion it is fully adequate, in scope and in quality, as a thesis for the degree of Master of Science.
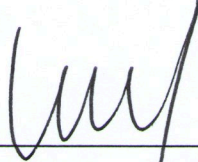
Asst. Prof. Dr. Özge ŞAHİN

Supervisor

Asst. Prof. Dr. Derya BİRANT

(Jury Member)

Asst. Prof. Dr. Selçuk KILINÇ

(Jury Member)

Prof. Dr. Mustafa SABUNCU

Director

Graduate School of Natural and Applied Sciences

ACKNOWLEDGEMENTS

DESIGN AND ANALYSIS OF PROJECTED CAPACITIVE METHODS FOR TOUCH SENSING

ABSTRACT

Touch sensing technologies that are used especially in mobile devices, now take place in every part of our lives, from consumer electronics to manufacturing industry, from automotive to health sector. In this study, design and analysis of touch sensitive capacitive sensors are examined. Capacitive methods are very sensitive to environmental changes and, especially, devices that use mains as a kind of power supply are very vulnerable to electrical noise that exists in the environment or network and can cause false detections. For this purpose, two different touch sensing cards with two separate methods, one with mutual capacitive and the other with self capacitive, have been designed in this thesis, and during this study, software has been developed on the basis of these cards.

Before the discussion of the design process, information about touch sensing technologies is given and the working principles of applied capacitive methods are explained in the first part of the thesis. Then, tests are implemented to designed cards in order to simulate a set of the environmental effects, and the test results are analyzed in graphical form. Some studies have been performed in order to reduce the effects of noise and crosstalk that have been encountered during the tests. On the other hand, a way of switching to a noiseless frequency is carried out when it is impossible to reduce the noise.

The "frequency hopping" tecnique that is used more often in data transfer and cryptology methods in order to increase SNR, is completely used for operating the capacitive sensors on noiseless frequency bands. When SNR gets lower, capacitive sensors switch to an undisturbed frequency band. For this purpose, software algorithms that detect and reduce noises have been developed and implemented.

Keywords: touch sensor, capacitive sensor, mutual capacitance, self capacitance, frequency hopping, spread spectrum, temperature, humidity, EMC.

DOKUNMA ALGILAMAYA YÖNELİK PROJECTED KAPASİTİF YÖNTEMLERİNİN TASARLANMASI VE ANALİZİ

ÖZ

Özellikle mobil aygıtlarda kullanılan dokunmatik teknolojiler, artık tüketici elektroniğinden üretim endüstrisine, otomotivden sağlık sektörüne kadar hayatımızın her alanında kendine yer bulmaktadır. Bu çalışmada, dokunmaya duyarlı kapasitif sensörlerin tasarımı ve analizleri yapılmıştır. Kapasitif yöntemler çevresel değişimlere oldukça duyarlıdır, özellikle güç kaynağını şehir şebekesinden alan aygıtlar, şebekede ya da çevrede var olan elektriksel gürültüye karşı çok hassas olup yanlış algılama yapabilmektedir. Bu amaçla, bu tezde biri karşılıklı kapasitif, diğeri öz kapasitif olmak üzere iki ayrı metotla iki farklı dokunmatik kart tasarlanmış ve bu çalışma süresince de üzerinde yazılım geliştirmesi yapılmıştır.

Tasarım sürecinin anlatılmasından önce dokunmatik teknolojiler hakkında bilgi verilmiş ve tezin ilk bölümünde uygulanan kapasitif metotların çalışma prensibi anlatılmıştır. Daha sonra tasarlanan kartlara bir takım çevresel etkileri simüle edecek şekilde testler yapılıp, test sonuçları grafik şeklinde analiz edilmiştir. Testler ve çalışma süresince görülen gürültü ve çapraz-karışma etkisini azaltmak için çalışma yapılmış, gürültüyü oranının azaltılamadığı yerde gürültüsüz bir frekansa geçmek gibi bir yöntem izlenmiştir.

Daha çok veri transferlerinde ve kriptolama işlemlerinde SNR oranını arttırmak için kullanılan "frekans atlama" tekniği, bu tezde kapasitif sensörlerin daha temiz ve gürültüsüz bir frekans bandında çalışması için kullanılmıştır. Böylelikle SNR oranının çok düşük kaldığı zamanlarda, sensörlerlerin daha temiz bir frekans bandında çalışması sağlanarak SNR oranı arttırılmıştır. Bunun için gürültüyü tespit eden ve azaltan yazılım algoritmaları geliştirilmiş ve uygulanmıştır.

Anahtar sözcükler: dokunmatik sensör, kapasitif sensör, karşılıklı kapasitans, öz kapasitans, frekans atlama, yayılı spektrum, sıcaklık, nem, EMC.

CONTENTS

CHAPTER ONE

INTRODUCTION

1.1 An Overview Touch Technologies

In recent years, touch technologies are increasingly improved and widely adopted as operator and customer interfaces in modern life. Lots of restaurants and hotels use touch-operated device such as touch screen for order entry or transaction finalization. The main factor influencing the widespread adoption of touch-operated devices is their function that is easy to use. Today all people use ATM machines because of credits card and almost all ATM machines are touch-operated. In addition to ATMs, most handheld devices such as cell phones and personal digital assistants (PDAs) etc. are using increasingly touch screens nowadays.

Although there are lots of touch-sensitive devices, touch screens are more popular than the others. The first official touch sensor was created in 1971 by Dr. Sam Hurst (founder of Elographics) and it was called "Elograph". In spite of the fact that it was not transparent like today's touch mechanism, it is significantly accepted as a kind of milestone in touch technology. The first transparent touch technology was developed by Sam Hurst and Elographics. Afterwards, wire resistive technology was developed and it is recognized as the most popular technology in use today. Over the past thirty years, touch technology has got the potential to replace most function of the mouse and keyboard; furthermore, they have taken a solid step in modern computers (Wikimedia Foundation Inc., 2011).

Touch technology does not refer to the screen type itself. On the other hand, all of them register contact as a "touch". "The major approaches of sensing 'touch' in general can be categorized as a) Minute physical deformation, b) Obstructing the path of sonic waves, c) Frustrated Total Internal Reflection (FTIR) and d) Change in capacitance. …. d) the touch is used to cause changes in the capacitance value of sensor elements…." (Chatterjee, R., & Matsuno, F., 2008, p. 2299). Although there

are more than a dozen different touch screen technologies used in touch-sensitive device, four major types traditionally more popular:

- Resistive;
    - 4, 5, 6 , 8 and X-Wires (Based on 4 Wires)

- Capacitive;
    - Surface Capacitive;
    - Projected Capacitive(PCT);
        1. Mutual Capacitive
        2. Self Capacitive

- Surface Acoustic Wave (SAW);

- Infrared.

These technologies have their own distinct characteristics, both beneficial and disadvantageous.

Additionally, there are some of other types of touch called as:

- Optical Imaging;
- Acoustic Pulse Recognition;
- Dispersive Signal Technology (DST);
- Strain Gauge
- Force sensing
- LCD in-cell optical

Each technology features unique attributes that directly impact how applicable or good the technology is in a particular environment.

1.1.1 Resistive

Resistive is the most common type of touch technology. It consists of two thin electrically conductive sheets, which is transparent resistive material called indium tin oxide (ITO), that are kept separated by a pattern of very small transparent insulating dots. When an object, such as finger or stylus, presses down on a point on the ITO layers get in contact with each other and that causes changes in the electrical current which is registered as a touch event.

Resistive is common type of touch because of simple, relatively inexpensive and low cost solution. A primary limitation of resistive is inability of multi-touch simultaneously. The primary types of resistive overlays are 4-wire, 5-wire, and 8-wire. Another type is X-wire resistive and it is multi-touch. It employs the same basic principal as single touch but break the large single sheet into a matrix of smaller sheets. In this way, touch- sensitive device has more 4-wire sensor instead of one and it can detect multi-touch events at the same time.

1.1.2 Capacitive

Capacitive touch sensors are getting more important, lately. They work always by measuring the capacitance of the closer object to the sensors. They can be several kind of form such as a button, slider or touch screens. While a conductive object, human body is also a conductor, is getting closer to capacitive sensor or touching the surface of it result in a distortion of the sensor electrostatic field. The decision of whether to touch any object to sensor or not is obtained by measuring the distortion of the electrostatic field or the shift capacitance in circuitry.

Different technologies may be used to determine the touch.

- Surface Capacitance: Surface capacitive technology consists of a uniform conductive coating on a glass panel. Electrodes around the panel's edge evenly distribute a low voltage across the conductive layer, creating a

uniform electric field. A human body is an electric conductor, so when you touch the screen with a finger, a slight amount of current is drawn, creating a voltage drop. The current respectively drifts to the electrodes on the four corners. Theoretically, the amount of current that drifts through the four electrodes should be proportional to the distance from the touch point to the four corners. The controller precisely calculates the proportion of the current passed through the four electrodes and figures out the X/Y coordinate of a touch point (WEB_1, n.d.).
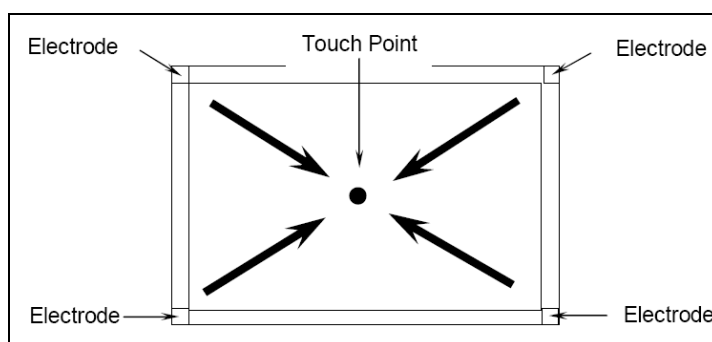
Figure 1.1 Surface capacitance working principle

- Projected Capacitance (PCT): There are two basic ways of arranging and measuring the change in capacitance: Self-capacitance and mutual capacitance. Self capacitance is based on measuring the capacitance of a single electrode with respect to ground. When a finger is near the electrode, the human-body capacitance changes the self-capacitance of the electrode. Because of existing single electrode, one the touch can be detected simultaneously. Mutual-capacitance is other more common type of projected capacitance method which has the transmitting and the receiving electrodes. When a finger gets closer to electrodes, changes the local electrostatic field which reduces the mutual capacitance. It allows an unlimited number of unambiguous touches (Carey J. 2009).
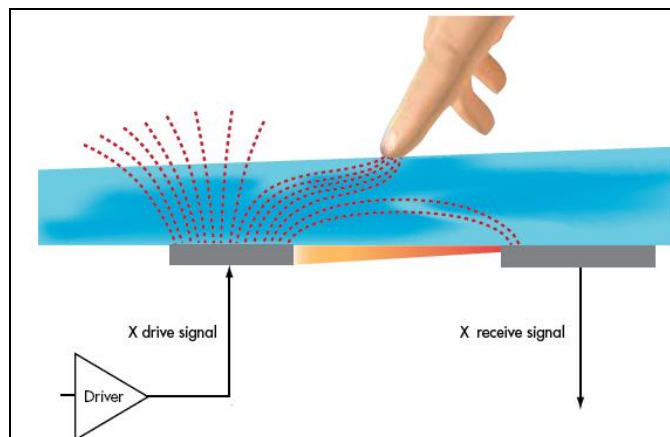
Figure 1.2 Projected capacitive touch screen (Zheng, Q., n.d.)

1.1.3 Surface Acoustic Wave

Surface acoustic wave touch screens have transducers and reflectors in the edges that send out and register acoustic waves. If a soft object touches the screen the waves is absorbed and the sensors can calculate where the touch is located. The advantage of using this technique is that no coating is needed on the screen, which allows this technique to have the highest screen clarity. The technique has a high touch resolution but it can only register touches from soft objects like a finger or a stylus with a rubber top. Touching it with a hard object will not absorb the acoustic waves and therefore no touch event will be registered (Stenmark, F., 2008, pp. 5-7).

1.1.4 Infrared

Infrared touch screens have a panel around it where two of the four sides have transmitters that send out infrared light in a matrix. On the other two sides there are receivers that receive the infrared light. When a finger or other object stops the infrared light from reaching the receiver a touch event is registered. One disadvantage with this technique is that the touch even can be triggered before the screen is touched. But the positive side is that the lifetime of the screen does not depend on the touch technique since it is not integrated into the screen (Stenmark, F., 2008, pp. 5-7).

1.2 Research Objective and Aim of Thesis

Main objectives of this thesis can be listed as follows:

- To investigate theories of capacitive sensing.
- To design two PCBs to implement both mutual and self capacitive sensing methods.
- To conduct tests for both of the methods and compare the measurement results for both of them to evaluate advantages and disadvantages of each method.
- To investigate the affects of various software filters applied on the measurement results.
- To investigate how to pass EMC tests.

The main purpose of the thesis is to develop projected capacitive sensors which can reliably be operated in harsh industrial and extreme conditions such as high temperature or humidity environment. Also, the frequency hopping algorithms are applied to guarantee safe operation of capacitive sensors by using a touch library which runs only at a constant frequency.

There are many researches in the literature related to various capacitive sensors. Nearly all of them need to include some external readout circuits or some of specific modules in microcontrollers. This makes the sensors more expensive and susceptible to noise and external interference. So, this thesis is also aimed to develop a novel low-cost capacitive sensor interface by considering Gaitan-Pitre, J.E., Gasulla, M., & Pallas-Areny, R.(2007), Reverter, F., Gasulla, M., & Pallas-Areny, R.(2004), Dietz, P.H., Leigh, D., & Yerazunis, W.S.(2002) low-cost researches along with frequency hopping method. These researches are direct interface based on charge transfer method. Direct interfeace means "capacitive sensors have been implemented, where the sensor is directly connected to a microcontroller (MCU). The MCU performs the capacitance-to-digital conversion without any external circuit for signal

conditioning or analog-to-digital voltage conversion."(Gaitan-Pitre and other, 2007, p.1). These researches are appropriate for this thesis.

Some other researches related to capacitive sensors, such as Kero, N., Nachtnebel, H., Pommer, H., & Sauter, T. (2002), Chou, W.C., Hsu, Y.C., &Liao, L.P. (18-20 Oct. 2006), Sheu, M.L., Lai, C.K., Hsu, W.H., & Yang, H. M.(2005), Nam, C., Pu, Y.G., & Lee, K. Y. (2009), include external signal processing circuits or microcontroller modules (sigma-delta, pseudo random or clock generator, modulator /demodulator etc.) in order to filter noises and increase SNR. For this reason, these are inappropriate for our system. But instead of these modules and circuits, all filtering and increasing SNR process are performed by software algorithms in this study. On the other hand, a low-cost microcontroller must be used. Therefore, noise detection and filtering algorithms should be efficient and required small size memory.

1.3 Scope and Organization of the Thesis

While designing touch sensor PCB (Printed Circuit Board), there are many issues that must be considered together such as PCB layout, sensor shapes, controller design, software architecture, digital software filters, MCU running clock frequency and so on. Significant amount of technical literature is available in the form of papers and journals on the IEEE website, and as product datasheets and application notes in the website of many manufacturers.

In the first chapter, capacitive sensing, which is a technology based on electric field coupling is investigated. Projected Capacitive Touch (PCT) can mainly be grouped into two headlines. These are self-capacitance sensors and mutual-capacitance sensors.

In the second chapter, the theory of the basic mutual capacitance is explained. After that, the theory of mutual capacitance sensing method is explained. All hardware design, modeling and control principles of the sensing implementation are also covered in this chapter. The basic characteristics and properties of QTouch

library and working principles are also explained. The basic PCB design rules for mutual-sensing circuits are also discussed in this chapter along with the effects of parasitic introduced by the PCB.

In the next chapter, all features for self and self touch sensing are explained. New PCB is designed and working principle is explained for self sensing. Operation of the mutual-capacitive sensing and self-capacitive sensing are more different than each other.

Chapter 4 is allocated for measurements and test results. Both mutual-sensing and self-sensing boards are tested under different conditions and got some measurements. The resulting waveforms of the given methods are revealed throughout the chapters. All results which are obtained during the tests of two sensing methods are evaluated and compared. The reason for why different measurements are obtained by using different methods is explained. The causes of the results are investigated. It is shown that, the different PCB design, applied digital software filters or working principles can cause different results. At the end of this section, the two applied methods are compared with advantages and disadvantages; then a conclusion is reached.

Chapter 5 is the conclusion chapter. A general overview about the thesis and some future work that can be carried out are included in that chapter.

CHAPTER TWO

THEORY OF MUTUAL CAPACITANCE AND IMPLEMENTATION OF PROPOSED CIRCUIT

2.1 Introduction

Capacitive sensors consist of the conductive areas on the PCB and they are connected to the microcontroller by means of the traces. The sensors on touch screens are the transparent indium tin oxide (ITO) substance. ITO, being a uniform conductive substance, can be placed both on glass and on plastics. The microcontrollers create an electric field on the sensors in order to check constantly whether the electric field changes or not. Any kind of conductive object or a finger, which is described as a conductive object, absorbs some electrical charge. As a result, the amount of total charges in touch system changes. The amount of changed charge is then measured by the MCU. This method is known as charge transfer method. Apart from this method, "several standard methods of capacitance measurement are available. some of them are, current to voltage phase shift measurement, charging time of RC circuit, capacitive voltage divider, charge transfer method, relaxation oscillator, etc." (Chatterjee, R., & Matsuno, F.2008, p. 2300).

The Atmel Qtouch libraries are used for this thesis and the charge or capacitance change in the system is measured by using the charge transfer method.

Charge transfer: A voltage is applied to the sensor, which causes it to accumulate some charge. Then this charge is transferred to an integrated capacitor. This process is repeated until a voltage threshold is reached. The capacitance of the sensor is determined by the voltage in the integrated capacitor (and the ADC, or a simple comparator could be used to extract the threshold information) and the number of cycles it took to reach the predetermined voltage level (Salas, M., & Marcos, A., n.d.).

2.2 Mutual Capacitance Basics

2.2.1 Mutual Capacitance Theory

Capacitance is the capacity of a substance to hold electrical charge. According to another definition, it is the value referring to the stored charge between two potentials. On the other hand, mutual capacitance can be described as capacitance, for it consists of the potential difference between two conductive plates. If there is a potential difference between two conductors, this may lead to the occurrence of an electric field. This electric field can also be described as electric field coupling.

The operation principle of mutual-capacitance type sensors is based on this theory. There are two electrodes on the PCB and these electrodes are quite close to each other. Earth or PCB is the dielectric substance between these electrodes. Consequently, the charge flow occurs from one electrode to the other. The change in the charge flow or the capacitance is detected by means of the charge transfer method.

2.2.2 QMatrix Acquisition Method

Each sensing electrode pair contains a field between drive electrode and a receive electrode (domanstrated in Figure 2.1). The emitting electrode is driven as a digital burst of logic pulses; the receive electrode normally collects most of the charge that is coupled from the emitting electrode via the overlying dielectric front panel.

This field coupling is attenuated by human touch, since the human body conducts away a portion of the fields which arc through the front panel; the absorbed part of the field is re-radiated by the human body back to the product via various capacitive paths.
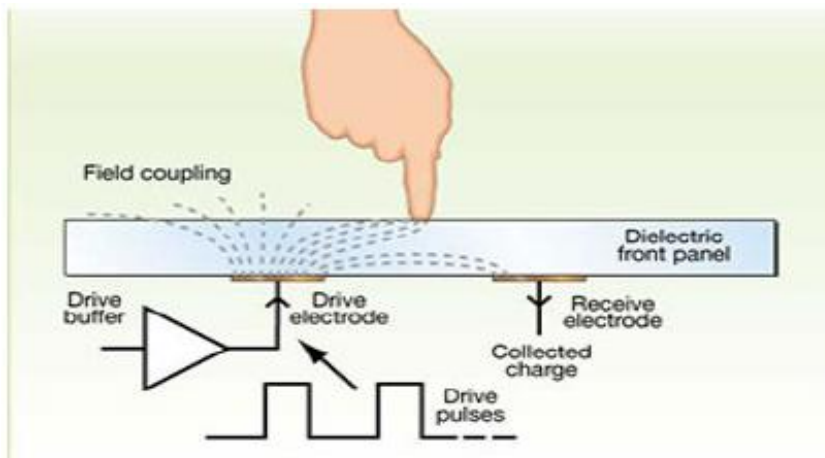
Figure 2.1 Qmatrix acquisition method, electric coupling field flows between electrodes. Touch absorbs the field, reducing collected charge (Atmel, 2010).

Signal that couples through the mutual capacitance of the electrode structure is collected onto a sample capacitor which is switched by the chip synchronously with the drive pulses (see Figure 2.2). A burst of pulses is used to improve the signal to noise ratio; the number of pulses in each burst also affects the gain of the circuit, since more pulses will result in more collected charge and hence more signal. By modifying the burst pulse length, the gain of the circuit can be easily changed to suit various key sizes, panel materials, and panel thicknesses.
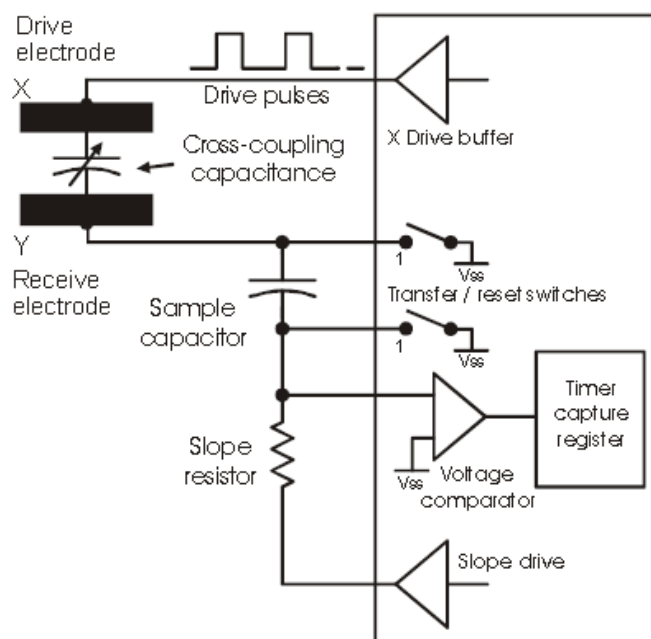
Figure 2.2 QMatrix dual-slope charge transfer principle(ORG, n.d.)

After the burst completes, the charge on the sample capacitor is converted using a slope conversion resistor which is driven high, and a zero crossing is detected to result in a timer value which is proportional to the X-Y electrode charge coupling which also reflects charge absorption caused by finger touches. Finger touches absorb charge, so the measured signal decreases with touch. The burst phase causes the charge on the sample capacitor to ramp in a negative direction, and the slope conversion causes a ramp in the positive direction on the capacitor; the net effect is that the conversion process is 'dual slope', and is largely independent of the value of the sample capacitor and is highly stable over time and temperature (Quantum Research Group [QRG], 2006).

The afore-mentioned process is illustrated in Figure 2.3. Here the finger may be regarded as a capacitor intervening between two electrodes. When the finger comes close to the electrode, a part of the charge diverts to the earth. So the sample capacitor is less charged by every pulse.
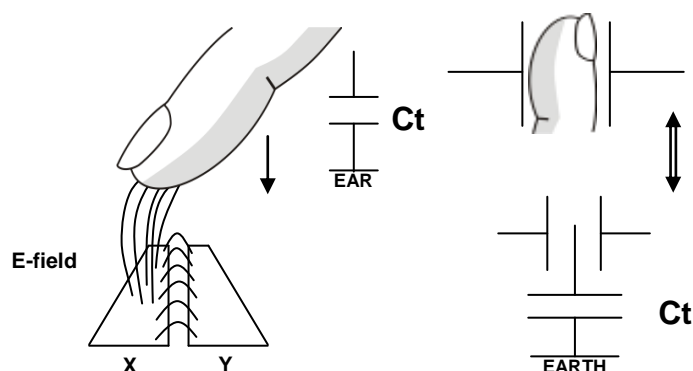
Figure 2.3 Processing of how to be diverted electrical filed coupling (ORG, n.d.).

The electrode pairs are driven as matrix in QMatrix method. Figure 2.4 illustrates just a single electrode pair and the circuit. While GND refers to local circuit return, EARTH means free space return. The Ct and *Cx* are most significant capacitors to us.
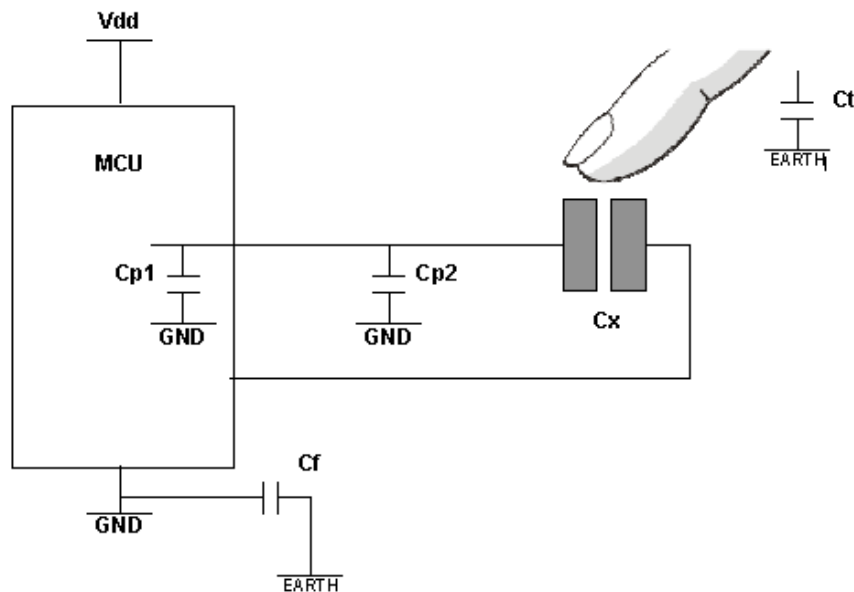
Figure 2.4 Basic mutual capacitance equivalent circuit (QRG, n.d.)

$Cp1$: Parasitic pin capacitance to GND (1-2 pF)

$Cp2$: Wiring capacitance to GND (few pF)

Cx : Electrode self coupling capacitance (2-10 pF)

Ct : Touch capacitance to earth (few pF)

Cf : Coupling capacitance between circuit GND and earth (few pF)

For simplification it is assumed;

$$Cx >> Cp1, \ Cp2 \qquad Cf >> Cx, \ Ct$$

2.2.3 Sequence of Operation

2.2.3.1 Switched Capacitor Technique

The switch-capacitor (SC) technique is based on the idea that a periodically switched capacitor can be used to simulate a resistor (provided that the switching frequency is much higher than the frequencies of the interest). This idea was proposed by Maxwell in 1891, although at the time there was no practical application (Toumazou, Hughes, & Battersby, 1993, pp. 13-14).
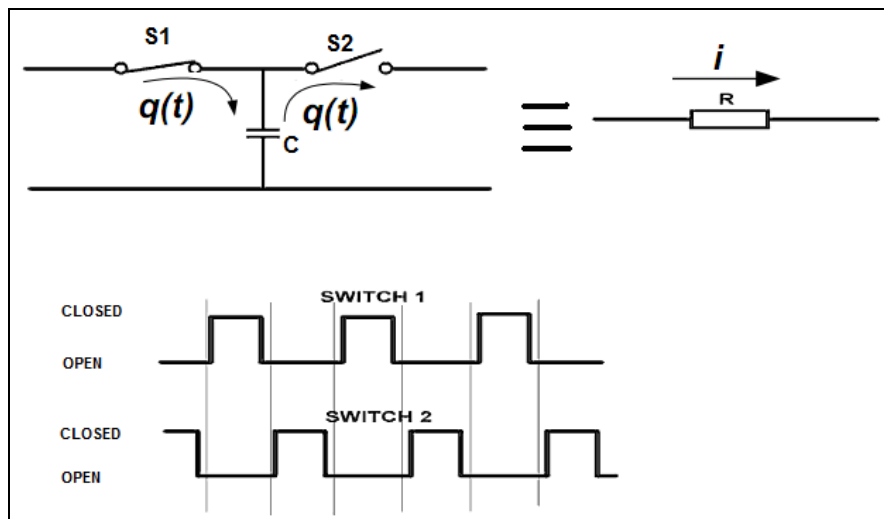
Figure 2.5 Implementation of resistor by using switched capacitor with moving
charge (Winder, S., 1997, pp. 340)

The circuit in Figure 2.5 is just one of several possible designs. The equivalent resistance depends on the capacitor value and the switching frequency used. A charge of Q= CV coulombs is stored when the first switch is closed and the capacitor (C) charges up. A charge of CV coulombs discharges in to the load, if the load is N clock cycle per second (f=N), there is a total charge flow of NCV coulombs per second; in the other words NCV amperes (since one ampere equals one coulombs per second) (Winder, S., 1997, chap. 14).

R = V/I or, substituting for I,

$$R = \frac{V}{NVC} = \frac{1}{NC},$$ (2-1)

Since N=f, that is, the clock frequency, $R = \frac{1}{fC}$ (2-2)

For example;

C = 1 pF,   f = 150 kHz ➔ R= 1.5kΩ

2.2.3.2 Charge Phase with Switched Capacitor Technique

A sensor circuit consists of two parts. The first part includes the microcontroller and the timer and comparator modules for the sensor, while the second part consists of Rsmp, Cs and Cx. The capacitive sensors charge the Cs capacitor on each loop by using the switched capacitor technique. Figure 2.6 shows the charge transfer circuit, while table 2.1 indicates the switching sequence.
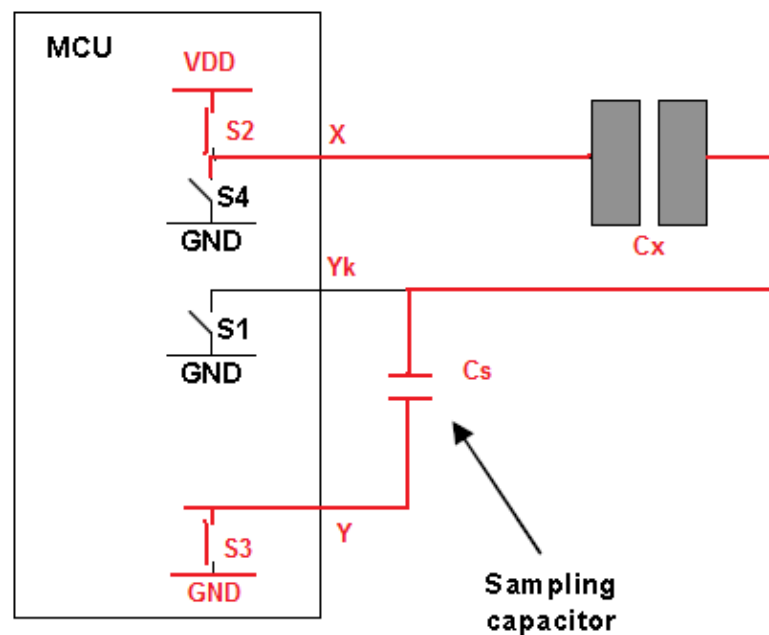
Figure 2.6 Charge transfer circuit. Capacitive sensors work on principle
called charge transfer method and use switched capacitor technique(QRG, n.d.)

Cx : Coupling capacitance of electrode

Cs : Sampling capacitor

X : X-line is the drive line and connected to the emitting electrode

Y : Y-line is the receiver line and connected to the receive electrode

Vcs : The voltage accumulated during the burst phase of the acquisition.

The actual value of Cs within the charge transfer circuit is larger than Cx. The difference between the values is assumed about 1000 times. This means that Cs is about 1000 times larger than Cx. The displayed switch controllers are the CMOS IO pins. They switch between GND, Z and Vdd.

Table 2.1 Burst switch states of the mutual capacitace's sequence diagram (***QRG***, n.d.)

	S1	S2	S3	S4	NOTES
1	CLOSED	OPEN	CLOSED	CLOSED	Cx and Cs discharge
#2	OPEN	OPEN	OPEN	CLOSED	Float State
#3	OPEN	CLOSED	OPEN	OPEN	Pre-charge X-line
#4	OPEN	CLOSED	CLOSED	OPEN	Charge transfer
#5	OPEN	CLOSED	OPEN	OPEN	Float State
#6	CLOSED	CLOSED	OPEN	OPEN	Isolate Cs charge
#7	CLOSED	OPEN	OPEN	CLOSED	Discharge Cx

State-1: Cx and Cs capacitors need to be discharges in this state before the first pulse is sent at start of acquisition.

State -2: This state prevents the simultaneous change of the S1 and S2 switches in order to ensure that Cs capacitor is not charged instantly. Charge repeat loop starts from state #2 and continues to #7.

State -3: All stray capacitances in the X pin and the X track are pre-charged at this state. The pulses sent after this state is not to charge other capacitors apart from Cs.

State -4: This state is the charge transfer state. The S3 switch is closed in order to ensure that charge is transferred through Cx to Cs. The duration of this state can be programmed. If stray capacitance is the circuit is much, this step may take long time. So the duty cycle of the send pulses may be longer. The duration of this state is known as "Dwell Time".

State -5: The simultaneous switching of the S1 and S3 switches is prevented in order to hold charge in the Cs capacitor. These switches are the terminals of Cs and if they are grounded simultaneously, some of charge may be lost.

State -6: The Cs is isolated in this state.

State -7: The charge charged on *Cx* is discharged at this state, because one charging loop is completed. The loop restarts after having returned to state # 2.

This loop charges the sampling capacitor by being repeated several times for each sensor. Around 30-100 pulses are sent for each sensor on the mutual-capacitive sensing card.

In the first loop, the microcontroller drives the X pin for about a value of VDD. *Cx* and *Cs* are series capacitors in circuit. The flow goes through *Cx* to *Cs* on the falling edge of the Y pin (in Figure 2.6).

The charging current flowed through *Cx* to *Cs* shall be equal when they are in series. The charging current charges the capacitor having a serial connected equally without taking the capacitor values into account. The total voltage in a closed loop circuit shall be of zero according to Kirchhoff's voltage law (KVL), or the total of the voltage value on the capacitors shall be equal to the supply voltage. (Robertson, R.C., 2008, pp. 49-54). When it is assumed that every capacitor is charged with Q;

$$C = \frac{Q}{V} \quad \text{And} \quad Vdd = Vcx + Vcs \tag{2-3}$$

$$Vdd = \frac{Q}{Cx} + \frac{Q}{Cs} \quad \text{(Kirchhoff's Voltage Low)} \tag{2-4}$$

$$Vcs = \frac{Cx}{Cx + Cs} * Vdd \quad (Cx \text{ and } Cs \text{ voltage divider}) \tag{2-5}$$

$$\text{The ratio of } \frac{Cx}{Cs} = \frac{1}{1000} \quad \text{(approximately)} \tag{2-6}$$

Cx is now charged to 99.9% of Vdd in the first loop.

Repeating the charge transfer cycle for the 2nd time, the equations are the same but *Cs* already holds 1000th of Vdd and the next transfer will add approximately;

$$\frac{Cx}{Cx + Cs} * (0.999Vdd) \qquad (2\text{-}7)$$

Each next loop, Vcs rises by another small reducing.
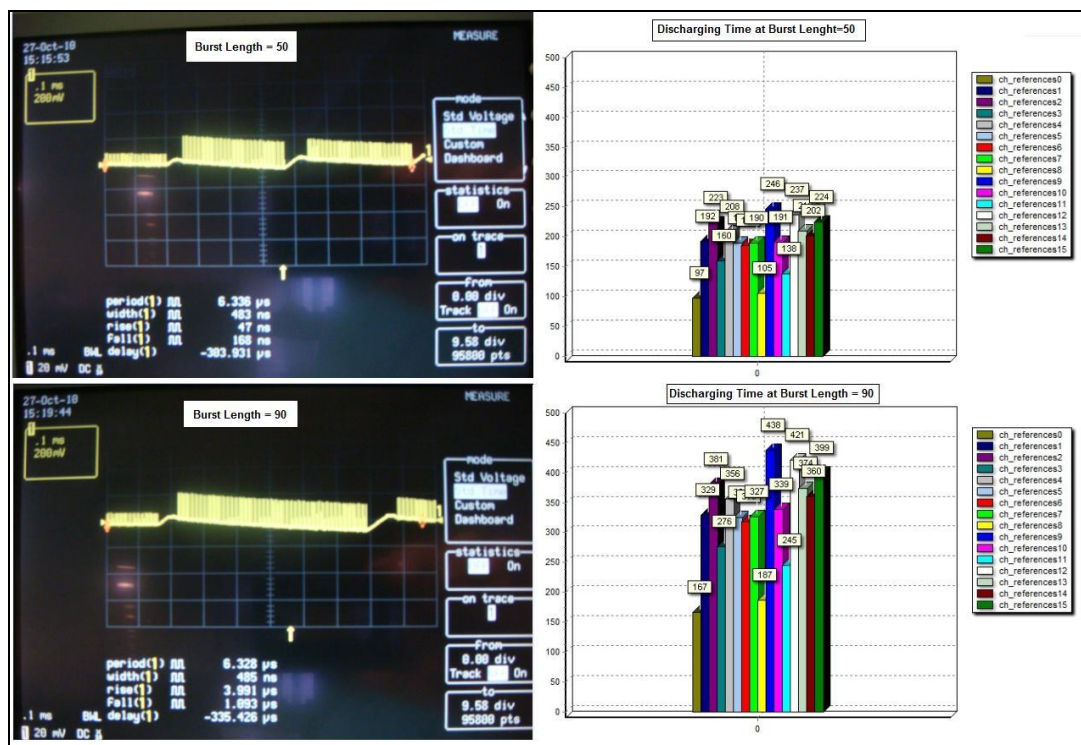
Figure 2.7 Typical voltage waveform across Cs capacitor in charge and discharge phase

Figure 2.7 shows the voltage waveforms on the *Cs* terminals. These graphics are obtained from the card designed for mutual-capacitance. The figures illustrate different burst lenghts and the relative pulses. The right side of the graphic displays the discharging duration of the capacitors. When the burst lenght increases, the capacitors are charged more and they are discharged in a longer period of time.

2.2.3.3 Measure Phase

After the burst completes, the charge on the sampling capacitor *Cs* is measured by using a resistor (Rsmp), a slope conversion resistor that is driven high, a counter and a comparator.After burst, counter is started and Rsmp is driven by closing S5 and opening S6 switch(see Figure 2.8), this causes Vcs to rump up towards to Vdd and zero crossing to GND is detected to result in an a timer value which is proportional to the charge that is stored on the sampling capacitor (QRG, n.d.).
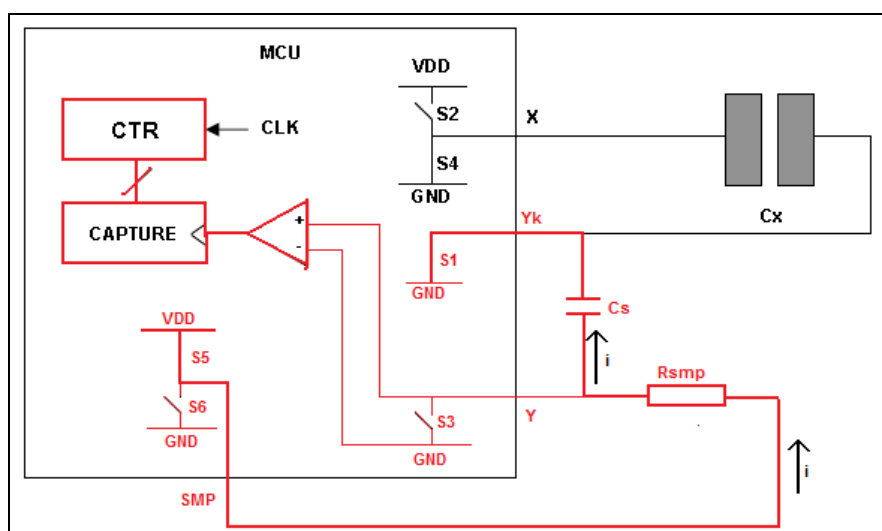
Figure 2.8 Charge transfer circuit with measure phase (QRG, n.d.)

When a finger comes close to the sensors, some charge are absorbed. So the *Cs* are charged less by each charging loop. When the burst phase is completed, the *Cs* terminal is expected to to be shown a lower voltage level. So the time required to discharge the *Cs* capacitor decreases. The difference between the discharging durations of the *Cs* capacitor is measured in order to determine whether the finger touched sensors or not.

Figure 2.9 illustrates the typical voltage waveforms across the sampling capacitor being charged less due to your finger. As seen in the figure, the change of voltage is dual-slope. The charging duration of the sampling capacitor affects the discharging duration in a linear way. The delta difference is then detected in order to determine whether the finger touched sensor or not.
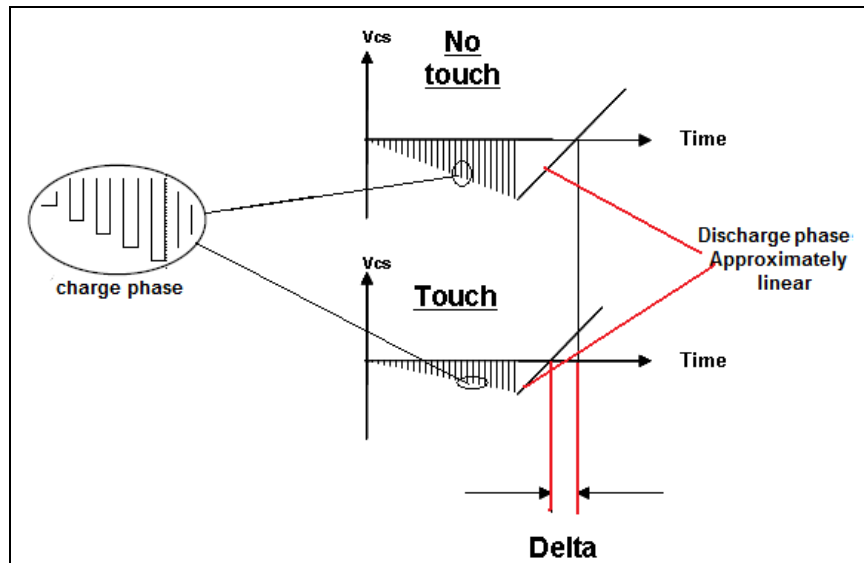
Figure 2.9 Typical voltage waveform across Vcs capacitor (QRG, n.d.)

Figure 2.10 illustrates the charging and the discharging graphics the burst length for 100. These graphics are obtained when MCU operates at 8MHz. The graphic above aimed at measuring the discharging duration by means of oscilloscope. The obtained value was then verified on the timer. This calculation was made for channel-9.

$Fosc = 8$ MHz

$$T = \frac{1}{8000000} \sec = 125ns \qquad (2\text{-}8)$$

Timer value is 468 cycles, that means;

468*125ns = 58.5 microseconds

The discharging time measured with oscilloscope is 60.32 us. The value displayed by Timer1 is close to the value measured on the oscilloscope.
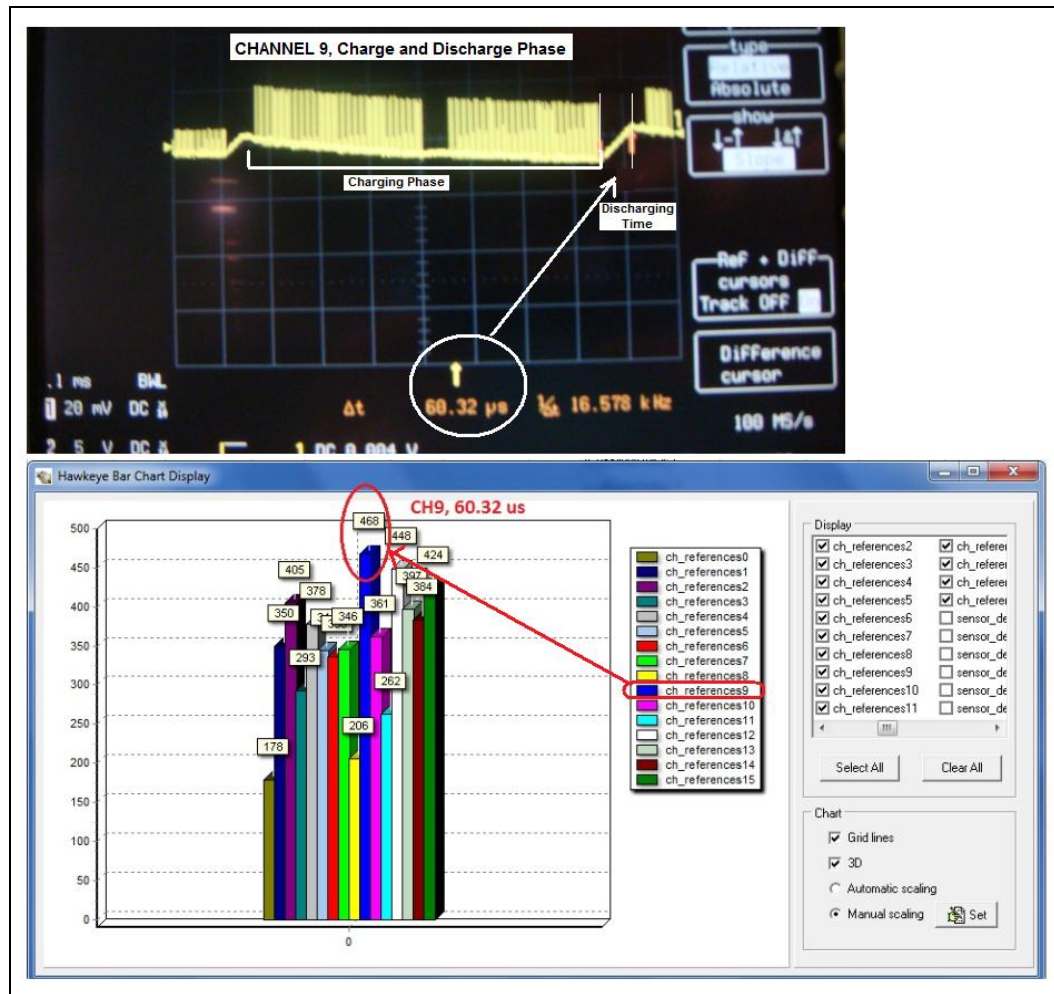
Figure 2.10 Typical voltage waveform of the channel-9 with the charging and discharging phases.

2.3 Hardware Design

The designed mutual capacitive sensing card consists of 10 buttons and 1 slider. There are led indicating whether the buttons are touched or not. Furthermore, there are white squares and strips on the upper layer of PCB in order to specify the places of the capacitive sensors. The buttons are also filled with white strips. Normally, the upper layer of PCB does not include any sensors or sensor traces. Therefore, the white strips are clues that specify where the electrodes are places on the lower surface. The general view of card is shown in Figure 2.11.
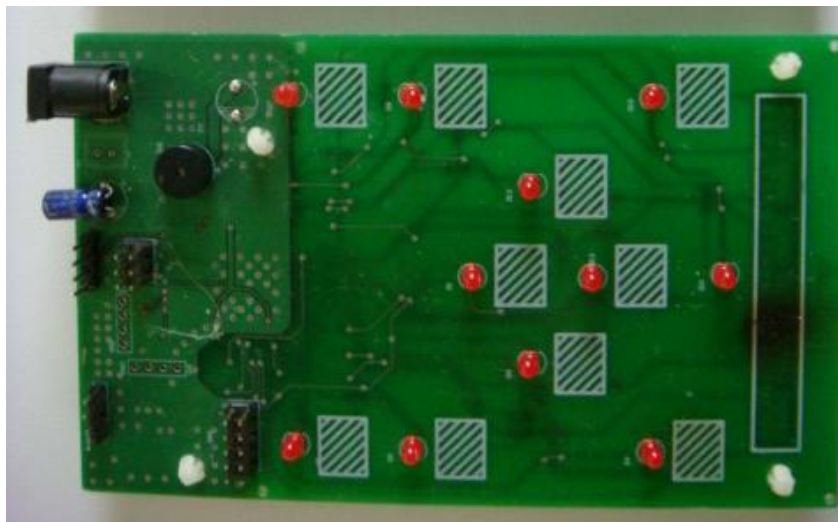
Figure 2.11 Mutual-capacitive sensing card top appearance

There is a buzzer on the card. The buzzer sounds, when any button is touched. There are 2 units of 8 and 6 connectors in order to program the card via JTAG and ISP. Furthermore, there is a connector of 4 to debug the card. There is a connector to transfer information to the computer through RS232 and a Max 232 Ic is available. The software is able to send data to the computer whenever the buttons are touched.

2.3.1 Sensors

The sensors on this card are composed of 8x2 (8X lines, 2Y lines) matrixes. There are 16 channels in total. There are 8 channels on each Y line. The buttons on this card consist of one channel, while the slider includes 6 channels. Since the slider traces need to be on the same Y line, the slider in this design can include maximum 8 channels.

The arrangement of capacitive sensor elements may be broadly categorized as; single, slider and 2D mesh(Chatterjee, R., & Matsuno, F.2008, p. 2301)

Single Element Sensor (Zero-Dimensional): This is a simple touch switch. Based on the requirement it can be designed to act as a simple on/off (Touch/No-Touch) sensor, or to measure the proximity of a conductive element like a finger, or to

measure the degree of partial touch in the sense that how much portion of the sensor element is covered by the touching entity like a finger.

Slider (One-Dimensional): This is a linear array of independent sensor elements. Usually a linear arrangement is common for the purpose of interfaces to use a sliding action for increasing or decreasing any parameter. Though for special applications non-linearly, e.g., concentrically placed element sequences can also be desined with same sensing principles…. The touch position is usually computed by weighted averaging the degree of touch over the sensor array.

2D Mesh (Two-Dimension)**:** This type of sensor arrangements is required for sensing the touch position in a two dimensional surface and can be broadly classified in two types. The more common one is a Matrix arrangement of two sets of slider type sensor arrays in mutually orthogonal direction (or at any other angle). The other arrangement is a 2D layout of independent sensor elements without any connection between neighboring elements. This arrangement is the one which allow sensing of multiple-touch using capacitive touch sensing.

Zero-dimensional (for buttons) and one-dimensional (for sliders) sensors are used for this design. The X and Y electrodes can either be located on the same layer of PCB or on separate layers of PCB. Both electrodes are on the same layer in this design. Figure 2.12 shows a few various sensor shapes.
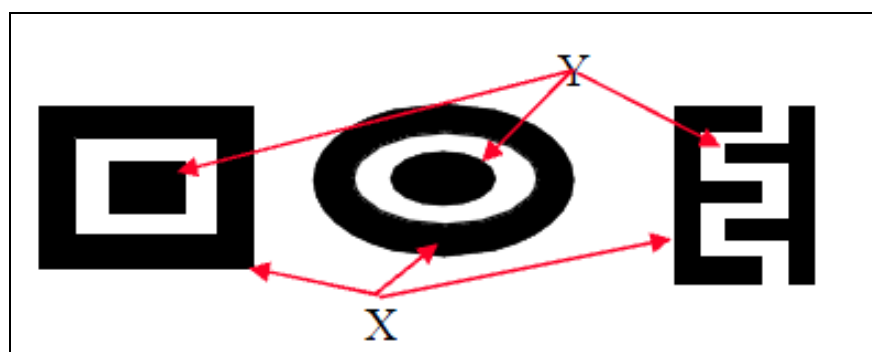
Figure 2.12 Mutual capacitive sensor shapes on the same layer of PCB (QRG, n.d.)

2.3.1.1 Sensor Circuit

Figure 2.13 illustrates the sensor circuit and the sensor shape used in this design. Furthermore, the X and Y traces and the resistor and capacitor values are displayed.
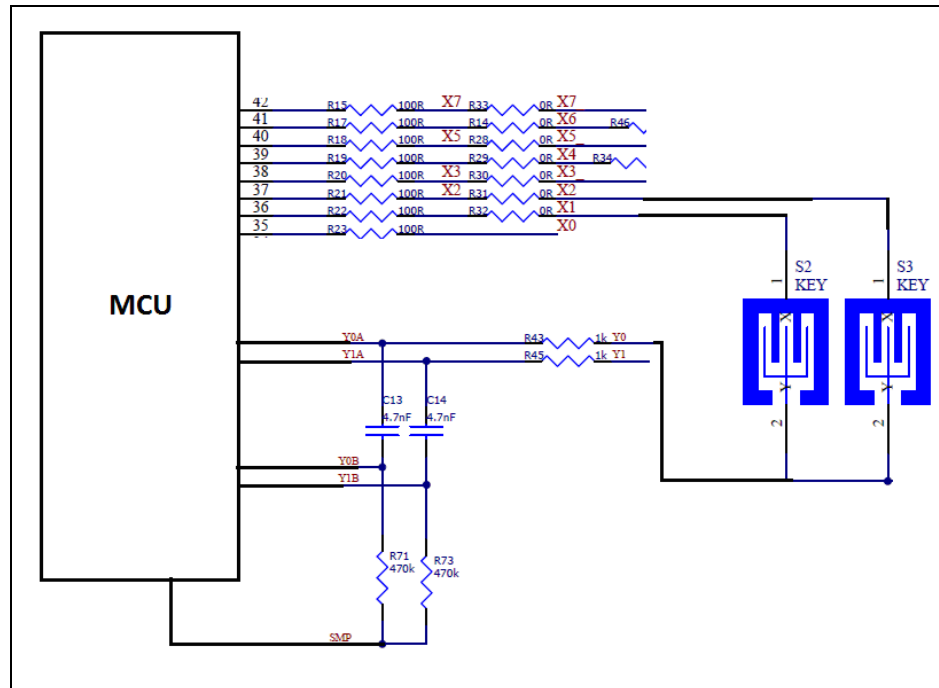
Figure 2.13 Sensor circuit with two example buttons connection

2.3.1.2 Touch Button

Since no front panel such as glass is used, both the electrodes and the traces for the sensor are constructed on the same plane of the PCB. Front panel is the PCB itself. The X and Y electrodes are interdigitated, that is they form interlocking "fingers". Typically the X electrode surrounds the Y electrode, as it helps to contain the field between the two. The other goal with this interdigitated design is optimize SNR value by maximizing coupling length between the X and Y electrodes (Atmel, 2009).

The designed sensors have two of the X fingers and three of the Y fingers.
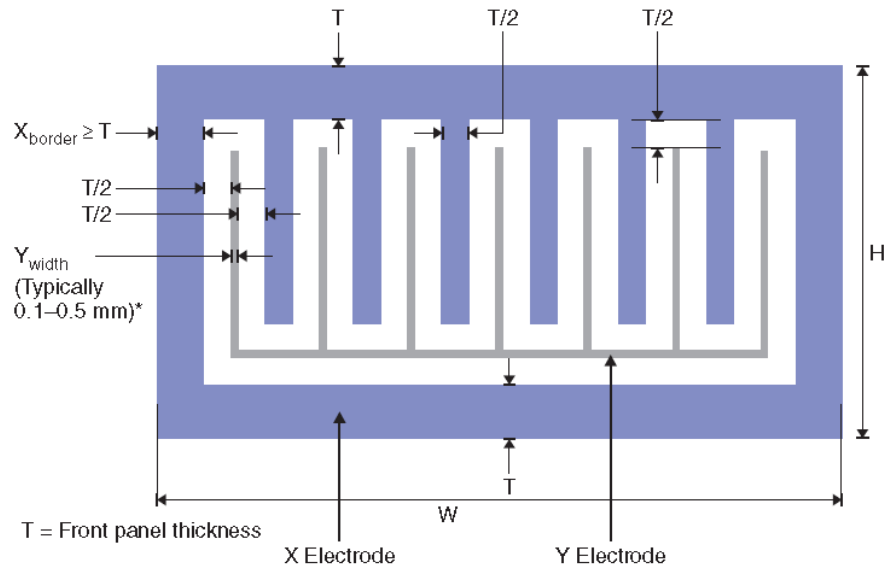
Figure 2.14 With planar construction, both the electrodes and the traces for the sensors are fabricated on the same plane of the insulating substrate (Atmel, 2009)

$$X_{fingers} = [(W - 3T - Y_{width}) / (1.5T + Y_{width})] \qquad (2\text{-}9)$$

$$X_{border} = (W - T - Y_{width} - X_{fingers}(1.5T + Y_{width})) / 2 \qquad (2\text{-}10)$$

If $X_{fingers}$ is not integer value, it rounds down to the nearest integer. In our design these values and obtained results are as follows:

T = 1.6mm

W = 10mm

H = 8mm

Y = 0.3mm   (the thinnest trace due to PCB manufacturer restriction)

10 x 8 mm²   (Area of sensor is a normal area of finger's press)

$X_{fingers} = [(10 - 3*1.6 - 0.3) / (1.5*1.6 + 0.3)]$

      $= 1.75$

      $= 1$ (we accepted that $X_{fingers}$ is 2 due to bad design)

$X_{border} = (10.5 - 1.6 - 0.3 - 2(1.5*1.6 + 0.3)) / 2$

      $= 1.6$ mm

The number of $X_{fingers}$ is very small and there is only one X fingers. The resulting key is far from ideal and has lack of interdigitation. This leads to very low *Cx* and a lack of sensitivity. The number of Xfingers is two due to the key size and panel thickness.

If there was a front panel made of glass, the electrodes and the traces were to take place on two layers on PCB. In a study that I conducted apart from this thesis I preferred to use a glass of 3 mm thickness and the sensors were designed by taking this glass and the dielectric constant into account. The dielectric constant of glass is higher than of plastics.This means that electric field propagates efficiently in glass.

Flooded- X two-layer method is used for the sensor design in this project. In this method, the X and Y electrodes are placed in an overlapping way on two layers on PCB. The X electrode is placed generally on the lower layer, while the Y electrode takes place on the upper layer, which is close to the area of touch. The X electrode placed on the lower layer covers the Y electrode, which is upper layer. All edges of the electrodes on the lower layer shall be 2mm longer than the electrode edges on the upper layer. The electro shapes are not quite significant, but it would be beneficial if these shapes are the same. The thickness of electrode Y shall be in between 0.1 mm and 0.5 mm. Figure 2.15 illustrates the side views and the top spot of the sensors existing on both side of PCB.
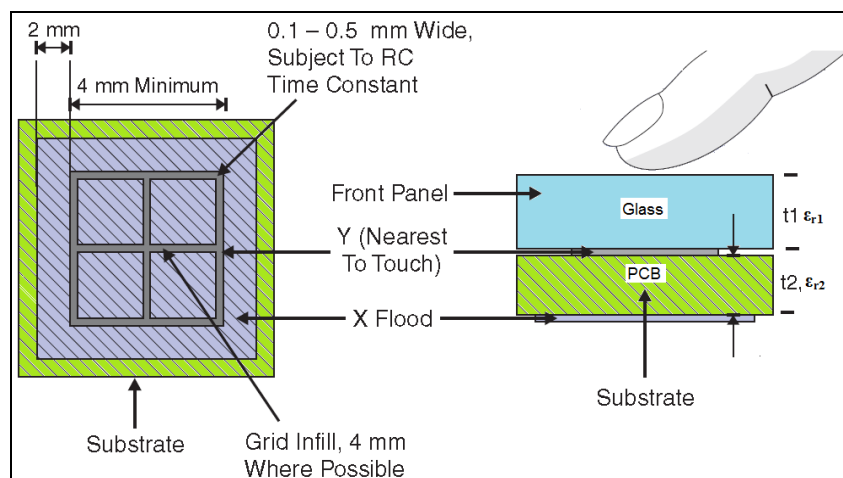
Figure 2.15 Flooded-X Two-layer Method (Atmel, 2009)

The sensitivity calculations are performed according to the thickness of the materials and their dielectric constants used in these kinds of designs, because electric field propagates better by materials having a higher dielectric constant (ε_r).

Sensivity Factor (S):

$S = \varepsilon_r / t$ (for only one layer) (2-11)

$1/ S_{STACK} = Sum (1/ S_{LAYER\,[\mathbf{n}]})$ (for a stack of materials) (2-12)

Where:

t is the thickness of the layer

ε_r is the dielectric constant of the layer

n is the number of layers

Ideally, the X to Y layer separation should meet equation (2.13).

X to Y Layer Separation:

$2 \leq (\ S_{YtoXstack} / S_{TouchtoXstack}) \leq 12$ (2-13)

$S_{YtoXstack} = \varepsilon_{r2} / t_2$

$$S_{TouchtoXstack} = \frac{1}{\left(\dfrac{t1}{Er1} + \dfrac{t2}{Er2} \right)}$$

In our non-planar mutual capacitive sensor construction

$t_1 = 3$ mm (thickness of the glass)

$t_2 = 1.6$ mm (thickness of the substrate, PCB)

$\varepsilon_{r1} = 3.7$ to 10 (dielectric constant of the glass, accepted 3.7)

$\varepsilon_{r2} = 4.2$ (dielectric constant of the FR4 pcb)

$Y_{width} = 0.25$ mm (This PCB coming from China manufacturer)

$S_{YtoXstack} = $ 4.2 / 1.6

$\qquad = 2.625$ \qquad\qquad\qquad (FR4 PCB)

$$S_{TouchtoXstack} = \frac{1}{\left(\dfrac{3}{3.7} + \dfrac{1.6}{4.2}\right)}$$

$\qquad = $ 0. 839093 \qquad\qquad (Touch to X electrode)

In result:

$S_{YtoXstack} / S_{TouchtoXstack}$

$\qquad = 2.625 / 0. 839093$

$\qquad = 3.128$ \qquad\qquad\qquad (this is good sensitivity)

Zero-dimensional types of planar and non-planar mutual capacitive sensors are attached in appendix A.

2.3.1.3 Slider

This part described how the slider sensor is designed. At all times the channels on the same Y line are used to design the slider. As a Y line in this design has maximum 8 channels, the slider is to consist of maximum 8 channels. However, the slider on this card consists of only 6 channels.

There are two types of one-dimensional sensors:

-Spatially Interpolated
-Resistively Interpolated

A Spatially Interpolated type sensor is used for this design, as the slider on the card having 6 channels is 6 cm long. There are many ways to arrange a spatially interpolated slider. The slider in this study is based on a design, in which the channels are laid together side by side. Figure 2.16 illustrates the structure of a slider. This slider acts as a broad "super key". There are no borders between the channels. However, there are borders on the edges of the slider. An extra Y finger is applied, for there are no borders between two channels.
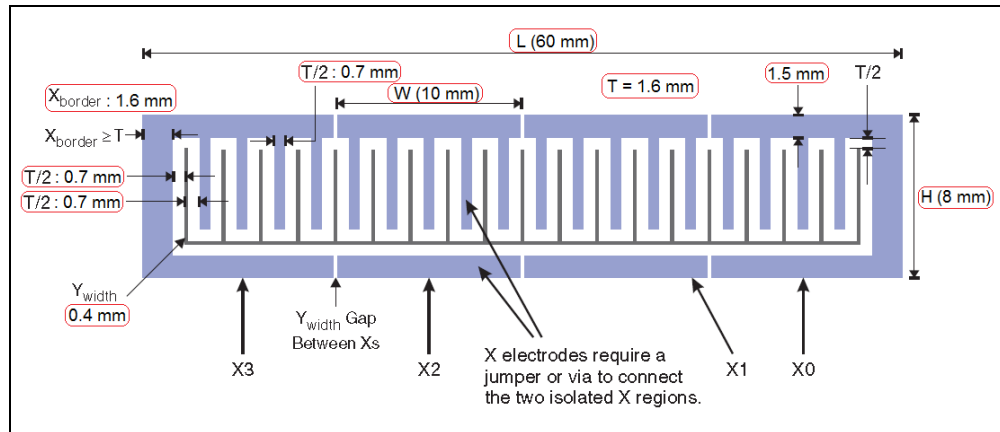
Figure 2.16 One - layer small slider (Spatially Interpolated). (Atmel, 2009)

Calculation $X_{fingers}$ and X_{border} for the slider on the same layer:

$$X_{nominalfingers} = [(L - 3T - Y_{width}) / (1.5T + Y_{width})] \qquad (2\text{-}14)$$

$$X_{fingers} = ((([(X_{nominalfingers} + 2) / keys]) * keys) + 2 \qquad (2\text{-}15)$$

$$X_{border} = (L - X_{fingers} (1.5T + Y_{width}) - T - Y_{width}) / 2 \qquad (2\text{-}16)$$

Some parameters in the slider of the mutual capacitive design:

L   : 60 mm

H   : 8 mm

W   : 10 mm

T   : 1.6 mm

Y_{width} : 0. 4 mm

Keys   : 6

$X_{nominalfingers} = [(60 - 3*1.6 - 0.4) / (1.5*1.6 + 0.4)]$

$\qquad\qquad = 19.57$

$\qquad\qquad = 19$

$X_{fingers} = ((([(19 + 2) / 6]) * 6) + 2$

$\qquad\quad = 20$

$$X_{border} = (60 - 20(1.5*1.6 + 0.4) - 1.6 - 0.4) / 2$$
$$= 1 \text{ mm}$$

The number of Xfingers is 22 instead of 20 and Xborder is 0.7 mm instead of 1 mm. Y_{width} is 0.4 mm in slider construction while it is 0.3 mm in button construction.

In another study, we designed s slider having electrodes of 12 cm on both layers. What is more, there were only 4 channels that we could use for this slider. Therefore, the resistively interpolated method was preferred instead of the spatially interpolated method. This method requires the use of array of electrode segments connected to each other with resistors. The advantage of this method is that each key or each channel may consist of one or more segments.

Figure 2.17 shows the segments together with the slider. There are 3 units of Y line on the upper layer in order to increase the mutual lenght. The following parameters are taken into account to design this slider:

N : 10 (the number of segment)
W : 12.15 mm (length of each segment)
H : 9 mm (height of each segment)
L : 121.5 (total slider length)
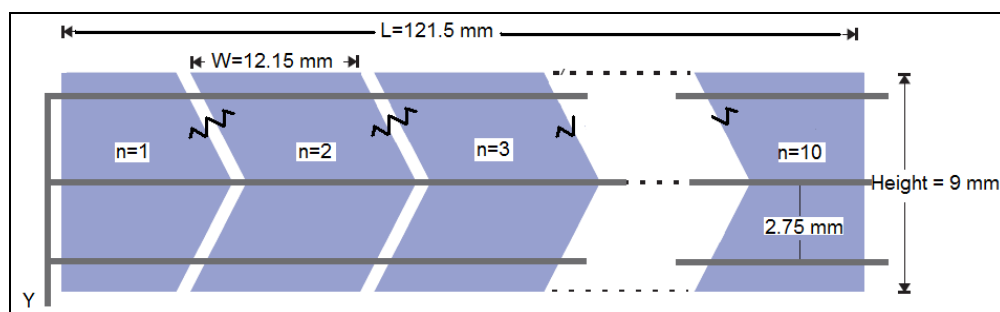
Figure 2.17 Two-layer large slider (Resistively interpolated) (Atmel, 2009)

One-dimensional types of planar and non-planar mutual capacitive sensors are attached in appendix A.

2.3.2 PCB Design Considerations

It is quite important to know the basic capacitance equation in order to design capacitive sensors. In a capacitive sensor, the physical parameter being measured by varying one or more of the terms in the basic equation of capacitance

$$C = \frac{\varepsilon * A}{d}$$
(2-17)

where e is the permittivity of the dielectric, A is the overlap area of the capacitor plates, and d is the distance between the plates. For example, humidity sensors typically work by varying the permittivity e, pressure sensors by varying distance d and position sensors by varying area A or distance d (O'Dowd, J., Callanan, A., & Banarie, G., 2005, p. 951).

In touching sensors, d will decrease when the finger comes close to the sensor, while the sensitivity increases. If the sensor area increases as well as the dielectric constant of the material, sensivity is to decrease.

$$C_{sum} = C_{parasitic} + C_{Fingers}$$
(2-18)

Where:

C_{sum} is total capacitance

$C_{parasitic}$ is the parasitic capacitance

$C_{fingers}$ is the finger's capacitance

Equation 2-18 describes the effect of parasitic capacitance on the sensitivity of the system (Davison, B., 2010).

As the coupling capacitance between X-Y is measured for mutual capacitive sensors, the effect of parasitic capacitance is quite low. On the other hand, the effect of parasitic capacitance is high on self-capacitive sensors.

Mutual capacitative sensors operate on the basis of the charge-transfer principle. Stable and repeatable results are to be obtained only when charge-transfer pulses are not be attenuated under the effect of the RC Time constants. Charge pulses are to have flat tops and they shall be settled exactly before the end of the period. The rule of thumb for this is as: (Atmel, 2009)

$$RC << T \qquad\qquad\qquad\qquad (2\text{-}19)$$

Where

$RC = R_{series} * (C_x + C_{parasitic})$

RC is the time constant

T is the time period of charge-pulse

If the time constant is lower than the time period, both Cx and Cs capacitors can be charged and discharged immediately. If the signals of the electrodes on the sensors are displayed by oscilloscope, charge-pulses shall be viewed on the transmitting electrode, while the receiving electrode displays the spikes.

Figure 2.18 illustrates the signals received from the X and Y electrodes of any mutual capacitive sensor on this card. This graphic verifies the equation of 2-19 and reveals how short the settling time is. Cx is charged and discharged before the end of this period.
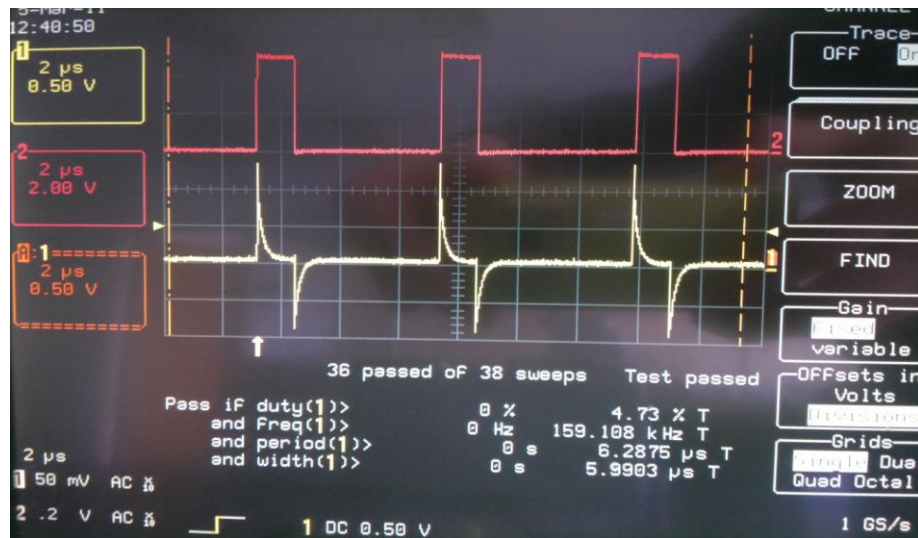
Figure 2.18 Voltage waveforms across sensor electrodes

Table 2.2 illustrates the rising time and the falling time of charge-pulses under different frequencies. This table reveals that the settling time is quite low when the pulse width is taken into account. This design shows that the RC time constant is small. This is the ideal form.

Table 2.2 Specifications of the sending charge-transfer pulses on a mutual capacitive sensor

Duty Clock Cycle	Freq (Khz)	Period (us)	Width (us)	Rising Time (ns)	Falling Time (ns)
2	179,7	5,55	0,5	16	18,5
4	172,2	5,8	0,75	16,1	18,5
6	164	6,1	1	16,1	18,1
8	158	6,33	1,25	15,5	18,1
10	152,15	6,57	1,5	15,5	18,1
20	110	9	2,75	15,5	18,1
50	60	16,45	9,95	15	17,9
100	32,4	30,75	12,75	14,9	17,7

The *Cx* and *Cs* capacitors are connected to each other by means of serial resistance. This refers to the copper trace resistance between these two capacitors. The effect on the RC time constant needs to be monitored. Normally, serial resistance improves electromagnetic interference (EMI) and ESD. Therefore, extra additional resistors are added to some designs. 1 kΩ resistors are used for the sensors on this card.

There is one integration capacitor (Cs) in this type of sensor. Normally Cs accumulates the coming charges. The measured level refers to the voltage difference between the terminals of Cs. As a result, this capacitor is the most important component of the measuring circuit. The circuit includes a ceramic capacitor of type X7R. This kind of capacitors has low tolerance value and high stability. Series resistors are not so critical. Serial resistors are able to tolerate an alteration of 10%, but such an alteration could not be tolerated in capacitors, especially when the alteration takes place under spontaneous conditions.

One of the most important problems related to the capacitive sensors is related to the sudden change of the Vdd value. The long term shifts in Vdd are compensated by the internal drift algorithms, but short term shifts are not compensated. 7805 integrity was used for the circuit with the aim of obtaining a linear regulated supply. The supply circuit can be seen on the schematic diagram of mutual capacitive touch sensing card in Appendix C.

Another important point related to the design of related with the placement of passive components such as Cs, because they need to be close to the chip. Especially, items belonging to the measuring circuit need to be placed closely to the chip. This help to the EMC compliance. Capacitive sensors are high-impedance input during the scanning process and they serve as high-frequency antennas. However, the series resistors used for the sensor circuit decrease the RF coupling both in sensor input and in sensor output. Therefore, traces used within this context are as short as possible (See Appendix C).

The traces of Y electrode in mutual capacitive sensors should be as thin as possible (0.1mm to 0.5mm). This minimizes the noise coupling possibility while touching. These thicknesses of traces also depend on PCB manufacturer. The Y traces of the buttons on this card are of 0.3 mm thickness; while the Y traces of the sliders are of 0.4 mm. Traces are not so important for X electrodes. Generally, the thickness of the overlaying panel is regarded as the basis for the calculations. X electrode is a partial shield for the Y electrode. This minimizes the noise coupling at

the Y electrode. The Y electrode is always the inner component for both the button and the slider in this card and the X electrode forms a partial shield for the Y electrode. The card layout shows the positions of X and Y electrodes to each other. The layout of the card is attached in appendix C.

The traces that routed on PCB are also as important as the thickness of the X and Y electrodes. X routing is not so important as long as the RC time constants are monitored. High frequency signals such as LCD and LED should be routed away from the X traces, because high frequency switching transient may disturb the charge transfer. As X routing is not touch sensitive, it can be easily routed from any layer on the PCB. Y routing is touch-sensitive. Therefore, this shall be routed carefully on the PCB.

The foreign signals around the Y traces increase the parasitic capacitance. Therefore, the Y traces are always routed away from other signals and the ground. Furthermore, it shall be kept away from the X traces, because apart from thesensor areas where the X and Y traces come close to each other, this may lead to a false key detection. Apart from the sensor area, if the finger touches an area where the X and Y sensors are close to each other, the touched area may act as a sensor. These lines may routed closely only in the sensor area. The distance between the X and Y lines for this design shall by minimum 8-10mm. As one led is used for every button, they simulate whether the finger touches the button or not. The led traces shall be routed away from the X and Y traces.

Since the mutual capacitance between the X and Y electrode are measured in mutual capacitive sensors, the coupling lenght on PCB should be as long as possible. This is important especially for sensor areas. As mentioned in the sensor design, the aim of interdigitated sensor method is to increase the mutual lenght.

The ground areas on PCB and the ground line lead always to an increase of parasitic capacitance (Cp). If ground floods or traces come close to the sensors, this may desensitize the sensors. While ground floods or traces sensors do not cause

much effect on the X element when they come close, they desentisize the sensors on the Y traces. However, ground traces are sometimes used in order to prevent crosstalk between the two sensors. See the ground traces between two sensors in appendix A.

Substrate is the most important component of the PCB design. Substrate is the base material that contains sensor electrodes and their traces. Nearly all insulating materials can be used for sensor design as substrate material. However, low-lost substrates are preferred. The PCB materials may be acrylics such as FR4, CEM-1 or Polyethylene Terephtalate (PET). However, the glass is a good material due to dielectric constant.

As seen in the sensitivity factor (S) equation, the thickness of the materials and the dielectric constant are the two main variables effecting sensitivity. Generally, thin materials having high dielectric constant are preferred. Furthermore, the dielectric constant shall be durable against the ambient conditions. FR4 type PCB shall be used for the mutual capacitive sensing card. X and Y traces can be easily routed, as it is possible to use both surfaces on FR4. The average dielectric coefficient of FR4 is 4. The thickness of PCB is 1.6 mm.

Figure 2.19 illustrates the field flow diagram of an electric field having two different dielectric constants.
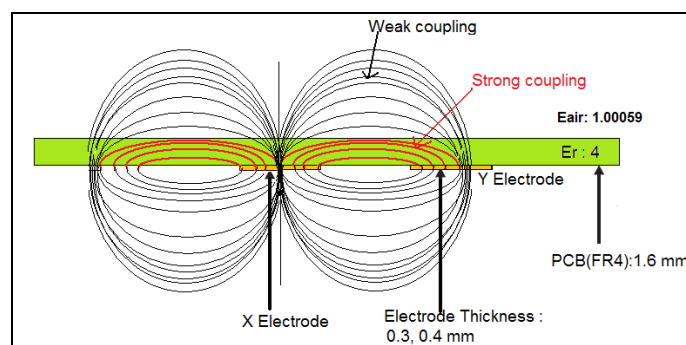

Figure 2.19 Diagram of the field flow in PCB and air

There may sometimes be a front panel in front of PCB in some designs. This design does not include springs, but if there were springs, there would be a front panel in order to prevent direct connection between the springs and user. Glass is the best example within this context, because the dielectric constant of glass is higher than plastics. Hence, glass materials do have a better electric field and sensitivity. Of course, the thickness of the material is important. The thinner the front material is, the higher would be the SNR rate and the sensitivity. Plexiglass, polycarbnate and PMMA could be also utilized as front panels apart from glass. The table in Appendix B shows the dielectric constants of some materials.

2.3.3 Microcontroller

In the mutual capacitance part of the thesis, ATMEL microcontroller is used because of ATMEL QTouch library which can run on it. And, the other reason for choosing this processor is to have CMOS pins instead of TTL pins. CMOS pins have smaller parasitic input/output capacitance to GND. This microcontroller is also used in self-capacitance part of the thesis.

In this project, ATmega329P that is 64-pin TQFP package is chosen. It is a low-power CMOS 8-bit microcontroller based on the AVR enhanced RISC architecture. It can execute an op-code in a single clock cycle. ATmega329P provides the following features (Atmel, 2009):

- 130 Powerful Instructions – Most Single Clock Cycle Execution
- 32K bytes of In-System Programmable Flash with Read-While-Write capabilities
- 1K bytes EEPROM, 2K byte SRAM
- Two 8-bit Timer/Counters with Separate Prescaler and Compare Mode
- One 16-bit Timer/Counter with Separate Prescaler, Compare Mode, and Capture Mode
- 8-channel, 10-bit ADC
- Programmable Serial USART

- Master/Slave SPI Serial Interface

- Programmable Watchdog Timer with Separate On-chip Oscillator

- On-chip Analog Comparator

- Interrupt and Wake-up on Pin Change

- Power-on Reset and Programmable Brown-out Detection

- Internal Calibrated Oscillator

- Up to 20 MIPS Throughput at 20 MHz

- -40°C to 85°C Industrial temperature range

- JTAG (IEEE std. 1149.1 compliant) Interface,

Pin diagram of ATmega329P IC is attached in appendix E.

2.4 Software Design

2.4.1 QTouch library

QTouch libraries are used for capacitive sensors. The firm offers separate library support for each microcontroller. The last version of QTouch Library 4.3 (revision 4.3 updated 7/10) is used for the mutual capacitive sensing card. This last release prefers "libavr5g3_16qm_8x_2y_krs_2rs.a" for ATmega 329P (WEB_2, 2010).

This library includes many limitations with regard to the library. For instance Y line or the reference line cannot be connected to every pin on the processor. The schematic diagram of the card was designed by taking all these limitations into account. Appendix C shows the pin connections and the schematic diagram of this card. Furthermore, this library uses some resources of this processor in run-time. The involved resources cannot be used, while the sensors drive. If used, this may lead to a failure regarding the measurement results.

Some constraints for QMatrix in this library are listed below:

- Timer1 and Analogue Comparator are used by the library.

- Software interrupts are disabled during the scanning process.

- The YB line is connected to the port ADC.

- The reference GND is connected to pin AIN0.

- As the slider channels are on the same Y line, the number of them may vary between 3 and 8.

The mutual capacitative card consists of 16 channels in total and this is explained by 8 x 2. Common settings can be performed for all channels by means of a software defines, but there are also sensor specific settings. See some of the sensor-related parameters and descriptions below:

- Detect Threshold: A limit used to define at what point a sensor should change states (Davison, B., 2010).

- Acquisition: A single capacitive measurement process

- Sensor: A channel or group of channel used to form a touch sensor. Sensors are of three types that are keys, rotors or sliders.

- Recalibration Threshold: Recalibration threshold is a level performing the automatic calibration procedures independently from the program. Generally, the detection threshold is described as the percentage of setting. For instance, the detection threshold is 20. 25% of the detection threshold is 5. If the threshold is falls below -5 or below, the library shall calibrate the sensors automatically.

- Detect Integration: The detection integration mechanism is used in order to confirm when any key is selected. Detection Integrator (DI) could be recognized as a simple software filter preventing false detection. For instance DI is 5 and the delta of any sensor exceeds the threshold one time. As DI is 5, the sensor delta is to be over the threshold level for a period of 5 acquisition. If the delta level is over the threshold during 5 acquisition processes, sensor declares to touch.

- Drift Hold Time: Drift Hold Time (DHT) is used to restrict drift on all sensors while one or more sensors are activated. It defines the length of time the drift is halted after a key detection. This feature is useful in cases of high density keypads where touching a key or floating a finger over the keypad would cause untouched keys to drift, and therefore create a sensitivity shift, and ultimately inhibit any touch detection. (Atmel, 2010)

- Maximum ON Duration: If an object unintentionally contacts a sensor resulting in a touch detection for a prolonged interval it is usually desirable to recalibrate the sensor in order to restore its function, perhaps after a time delay of some seconds. The Maximum on Duration timer monitors such detections; if detection exceeds the timer's settings, the sensor is automatically recalibrated. After a recalibration has taken place, the affected sensor once again functions normally even if it still in contact with the foreign object. (Atmel, 2010)

- Positive / Negative Drift: These parameters are used for the adjustment of the reference values of the sensors under specific conditions. The mechanism will stop, if one button is pressed. It is called as negative drift, if the reference level of the sensors fall. On the other hand, it is positive drift, if the reference value of a sensor increases. For instance, if the circumstances lead to a physical increase in the dielectric constant of the sensors, the sensitivity may also increase. Consequently, this will result in a positive drift. However, the point that needs deference here is related to the speed of the drift mechanism. For instance, if a finger closes slowly to the sensor, and if the drift mechanism is drifting fast in accordance with the movement of our finger, the system may not recognize our finger.

- Positive Recalibration Delay: If the delta of a sensor falls below a certain negative level as described above in the recalibration threshold, sensorsa re-calibrated automaticall y, but the library does not calibrate immediately. This

takes some time. The period of this time is determined by the positive recalibration delay.

- AKS: In designs where the sensors are close together or set for high sensitivity, multiple sensors might report detect simultaneously if touch is near them. When a group of sensors are in the same AKS group, then only the first strongest sensor will report detection. The sensor reporting detection will continue to report detection even if another sensor's delta becomes stronger. The sensor stays in detect until its delta falls below its detection threshold, and then if any more sensors in the AKS group are still in detect then the strongest will report detection. So at any given time only one sensor from each AKS group will be reported to be in detect. In this design, slider and two sensors which are close slider are the same AKS group (Atmel, 2010).

- Hysterisis: This setting is sensor detection hysteresis value. It is expressed as a percentage of the sensor detection threshold setting. Once a sensor goes into detect its threshold level is reduced (by the hysteresis value) in order to avoid the sensor either in and out of detect if the signal level is close to original threshold level (Atmel, 2010).

2.4.2 Software Process

Software first initializes software parameters and firmware parameters. After initialization it enters main loop. Main loop is implemented in "main.c" file.
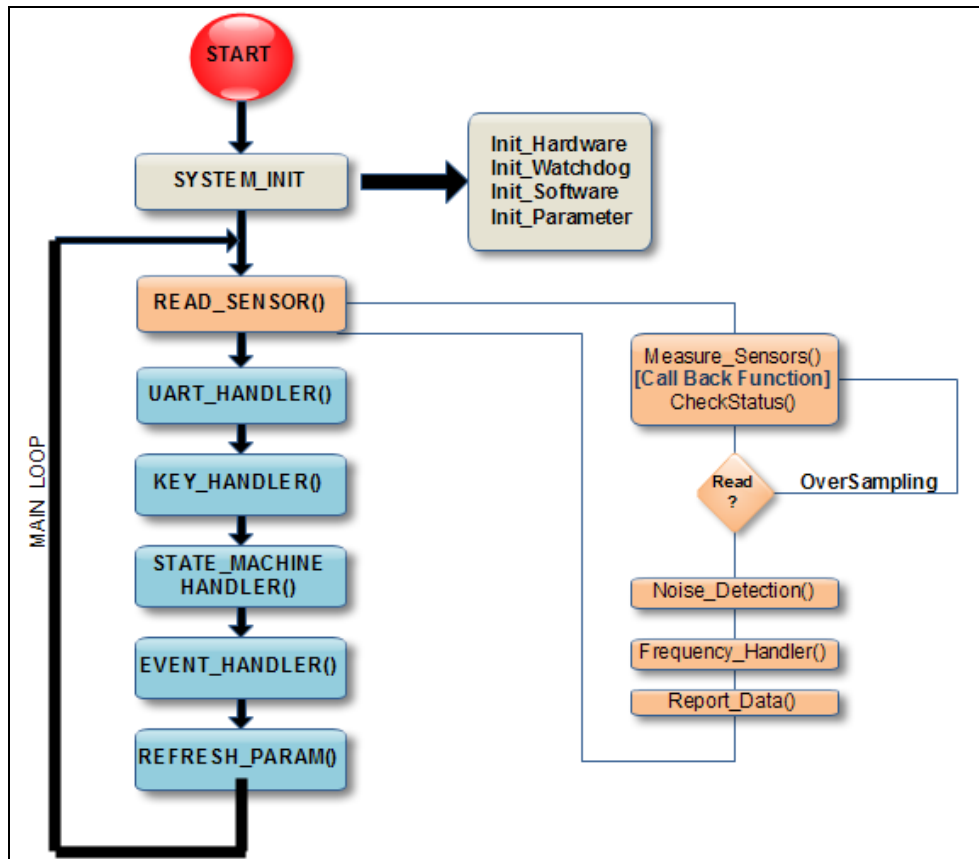
Figure 2.20 Flow diagram of main loop

Following jobs handled in main loop:

- Read Sensor: Main loop will constantly check appTouch_ReadSensors() for any button or slider detection. This function is checking touch button driver by calling qt_measure_sensors() library function. All jobs about which are frequency hoping and key decision are performed in this function. while leaving this function Report_debug_data is called to get all parameter that is related sensor.

- UART Handler: Main loop calls serial port to send message to the computer in order to simulate which key detected.

- Key Handler: Main loop will constantly check appTouch_ReadSensors() for any key event. This handler will generate a valid key event by checking structKeyAppInfo structure in sw.

- State Machine Handler: This handler receives key events from key handler and virtual events from timer handler and maps to a valid event according to state.

- Event Handler: Checks for any event in queue and executes the incoming event. It updates necessary parameters for the rest of the system. This handler uses timer handler for timer set, cancel or update. This notifies to user with buzzer and led indicators.

- Refresh Parameter: All parameters that belong to microcontroller system, buzzer and led are refreshed.

2.4.3 Software Filters

There are some basic limitations being taken into account, while designing capacitive sensors. The first limitation is SNR. Although the hardware design and the capacitive measuring technique are good, SNR is the most important component of the design part. If the SNR is high under normal operation conditions, the detection process can be performed easily and speedy without the need for a software filter. If the SNR is low in spite of all developments and enhancements, software filters shall be preferred in order to prevent false detection.

Another limitation is the memory of the processor and the response time of the action. For instance, speed is very important for systems related to games and security. The response is expected to come immediately. Therefore, the filters to be preferred may have a small code sizes and include fast filtering techniques (Davison, B., 2010, pp. 12-13).

There are many studies in the literature to increase the SNR and to filter noise. For instance, according to the study of W.C., Hsu, Y.C., and Liao, L.P(2006), the signals received are carried to a high frequency band by using modulator. Then, the signals are increased by means of an amplifier. After that, the increased signals are demodulated and are passed through a LP filter. Noise signals are reduced at output of LP filter, so SNR increased.

Some software filtering techniques are applied consecutively in this study. The goal is to pass some EMC tests and to have a more reliable and speedy measurement process. Figure 2.21 illustrates the filter structures and the flow diagram of the READ_SENSOR () function. The filters are called by means of the callback function. The callback function is called after every acquisition. The first measured signals are still raw data. This acquisition is performed by calling the qt_measure_sensors() function and the signal values are obtained from all channels. If there is a callback function for filtering, the address of this function is assigned to qt_filter_callback function that provided the library. The signal values for the sensors are being filtered before the qt_measure_sensors() is returned back in order to obtain the filtered values.
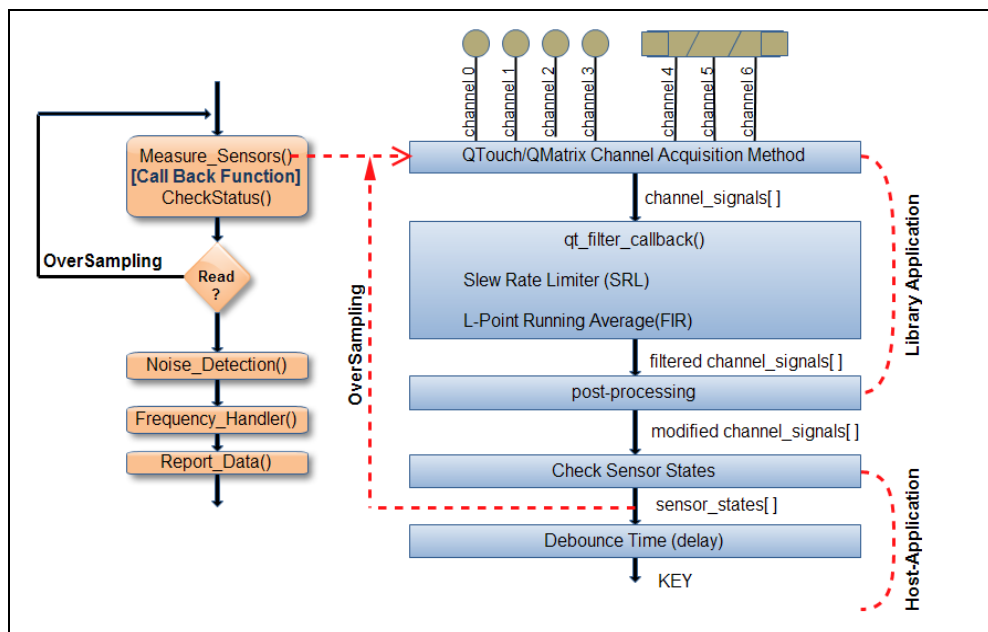

Figure 2.21 Block diagram to represent usage of filters with callback function

2.4.3.1 Oversampling

This process is the simpliest filter used in order to prevent false detection. This provides more acquisition sample per reading of sensors. There may be false key detection on the card due to the electrical noise. Especially, high impulses are injected to the card of high voltage during the EFT tests. In this case, it may be illusive to decide whether the sensor is detected or not just only by a single

acquisition sample. Therefore, there should be more than one acquisition in all sensors (Davison, B., 2010, p. 14).

This process is similar to the debounce time in push-pull buttons. When the logic pin is read for more then one time, it will be possible to determine whether the logic changes in hard buttons occur due to the electrical arc or due to touching. This prevents also the false detection possibility.

The oversampling filter may also be applied during the release or going out of detect procedures. The accuracy of the operation is going to be verified, when the keys are read for several times after the finger releases the button.

In this study, it is determined whether the sensor is touched or not after a period depending on 10 acquisition. There are 16 channels in the mutual capacitive sensing card and all channels can be read via a single acquisition. A single acquisition takes 10ms. Since there is a need for at least 10 acquisitions, this process takes about 100ms in total. This is a long period for systems, where quick response is demanded. Figure 2.22 shows the software codes realizing the oversampling process. It is determined whether the key is touched or not by calling the function qt_measure_sensors() for at least 10 times.

```
#define MEASURECOUNT            10

do
{
    qt_measure_sensors(s_u16CurrentTimeTouch);
    u8ReturnKey = appTouch_CheckSensorStates();
    if (u8ReturnKey == u8UpdateSensor)
    {
        --u8MeasureCount;
    }
    else
    {
        u8UpdateSensor = u8ReturnKey;
        u8MeasureCount = MEASURECOUNT;
    }
}while(u8MeasureCount > FALSE);
```

Figure 2.22 Example code implementation of the oversampling filter.

Another advantage of the oversampling method is to increase the SNR rate. In other words, this is going to reduce electrical noise in the system. Every value obtained herein is the average value, as it is obtained after several acquisitions (Davison, B., 2010, p.14).

Figure 2.23 and Figure 2.24 shows the oversampling examples. While the oversampling value is 2 in Figure 2.23, this will be 10 for Figure 2.24. Noise is injected from 150 kHz to 80 MHz. As seen from the figures, it is possible to obtain a more stable signal, when oversampling is 10. Consequently, the noise ratio falls.
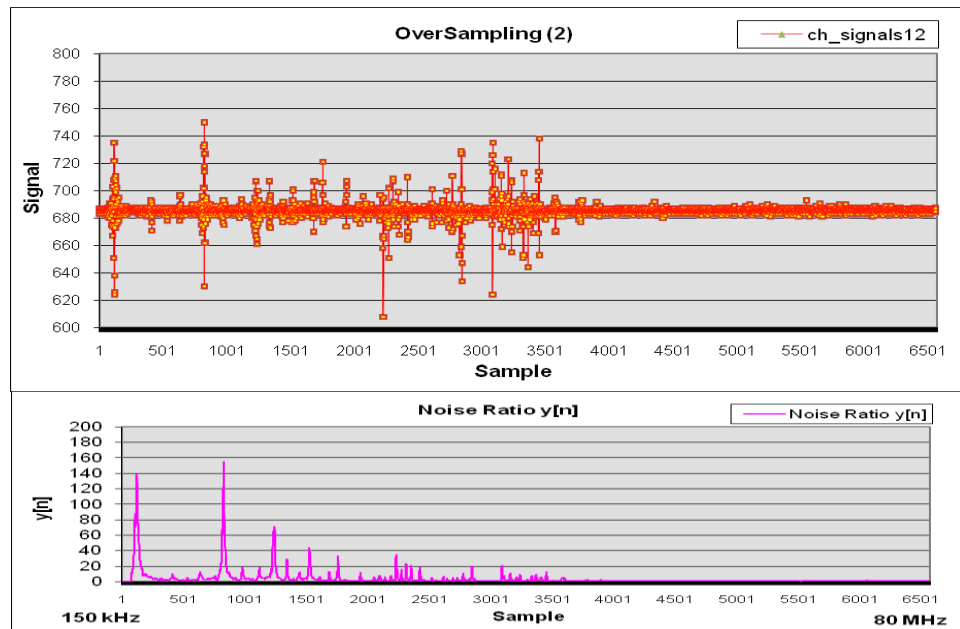

Figure 2.23 Example of oversampling when each per 'reading ' is 2. While noise is being injected, signal is distorted and noise ratio increases.
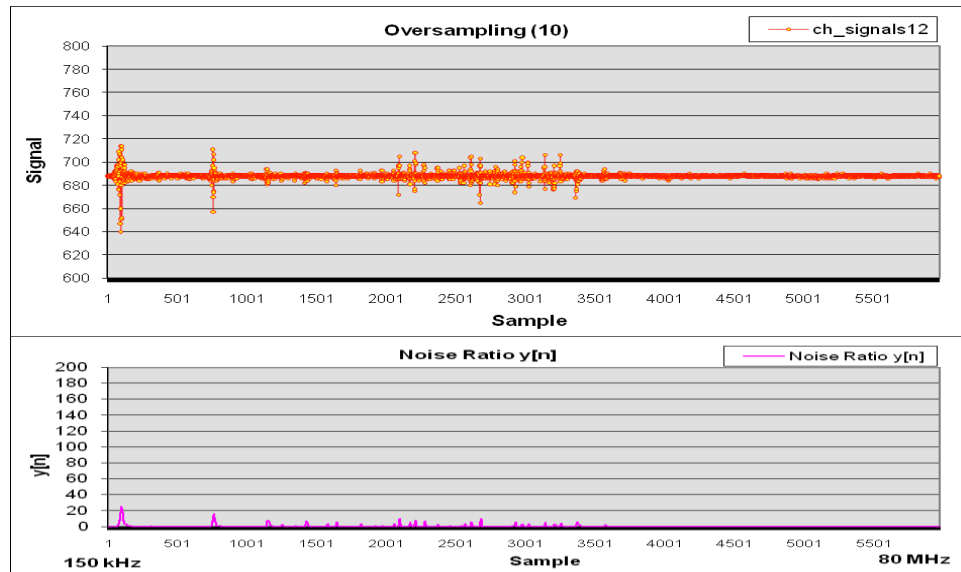
Figure 2.24 Example of oversampling when each per reading is 10. Increasing the oversampling increases the stability of the system and decreases the noise interference.

2.4.3.2 FIRs and IIRs

Digital filters are a very important part of digital signal processing. They can be used for most purposes but they in this thesis are used for signal separation when capacitive measurement signals has been distorted with interference, noise or other reasons.

There are two fundamental types of digital filters: finite impulse response (FIR) and infinite impulse response (IIR). As the terminology suggests, these classification refer to the filter's impulse response. Digital filters lend themselves to adaptive filtering applications simply because of the speed and ease with which filter characteristics can be changed by varying the filter coefficients. (Ashby, D., Baker, B., & Stuart, S., 2008, pp. 489-494)

FIR filters take a fixed number of previous inputs and to create a output such as average filters. Some FIR filter benefits:

- Always stable
- Simple implementation by looping a single instruction

- keeping previous values cause some problems

IIR filters take a current value and operate it in combination with past output value. It has a feedback mechanism and theoretically, the impulse response never reaches zero and is an infinite response. Some IIR filter benefits:

- Require less memeory
- Require less resources due to few multiply-accumulates processing
- More efficient and fast (Davison. B., 2010, p. 15)

2.4.3.3 Slew Rate Limiter (SRL)

The concept of this filtering technique is very simple. The value obtained for each channel is maintained in order to evaluate what the difference is between the current value and the previous value. If the current value is too high or too low, when compared with the previous value, the current value shall not be taken into account, as instead +1 or -1 is added to the previous value to obtain a valid value. The last value is deemed to be the current value that is read by means of the latest measuring system. As a result, very large and very small values occuring as a result of the noise is discarded (Davison. B., 2010, p. 15).

In this study, the moving-average filter is coming after the SLR filter. The moving-average filter is specific for each channel. Every value obtained for each channel is compared with the average of the moaving filter before being registered as input of the moving-average filter. If a value read in a channel is 25% higher or lower than the average value of the filter, this value shall not be taken into account. Instead ± 1 of the filter average is taken.

The size of the moving average filter is 10 for each channel. For instance, think that the moving-average filter value is 400 for a specific channel. This means that the average of the last 10 values is 400. $\pm 25\%$ of this value are 300 and 500. If the value obtained for this channel is lower than 300, this value shall not be taken into account, as 390 (=400-10) is deemed to be valid. As a result, the average of the filter falls to

399 (400*9+390)/10. Again the same method is applied in case the value is deemed to be higher. So the values being invalid due to any reason apart from the problems stemming from the EMC tests are smoothed.

This filter is used commonly in order to prevent noise being injected during the conductive immunity tests. Figure 2.25 illustrates the signals being obtained from the moving-average filter together the SRL filter. The SLR limits in this graphic are $\pm\%10$ of the moving-average filter. If attention is paid, this study reveals that the limits change, when the buton is pressed. The signal is maintained constantly, even if the testing conditions change.

Figure 2.25 Slew Rate Limiter ($\pm$ 10% limits of the moving-average filter)

Figure 2.26 illustrates another example of the slew-rate limiter. If the received signals are more or less than 10% of the signal itself, the current value shall not be taken into consideration. Instead ±1 of the signal average shall be taken into account. The yellow line is raw data in this graphics and this area is disturbed, when noise is injected to the system. On the other hand, the red-colored area is the slew-rate filter output and they do not change in the way as of the raw data. They are stable and smooth.
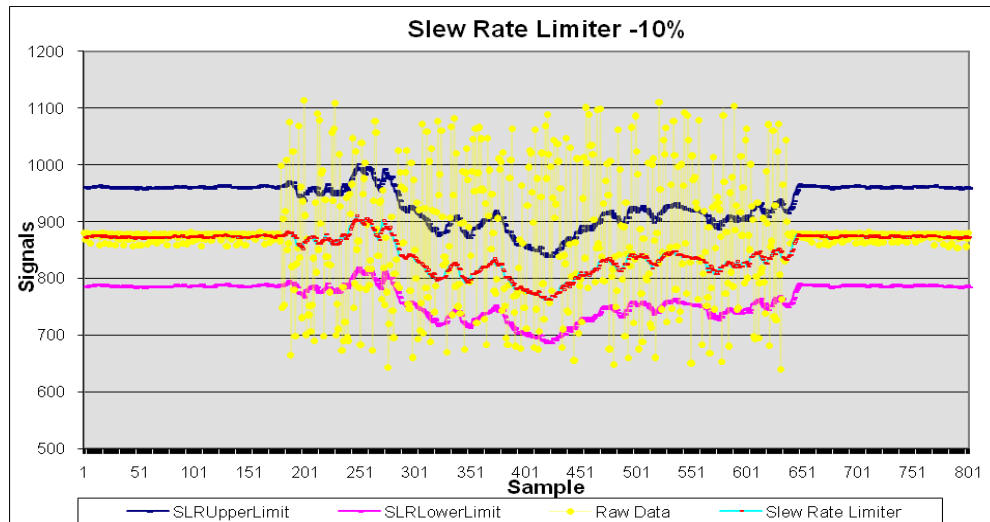
Figure 2.26 Slew Rate Limiter (Figure 2.25 is zoomed in.)

2.4.3.4 L-Point Running Average (FIR and IIR types)

The moving (running) average filter is defined as a type of FIR filter. Consider an L-point moving-average filter defines as formula;

$$y(n) = \frac{1}{L}[x(n) + x(n-1) + \ldots + x(n-L+1)]$$

$$= \frac{1}{L}\sum_{l=0}^{L-1}x(n-l) \qquad (2\text{-}20)$$

where each output signal is the average of L consecutive input sample.

Implementation of Equation 2.20 requires L-1 additions and L memory locations for storing signal samples $x(n), x(n-1), \ldots x(n-L+1)$ in a memory buffer. These types of filters are popular for smooting data. While EMC tests applying to the card, the effect of the noise causes signal samples to fluctuates from the original values, so the noise might be removed by averaging a few neighbour samples (Kuo, S.M., Lee, B.H, & Tian, W., 2006, pp.127-130).

In general, moving average filters are known as type of finite impulse response filter but actually they are two kind of filters. One of them is FIR type and other is first-order IIR type. Equation 2.20 always requires L memory locations and when a large L used, it increase memory cost. To solve this limitation of the filter the oldest sample $x(n-l)$ can be approximated by its average $y(n-l)$. Now the moving average filter can be defined again. It is approximated as

$$y(n) \cong \left(1 - \frac{1}{L}\right)y(n-1) + \frac{1}{L}x(n)$$

$$= (1-\alpha)y(n-1) + \alpha x(n)$$

Where $\alpha = \dfrac{1}{L}$ or

$$y[n] = y[n-1] + \frac{x[n] - y[n-1]}{L} \qquad (2\text{-}21)$$

This is simple first-order IIR filter. Two multiplications are need instead of one but, only need two memory locations instead of L+1. Thus, this is most efficient way of approximating a moving-average filtering.

The IIR type of moving average filter will be used noise detection algorithm in order to make decision whether these is noise along with FIR type moving average filter.
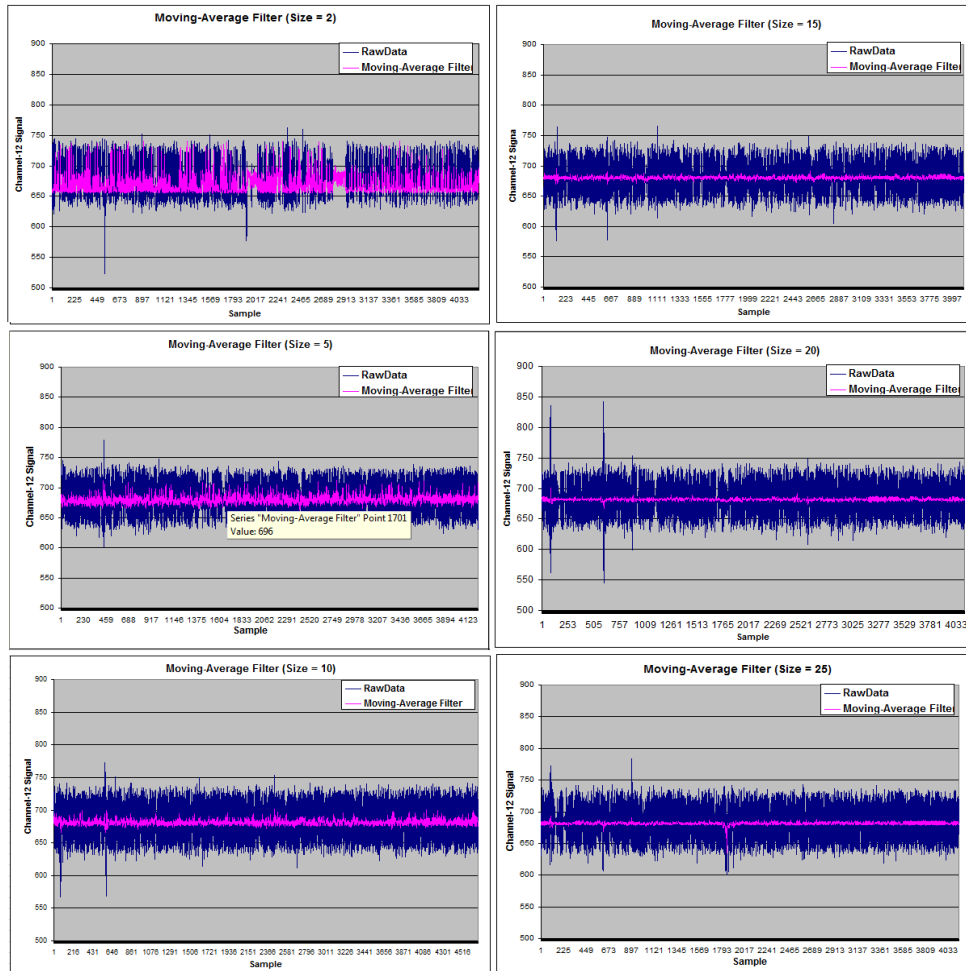
Figure 2.27 The output of moving average filter with different size of filter

The length of the moving-average filter shall be medium size. If the filter is too long, the update period shall take a long time after every acquisition. The response time may also decrease, which may result in a response delay. Sometimes the filter may not be updated and the keys may not be detected, although the key is pressed. The reason of this malfunction is related with the excessive length of the moving-average filter. Speed is an important factor for games and security systems. The size of the moving average filter for self-capacitance and the mutual-capacitance technique is 10 for this study. This is the optimal value for both cards.

Figure 2.28 shows the graphics and the possible outputs for different kinds of moving-average filter sizes. The response delay increases, when the filter size increases.
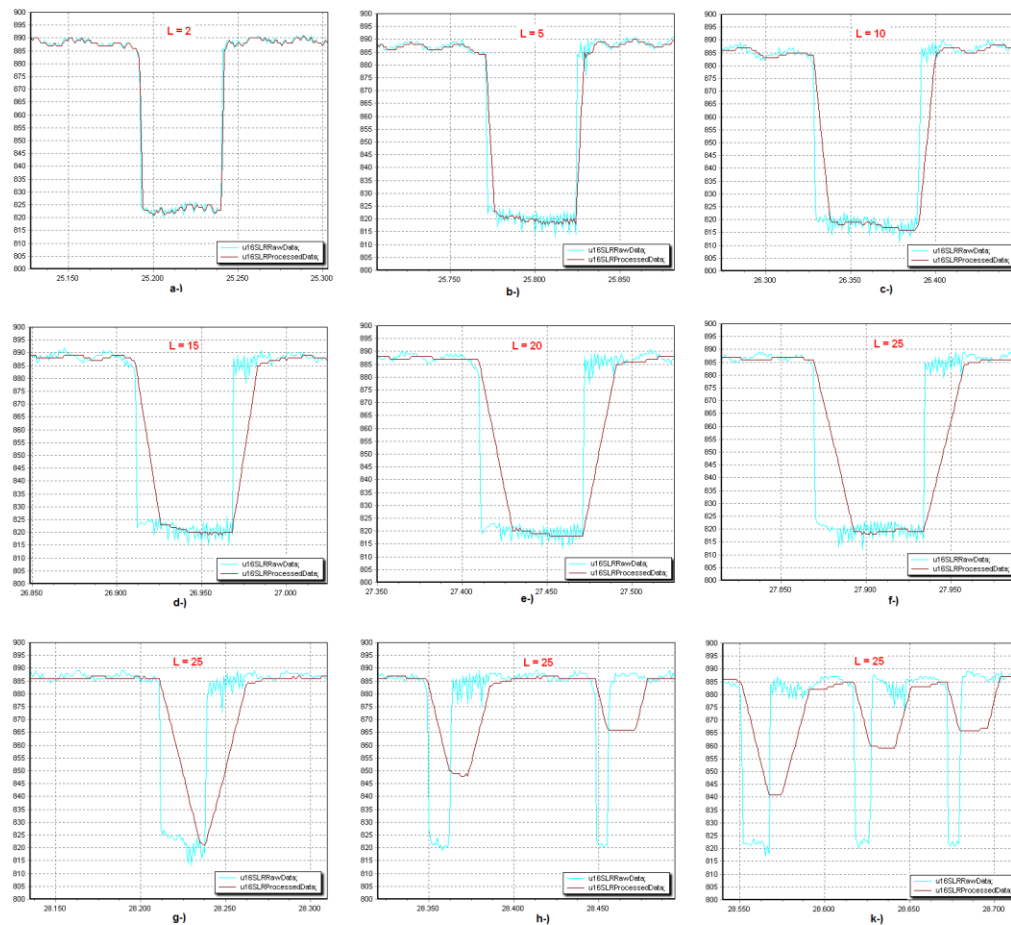
Figure 2.28 The output of moving average filter and the output of raw data with different size of filter. Increasing the filter size increases the response time and the response delay. It may causes some not touched as seen figure (h) and (k).

2.4.4 Frequency Hopping

Frequency hopping systems have been widely used in military communications to prevent hostile jamming, interception and detection. In traditional frequency hopping (FH) systems, hopping frequency selection at the transmitter end is controlled by a pseudo-random code sequence, and the receiver operates accordingly in exact synchronization with the transmitters hopping pattern…. Based on the hopping duration, FH systems can be further divided into two categories: fast hopping (FFH) scheme and slow hopping (SFH) scheme. In an FFH system, the carrier frequency will change or hop several times during the transmission of one symbol, while in an

SFH system, several symbols are transmitted during each hop (Ling, Q., Li, T., & Ding, Z., 2007, p. 5496).

Capacitive sensing devices that have to be operated under harsh environmental condition have to be feature a reliable and robust design. This doesn't mean that a resistant, non-invasive principle, but also robustness in terms of EMC performance. Although there are lots of approaches to improve EMC performance, only one of these is used in this thesis. The capacitive sensor can use more than one carrier frequency that means frequency hopping approach. It is also called frequency hopping spread spectrum.

Frequency hopping can guarantee safe operation of capacitive sensors by reducing any EMC problem. Normally, the capacitive sensors are driven at a constant carrier frequency f_{c1} for measurement. As long as the evaluation algortihm, actually it is noise detection algorithm, doesn't detect disturbances in the measurement signals, the carrier frequency f_{c1} retain unchanged. If there occurs any interference that is caused by line-powered system, the evaluation algorithm switches to the carrier frequency f_{c2} by changing microcontroller's clock. Generally, switching to another frequency will solve the remaining problem of EMC disturbances (Brasseur, G., 2002, pp. 141-144).

The frequency hopping in capacitive-based proximity sensors is patented by Gerphiede G. and Layton M. under the Patent Corporation Treaty (PCT, 1996).
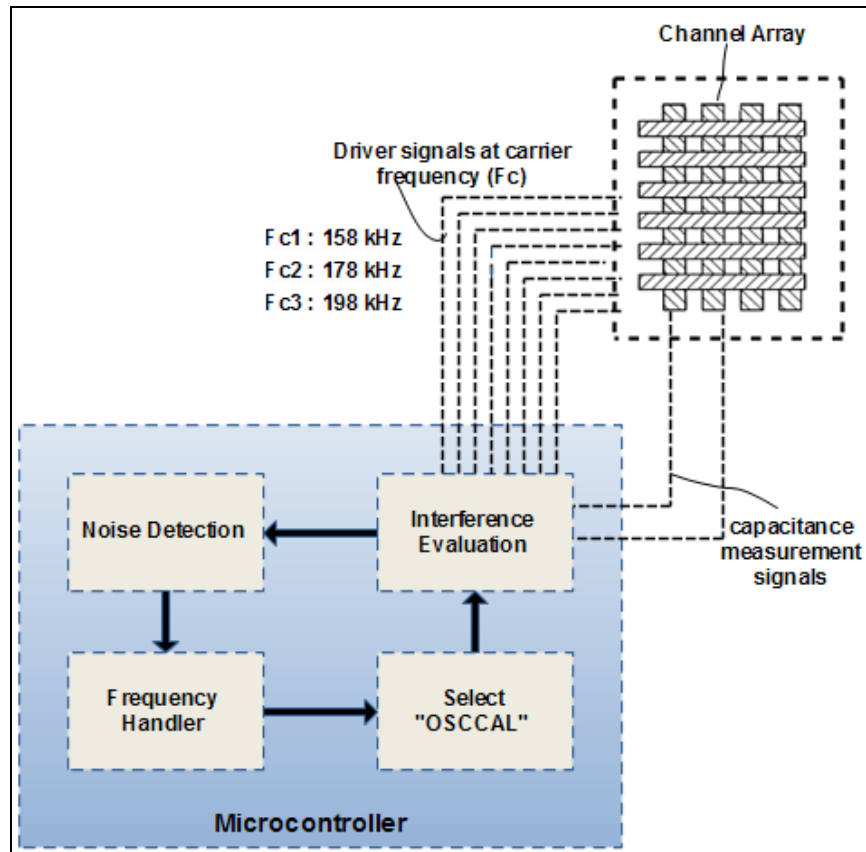
Figure 2.29 Frequency hopping approach based on capacitive sensors with interference rejection.

2.4.4.1 System Internal RC Clock

ATmega329P has an internal RC oscillator. It provides an approximate 8 MHz clock. Although voltage and temperature dependent, this clock can be very accurately calibrated by using OSCCAL register. By changing the OSCCAL register from software, it is possible to change system clock frequency. Internal RC has two range of operation. One of them is lowest frequency range; the other is highest frequency range (AVR, 2008).

As seen from the Figure 2.30, the frequency increases with increasing temperature and operating voltage. These characteristics will vary from device to device. For our project, three different OSCCAL values are determined. All values are built-in flash and are read by the main program and then copied into OSCCAL at run-time.
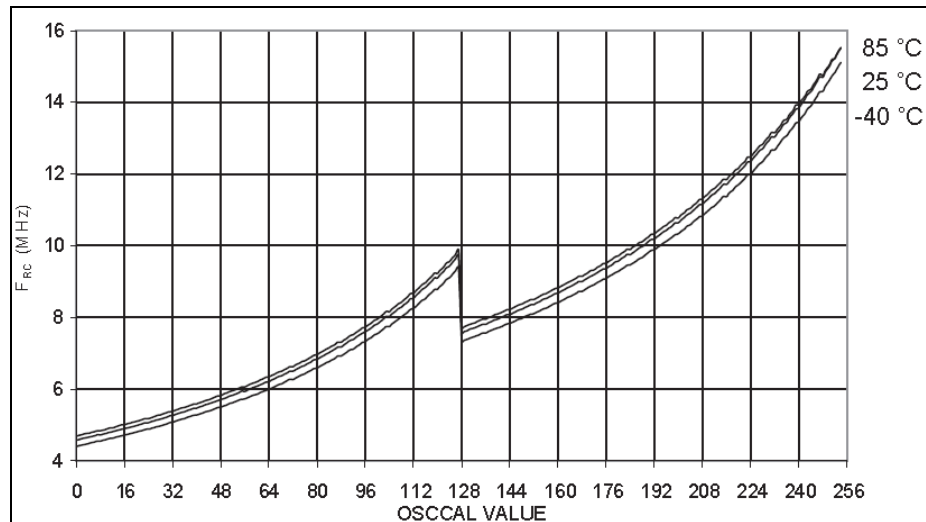
Figure 2.30 ATmega329 calibrated RC oscillator frequency as a function of the OSCCAL value. (AVR, 2008)

Table 2.3 Some frequencies corresponding to the values of OSCCAL in
mutual-capacitive sensing card's MCU

RCclk (MHz)	OSCCAL	RCclk (MHz)	OSCCAL
1	-	9	124 - 179
2	-	10	198
3	-	11	214
4.2	1	12	228
5	38	13	237
6	64	14	246
7	92	15	255
8	110 - 155	16	-

2.4.4.2 Noise Detection Algorithm

Above all, it is quite important to detect when noise coming in order to change the driving frequency of the sensors. If noise comes from the utility grid, this noise is expected to affect all channels. Therefore, all channels are to be examined in order to monitor the noise and the strength of noise. There are different kinds of methods to calculate the level of noise. The most common method is the standart deviation method.

An example of them, according to the study of Georg Brasseur (Brasseur, G., 2003, p. 1263): "…. The algorithm used to detect EMC problems compares the standard deviation of 50 consecutively taken measurement values with the average value of the same data. If a specific ratio $r = \sigma / \mu$ is reached or overtaken the carrier frequency is altered." Furthermore, this method is applied for just one sensor. If there is no interference, standart deviation shall remain within specific values. If there occur any EMC problem, this shall go beyond the limits of standart deviation and the carrier frequency of the sensor is switched.

The signal value of each channel is 2 byte in this design. If 50 values are obtained and recorded for every channel, the number of byt to be required for RAM would be:

16(channels)*2(byte)*50 = 1600 bytes.

The SRAM for ATmage 329P is 2048 byte. If the calculation is performed on this basis, the SRAM of the microcontroller would be insufficient. Another problem is related to the calculation of standart deviation. Standart "math.c" library is to be utilized in order to perform this method on the processor. Again any function within this context is to consume a large amount of byte from the ram and flash of the processor.

The precision of the signals received from the capacitive sensors are monitored constantly. This is a must in order to evaluate the reliability of the system. The noise detection algorithms need to be reliable. These algorithms in the safety critical applications are expected to react quickly to disturbances. Furthermore, the low-end processor is to perform the complex noise detection algorithms in a quick way. Sauter, T., & Nachtnebel, H. (2003) modified the standart deviation formula and new algorithms are developed in capacitive sensor applications for standart procedures. Furthermore, Kero, N., Nachtnebel, H., Pommer, H., & Sauter, T. (2002) introduced a combined frequency selection method in order to ensure that the sensors work on a noiseless frequency band. The SNR and the standart deviation is used again for this

method.   The aim in this study is to ensure that the selected frequency is an undisturbed frequency, rather than decreasing the cost.

   In this study, a new detection of interfering algorithm has been developed because of resources of the processor such as flash, ram and speed. The cards designed in the thesis, have lots of capacitive channels. The standart deviation algorithms, above mentioned, consume lots of resources of processor and power. If these proposed algorithms are applied to all channels, it may be disaster. Therefore, new efficient detection of interfering algorithm has been developed and used. It has small code size and is very efficient when used too many capacitive channels.

   This algorithm includes two different kinds of calculations. The first calculation (see equation 2-22) get the current measurement values of all channels and compares them with the previous measurements in order to detect noise strength. In this method, the calculations are not performed by obtaining 50 consecutive different results, but instead measurement values are received from 16 channels in order to detect the correlation of the channels towards noise. This is similar to the FIR type moving-average filter. However, there are consecutive values for FIR filters. Another advantage of this filter is that every channel records only the previous measurement value in the memory part. So SRAM does not consume so many bytes.

$$x[n] = \frac{1}{CH} \sum_{k=0}^{CH-1} \left| \Delta k[n-1] - \Delta k[n] \right| \tag{2-22}$$

   Where:

   $x[n]$ is the average channel noise strength

   $\Delta k[n]$ is the channel delta at time 'n'

   $\Delta k[n-1]$ is the channel's previous delta

   $\left| \Delta k[n-1] - \Delta k[n] \right|$ is the delta at k channel

   k is a channel counter variable

   CH is the number of channel

The channel noise strenght value received for all channels is to be processed by means of the IIR filter together with previous noise strenght value (equation 2-23). The result being obtained from the IIR filter is the noise ratio. This limit is not to exceed specific tolerance values under certain circumstances. This is the method described in the study of Georg Brasseur (Brasseur, G., 2003, p. 1263). The noise detection algorithm is displayed in Figure 2.31. The software code of this algorithm is shown in Figure 2.32.

$$y[n] = y[n-1] + \frac{x[n] - y[n-1]}{L} \qquad (2\text{-}23)$$

Where:

$y[n]$ is the noise ratio

$y[n-1]$ is the previous noise ratio
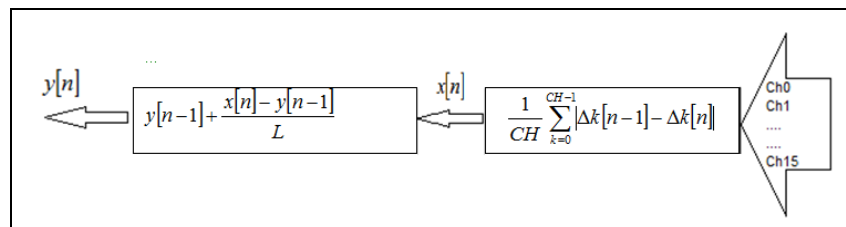
L is noise strength size

Figure 2.31 The flow chart of noise detection

```
/*------------------------------------------------------------------------------
 * Func. Name : appTouch_NoiseDetection
 * Description : try to detect noise.
 * Inputs      : None
 * Outputs     : pass to next frequency or still wait current frequency.
 * Return      : Correlation coffecient
 * Author      : Ferhat AKKOÇ
 * Date        : 04.12.2010
 ------------------------------------------------------------------------------*/
static U8 appTouch_NoiseDetection(void)
{
    S16 sensor_delta;
    U16 u16SumDeltaDiff=0;

    for(U8 i = 0u; i < QT_NUM_CHANNELS; i++ )
    {
        sensor_delta = (qt_measure_data.channel_references[i] - qt_measure_data.channel_signals[i]);
        u16SumDeltaDiff  += labs (g_stFrekans[enFreq].Channel[i].s16PreviousDelta - sensor_delta);
        g_stFrekans[enFreq].Channel[i].s16PreviousDelta =(S16)sensor_delta;
    }
    g_stFrekans[enFreq].u8Correlation = (((g_stFrekans[enFreq].u8Correlation) * 3) + (u16SumDeltaDiff / QT_NUM_CHANNELS)) >>2u;  /

    return (g_stFrekans[enFreq].u8Correlation);
}
```

Figure 2.32 Detection of interfering function

Figure 2.33 illustrates the signals received from 8 channels which exist on the Y line. This figure shows the data related to the sensors included herein my work. The noise being injected differs between 150 kHz and 80 Mhz. The sensors are scanned at 158 kHz. When the carrier frequency or its harmonics overlaps the noise frequenc, it will result in resonance. Consequently, the sensors are to receive noisy signals.
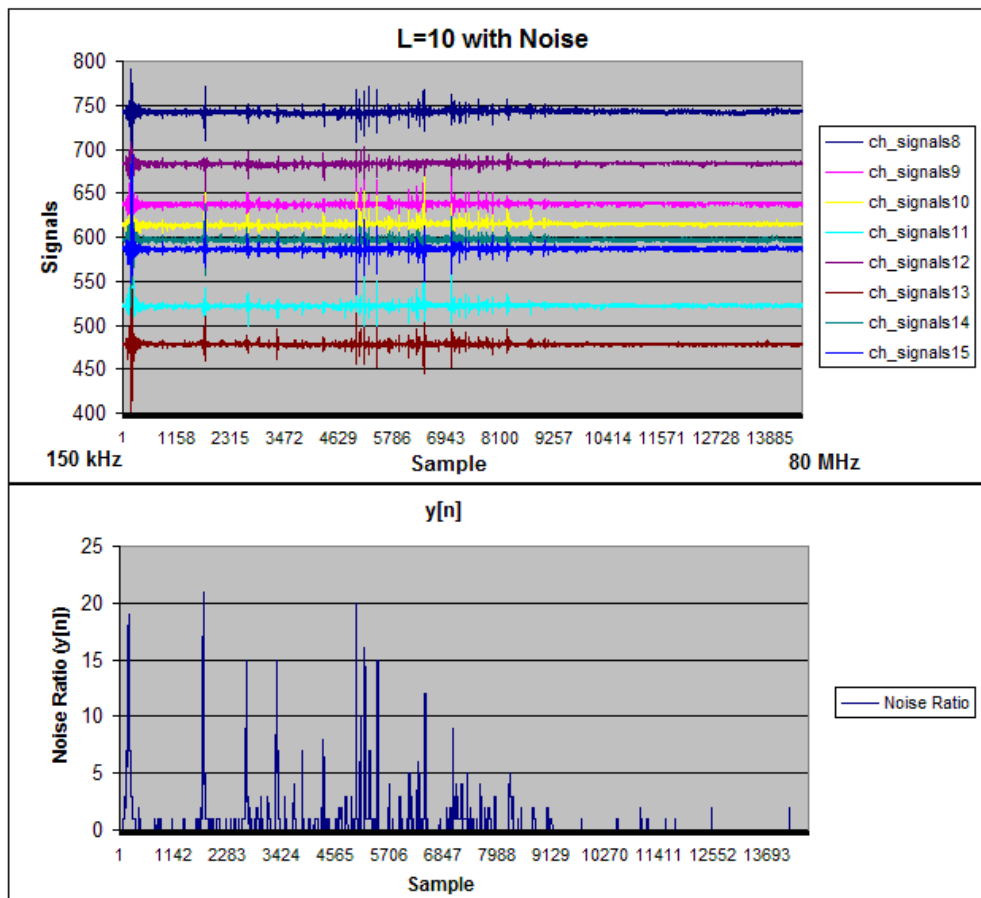
Figure 2.33 The output of noise detection algorithm with noisy signals. In this algorithm, L=10 means moving average filter size is 10.

2.4.4.3 Operation Frequency

The microcontroller do not operate under constant frequency due to the frequency hopping process, because there is no option being able to alter the carrier frequency of the sensors in QTouch Library at the run time. This library is designed to operate just with a single frequency and it holds the signal value. If the frequency hopping process is performed, the reference values and the signal values shall be hold separately for every carrier frequency. Moreover, as indicated above, most of the features being backed up by the library need to be supported separately for every frequency.

As the carrier frequency did not change in run-time, another method was applied in order to change the carrier frequency, which is changing the frequency of the processor. If the processor frequency of the area where the library runs changes, the library frequency shall also change automatically. Therefore, an internal RC oscillator was used instead of a stable crystal oscillator. As a result, the frequency of the processor could be changed spontaneously during the run-time.

There are many peripheral modules in the microcontroller. These peripheral modules are suplied by the clock of the processor. The clocks of these modules will change, when the CPU clock changes. The running frequency of modules such as uart and timer will also change simultaneously. To prevent this, the clock frequencies of the registers within the modules are set simultaneously, when the source clock of CPU is changed. Otherwise, communication will be interrupted or there will be a shift of time, as buadrate changes.

There are 3 different carrier frequencies in this study. The base frequency will be f_{c1}, if there is no EMC problem. Table 2.4 shows the carrier frequencies of the sensors and their respective OSCCAL values and the CPU clock frequency of the MCU. Normally, frequency hopping is realized in a very narrow frequency band range. There is a bandwidth of 20 kHz between every frequency. There is a frequency range of 40 kHz between the highest and the lowest frequency. This helps us to avoid from the disturbance that is based on EMC.

Table 2.4 Carrier frequencies (fc)

Carrier Freq.(f_c)	Fc (kHz)	RCclk (MHz)	OSCCAL
f_{c1}	158	8	155
f_{c2}	178	9	179
f_{c3}	198	10	198

As MCU has a SRAM of 2K, it is not possible to hold the reference values and the signal values for every carrier frequency. This means that the SRAM will be insufficient, for every frequency has additionally its own software filter. The method applied here is described as: The library and the software filters are used commonly for every carrier frequency. Additionally, the library is calibrated one by one for each

carrier frequency at start-up and the reference values of the carrier frequencies are recorded in SRAM. As there are 16 channels and an area of 2 byte for every channel in total, 32 byte in SRAM is used for every carrier frequency.

If there is noise detected from EMC, the microcontroller is to switch to the next frequency and the new OSCCAL value is set to the OSCCAL register. As the system clock of the entire system changes at this moment, the registers of other modules are also set simultaneously according to the new frequency. Moreover, the new reference values in SRAM are registered to the reference values stored in the library. At this moment the reference values and the filters are updated immediately to prevent the change of some values in the library due to this process, which results in a recalibration process. So the library operates on another frequency without interruption and calibration.

Figure 2.34 illustrates the frequency handler flowchart. If the frequency hopping process takes place just at the moment, when it is touched, the frequency shall hop, for the library is not calibrated. This results in finger detection.
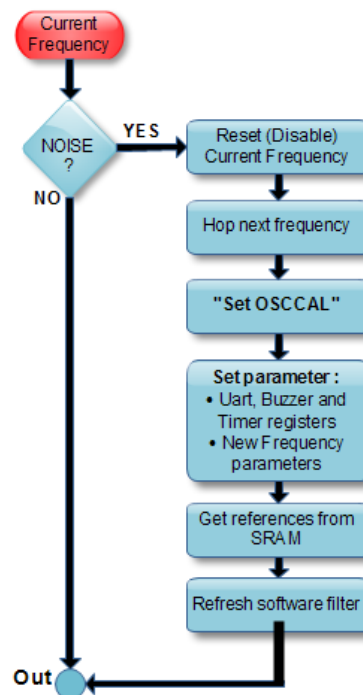

Figure 2.34 Flow chart of frequency handler

2.4.5 Programs & Tools

The software is written in embedded C language. The microcontroller used has 32K FLASH and 2K SRAM, so resource are plentiful. Some simulation programs and tools used are ordered in the following:

- Source Insight (source code editor)
- AVR Studio (V4.18.700) (Integrated Development Enviroment)
- WinAVR (20090313) (GNU GCC compiler for C and C++)
- JTAGICE mkll tool (programmer and debugger)
- Altium Designer Dxp 2004 (shematic and pcb layout)
- EVK2080B Evaluation Board (to get channel data)
- Hawkeye Atmel Software (simulator for channel parameters on computer)
- Edraw Network Diagram (trial version) (to prepare flowchart diagrams)

CHAPTER THREE

THEORY OF SELF CAPACITANCE AND IMPLEMENTATION OF PROPOSED CIRCUIT

3.1 Introduction

There are two ways to measure the changes of capacitance in the projected capacitance touch technology. The previous chapter focuses on the mutual-capacitance method. This chapter clarifies the self-capacitance method. As indicated in the previous chapter, mutual-capacitance is a method used in order to measure the capacitance change between two electrodes on a planar or non-planar layer. On the other hand, the self-capacitance method is used with the aim of measuring the capacitance change of a single electrode by taking ground as a basic element.

The design is created in a way, so that one card of the mutual-capacitive card could be used for the self-capacitive sensing card. The aim of this idea is to ensure that the tests and the test results are more consistent. The charge transfer method is then applied in the same way. The library and the microcontroller (329P) used within this scope are the same, when compared with those used in the mutual capacitive technique. The components and the layout of the card and the location of the components on the card obviously affect the EMC tests and the sensitivity. The method applied in order to obtain a more scientific and comparable result is the same and the hardware design is created by taking the self-capacitive sensing card into consideration.

3.2 Self Capacitance Basics

3.2.1 Self Capacitance Theory

According to Chapter 2, mutual capacitance is described as a kind of capacitance occurring between two conductive electrodes. On the other hand, self-capacitance is described as the kind of capacitance on the same conductive component. Each conductive component has a Q charge and this Q charge creates a static electric field

to outside direction of itself. The V potential occurring as a result of Q is in linear proportion with the Q charge.

$$V = \frac{Q}{C}$$ (3-1)

When equation 3-1 is examined, one can say that self-capacitance can be described as the proportion of the load to the voltage on the same conductor (The ratio of charge to voltage is capacitance C). Any conductive object has its own capacitance and this capacitance depends on the geometry and the dimensions of the relevant object. Although there is no need for a second conductive object, it would be beneficial to use a second object in order to analyses the circuit theory. The second material herein is the ground.

The operation principle of the self-capacitance type sensors is based on measuring the capacitance changes between the ground and the relevant conductive object. The ground here is the finger of a human. Self-capacitance is measured, when there is no finger.
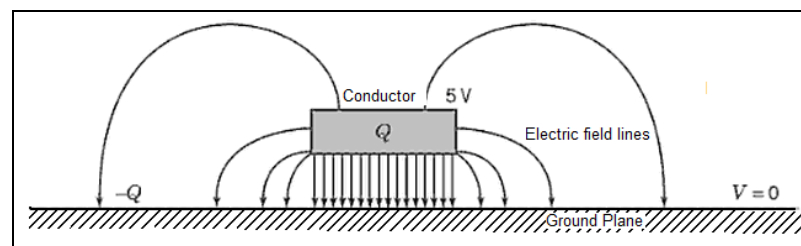
Figure 3.1 The electric field pattern of a circuit trace over a ground plane

Capacitance is a geometric concept. All conductor geometries can store some electric field energy, therefore they all have capacitance. Example of self-capacitance is shown in Figure 3.1 (Morrison, R., 2007, chap. 1).

3.2.2 QTouch Acquisition Method

According to the QTouch theory, a self-capacitive sensor consists of a single electrode. This electrode can be considered as a transmitter electrode. There is no

receiver electrode for these types of sensors. Therefore, base capacitance refers to parasitic capacitance.

The pulses are send by the microcontroller creates a static electric field going out of the sense electrode. So when a finger is getting closer to these sensors, the charge to be diverted from that electrode shall be caught by the finger. Consequently, this charge flows to the ground. The diverted charge is then measured by means of the microcontroller and the system decided whether the sensor is touched or not. This process is illustrated in Figure 3.2.
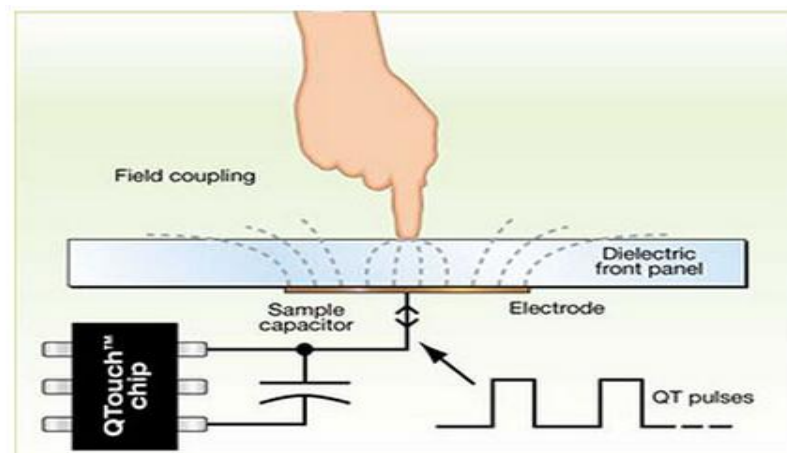
Figure 3.2 QTouch acquisition methods, electric coupling field flow to ground or the electrode itself. (Atmel, 2010)

The charge being coupled to the ground or earth from the relevant sensor electrode is then accumulated on the sampling capacitor. Each pulse collects some charge on the sampling capacitor and this increases the voltage of the involved capacitor. The microcontroller checks the level of voltage on these capacitors after each pulse. This process continues until the Vih level, which refers to the threshold level that can be detected by the microcontroller, is obtained on the sampling capacitors. The threshold level is also called as "logic high" or "logic 1".

When the microcontroller pin connected to the sampling capacitor reaches to the logic high, the pulsing step shall come to an end and it is then recorded how many pulse is sent to the electrode within the relevant period of time (QRG, n.d.).

In contrast to the QMatrix method, the sampling capacitor is not charged and discharged in the QTouch method. Therefore, there is no effect of dual slope. Within this context, QTouch has a simple process when compared with QMatrix. Differently from QMatrix, each sensor has its own sampling capacitor and each sensor is connected to two pins of MCU. So when compared with QMatrix, one can say that the number of pins used under the QTouch theory is more than the QMatrix theory, when the goal is to obtain equal sensors.

See Figure 3.3 in order to examine a self-capacitance sensor and the relevant circuit structure. While "GND" refers to local circuit return, "EARTH" is described as free space return. The Ct and *Cx* capacitances are most significant to this studying.
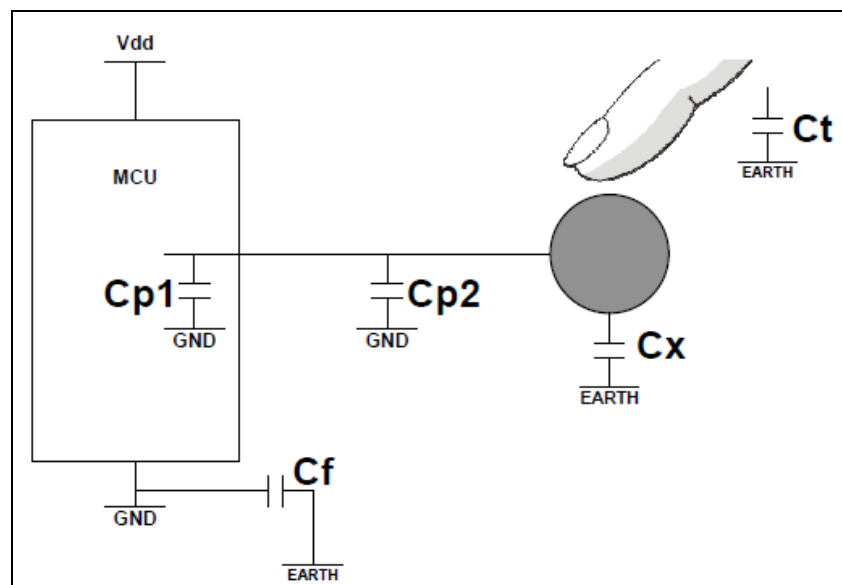
Figure 3.3 Basic self-capacitance equivalent circuit (QRG, n.d.)

*Cp*1 : Parasitic IO pin capacitance to GND

*Cp*2 : Wiring capacitance to GND

Cx : Electrode capacitance to earth

Ct: Touch capacitance to earth (few pF)

Cf : Coupling capacitance between circuit GND and earth (few pF)

For simplification it is assumed;

$$Cx >> Cp1 \, , \ Cp2 \qquad Cf >> Cx \, , \ Ct$$

3.2.3 Sequence of Operation

3.2.3.1 Charge Phase

The sensor circuit of a self-capacitance mechanism is not as complex as the sensor circuit of a mutual capacitance mechanism. As the circuit is simpler, there is no need for a timer-counter or an analogue comparator module. There is also no need a reference point. See the charge transfer circuit in Figure 3.4 and examine table 3.1 for the switching sequences of this method.
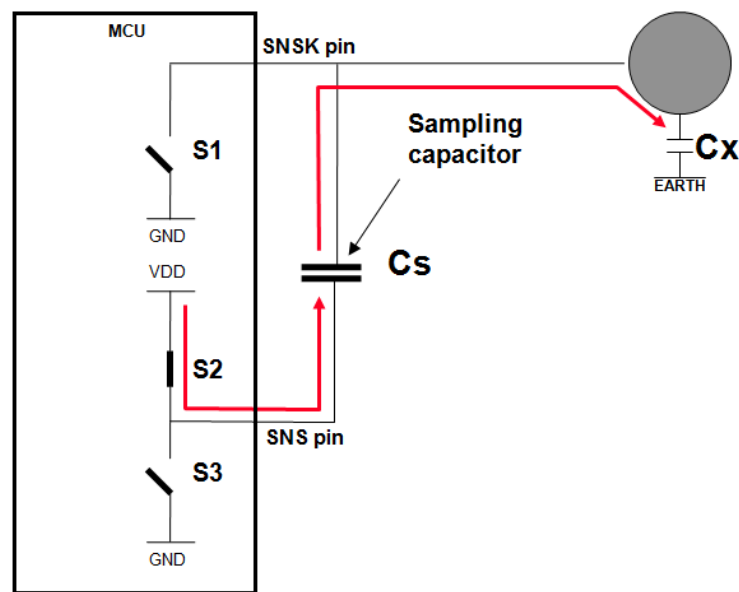
Figure 3.4 Charge transfer circuit. Rising edge on SNS pin drives charge through Cs to Cx (QRG, n.d.)

Cx: Electrode capacitance to earth

Cs: Sampling capacitor

S1, S2 and S3 are CMOS IO pins

SNS pin: charge pin

SNSK pin: discharge and measurement pin (switching between GND, Z and Vdd)

Vih : The logic high or the logic '1' threshold voltage for digital IO.

Cs is much more than Cx according to this illustration. It is accepted that Cs is about 1000 times larger than Cx.

Table 3.1 QTouch burst switching sequence (QRG, n.d.)

	S1	S2	S3	NOTES
1	CLOSED	OPEN	CLOSED	Cx and Cs discharge
#2	OPEN	OPEN	OPEN	Float Cs
#3	OPEN	CLOSED	OPEN	Charge transfer
#4	OPEN	OPEN	OPEN	Float Cs and settling time
#5	CLOSED	OPEN	OPEN	Measure Vcs and discharge Cx

State-1: Provides the initial condition at the start of acquisition (needs time). In this state Cx and Cs capacitors are discharged for reliable measurement.

State-2: It is needed in order to prevent cross-conduction between P and N-channel transistors in SNS and SNSK IO pins. Cross conduction is a disaster for charge conversation in Cs.

State-3: This is charge phase. Each burst pulse is given in this state. The rising edge of the pulse drives charge through Cs into Cx and then both of them are charged.

State-4: As state-2 that allows settling time.

State-5: Cx capacitor is discharged by clamping SNSK to GND, in the event one side of Cs capacitor is open and in this way, it can be measured. Cs charge has increased and the charge is conserved. Up to this state, one loop is completed and the next loop will be start by hopping to the state-2.

These iterations continue until the SNS pin reaches Vih. Burst lengths vary between 100 and 1000 according to the design.

3.2.3.2 Measure Phase

Both the charge phase and the measure phase take place on each loop in the QTouch method. While State-3 is the charge phase, state-5 refers to the measure phase. This loop continues until the SNS pin reaches the logic high.

In the first iteration, the SNS pin in state-3 is driven approximately with Vdd. The charge flows through Cs to Cx. Since both capacitors are on the same serial, the flow is also the same and they store equal amounts of 'charge'. According to Kirchhoff's voltage low (KVL), it is possible to extract the sensor equation for mutual-capacitance, for the voltage refers to zero in the closed circuit loop. Consequently, thecharger transferred byVdd is the same in both capacitor (QRG,n.d.)

The finger coming close to the sensor steals some charge that is normally to flow towards the electrode. Since the finger interrupts to the process between the sensor and the EARTH, Cx capacitance here shall increase. Or as seen in Figure 3.5 of self-capacitance circuit, Ct (finger capacitance) shall form a capacitor in parallel with the Cx. Consequently, the capacitance on the sensor shall refer to Cx//Ct. Figure 3.5 illustrates the modeling process with regard to the finger and the circuit.
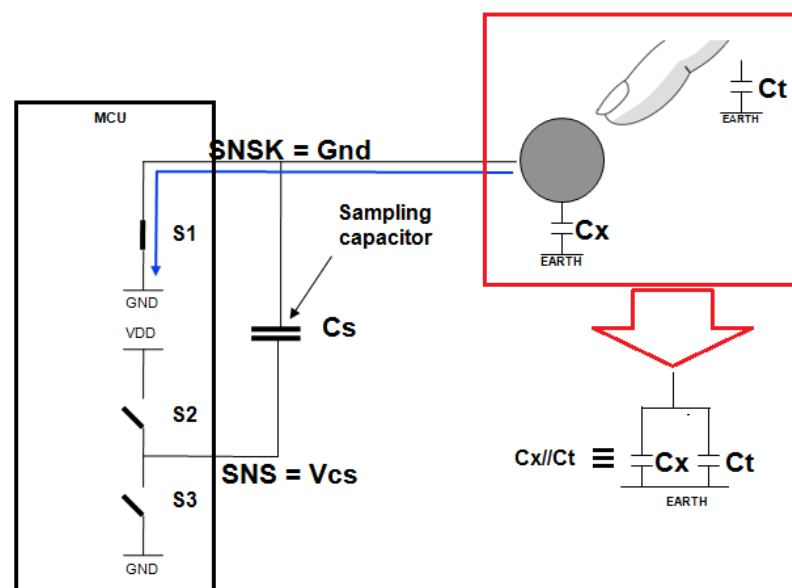

Figure 3.5 Measure phase of self-capacitance sensor (QRG, n.d.)

When the equations written for mutual-capacitance are re-written for self-capacitance:

$$Vcs = \frac{Cx}{Cx + Cs} * Vdd \qquad \text{(No touch at first iteration)} \qquad (3\text{-}2)$$

$$\frac{Cx // Ct}{(Cx // Ct) + Cs} * Vdd \qquad \text{(Touch at first iteration)} \qquad (3\text{-}3)$$

$$\frac{Cx // Ct}{(Cx // Ct) + Cs} * (0.999Vdd) \qquad \text{(At second iteration)} \qquad (3\text{-}4)$$

$$Vcs[n] = \frac{Cx}{Cx + Cs} Vdd + \frac{Cs}{Cx + Cs} Vcs[n-1] \qquad \text{(At } n^{\text{th}} \text{ iteration)} \qquad (3\text{-}5)$$

According to equation 3-2, *Cs* shall store more load for each charge phase. This may result in a faster increase of the voltage level. So the number of pulse required to reach the Vih shall decrease. The *Cs* is now able to be charged with a shorter burst length. The software firmware shall decide whether the button is touched or not by taking the burst length into consideration.

In Figure 3.6, the sampling capacitor is charged with less pulse. The typical voltage waveforms across the sampling capacitor are illustrated in this figure. As one can see from the figure, the Vih level is obtained with less pulse when touch. "Delta" refers to how few the numbers of pulses transferred when one touches the sensor. Delta is proportion with Ct.
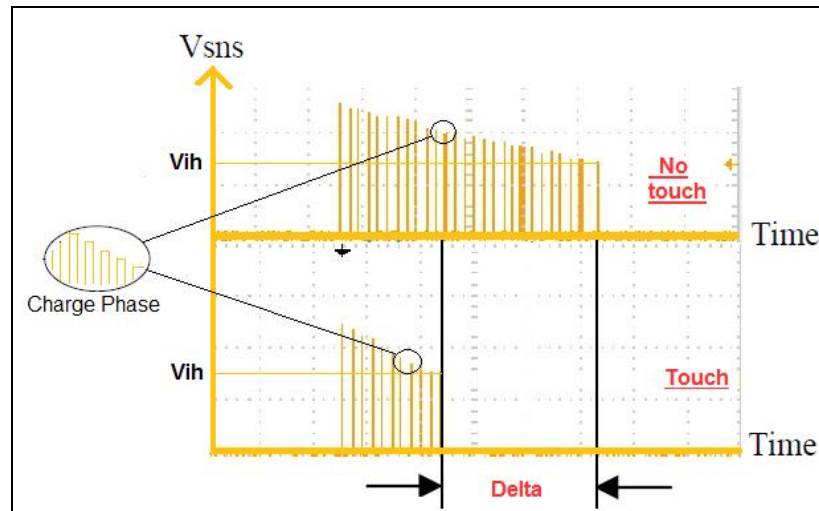
Figure 3.6 Typical voltage waveforms onto measure SNS pin

Figure 3.7 illustrates the voltage waveform of the Cs terminals of the 12th channel on the card designed for the self-capacitance on oscilloscope.
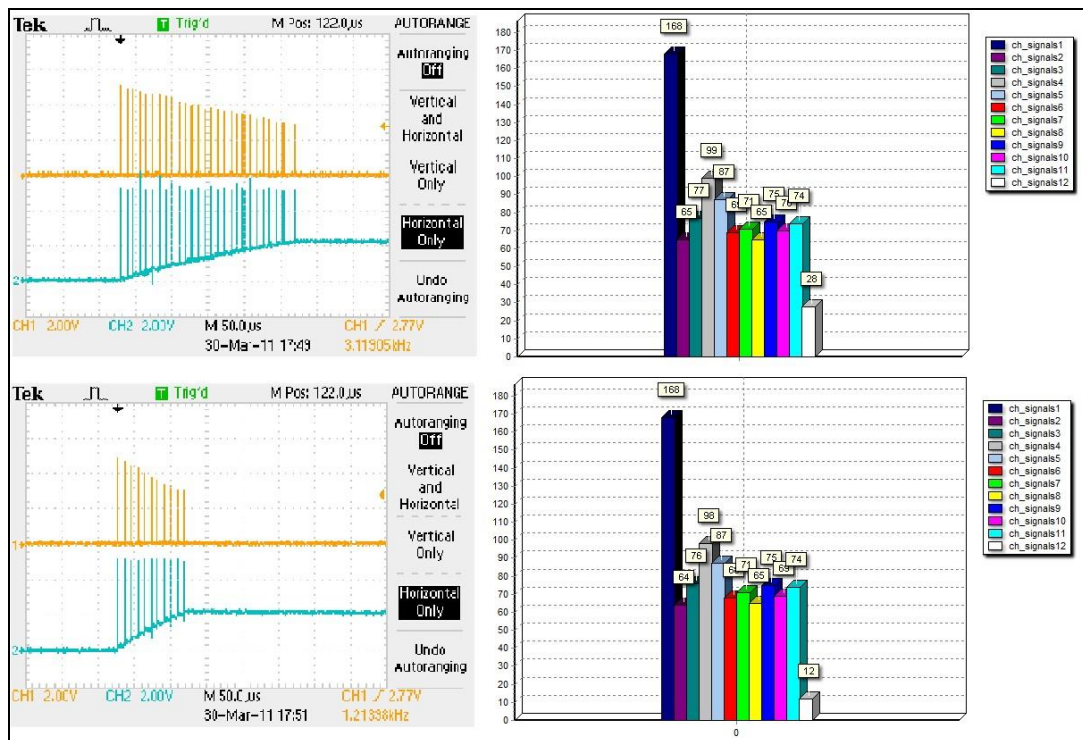

Figure 3.7 Typical voltage waveform across Cs capacitor in charge phase. The data is obtained from the twelfth channel. While touching the sensor, decreasing the number of the pulses, and the capacitor is quickly charged.

3.3 Hardware Design

The self- capacitive sensing card was designed as the same as mutual capacitive sensing card. This card has 11 sensors in total, which consist of 10 buttons and 1 slider. There are white strips and led lights to indicate whether the sensor is touched or not as well as a buzzer. There is no trace or sensor electrode on the upper layer of PCB. There are programming connectors, Max 232 IC, JTAG and ISP connectors for debug. Appendix D illustrates a general view of the self capacitive sensing card.

3.3.1 Sensors

The self-capacitive sensing card consists of independent channels and sensors. There are 11 sensors and 13 channels. The slider sensor includes 3 channels. The remaining 10 channels refer to the other single buttons. The slider sensor in the mutual capacitive sensing card included 6 channels.

Zero-dimensional sensors are for buttons and one-dimensional type sensor is for the slider used. Since all sensors consist of a single electrode, all channels are on single layer.

3.3.1.1 Sensor Circuit

Figure 3.8 illustrates the circuit structure of the slider sensors. The sensor type is much more different than the sensor shape on the PCB. This is just an illustration. Furthermore, the resistor and capacitor values are indicated for each sensor.
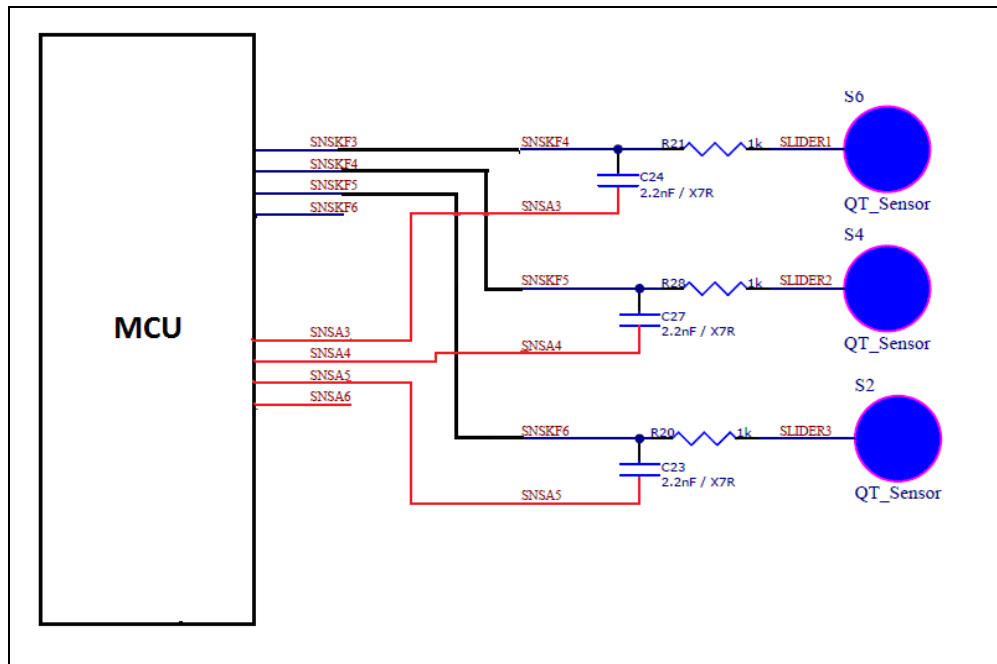
Figure 3.8 The slider sensor circuit in self-capacitive sensing card

3.3.1.2 Touch Button

The self-capacitance zero dimensional sensors have simple structures and they are copper area to be formed on a single layer. As it is simpler, the electrodes on this card have a square shape. There is no much limitation with regard to the dimensions of the electrodes. The only limitation is related to the shortest edge, which shall be equal to a value 4 times larger than the front panel. This design does not include a front panel like a glass. Only PCB is used as a front panel. The thickness of PCB is 1.6 mm. Another issue is related with the dimensions of the sensor to be drawn. It is expected that the dimensions of this sensor suit the dimensions of a human finger. Figure 3.9 illustrates the electrode structure and the dimensions used for the single sensors in this diagram.
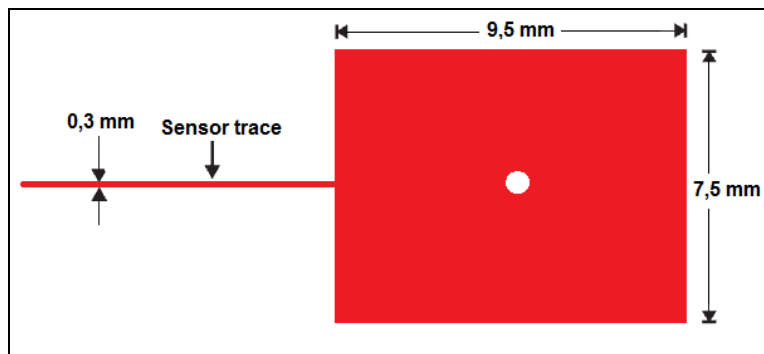
Figure 3.9 Self-capacitance electrode shape for a button

These sensors are not designed together with the ground lines having an interdigitating structure as in the sensors of mutual capacitance. In this case *Cx* shall increase and the gain of the sensor shall decrease. This results in low SNR. The sensor electrodes shall be as simple as possible and as far from ground lines as possible.

3.3.1.3 Slider

We described in the previous chapter that there are two different design methods in order to constitute one-dimensional slider sensors. The "Spatially Interpolated" method is used for this observation. The reason of this is that the slider is not too long. The slider consists of 3 channels.

Figure 3.10 illustrates the slider and electrode structure designed for this card. As you see in the figure, there are 4 pieces. However, the electrodes on the left and right side are half and they two represent a single electrode (or a single channel) as a whole. Normally, it would be possible to obtain a slider sensor by placing 3 square sensors side by side, but the length of the slider here is 60 mm. And the length of the sensors used for the buttons are 9.5 mm. If a medium sized slider sensor is to be obtained through 3 channels, "Spatially Interpolated" would be the best method. This method refers to the "two plus two half" method. Toothed electrodes are used instead of square electrodes. So when the finger moves, the resolution of the finger is expected to be equal anywhere on the slider.
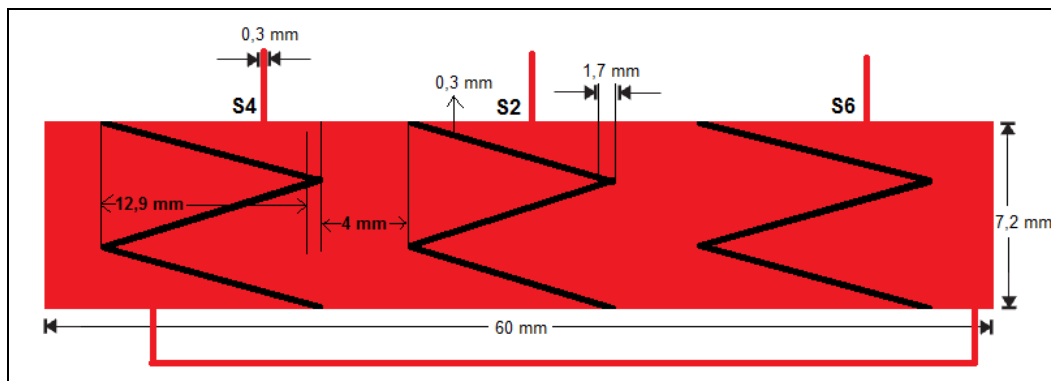
Figure 3.10 One-layer medium self-capacitive slider (Spatially Interpolated). This method is known as "two plus two half", with the highest channel split in half.

3.3.2 PCB Design Consideration

Any point requiring great deference in the mutual capacitive PCB design does also require deference in the self-capacitive PCB design. Additionally, some other points are to be underlined within this context.

The electrode shapes drawn for the sensors shall be smooth and simple. Complex or exotic drawings lead to an increase of parasitic capacitance and this result in a decrease of SNR. Shapes like interdigitating shall not be used. Each side of the drawn electrode shall be of at least 4-5 times larger thickness when compares with the PCB. FR4 type PCB is also used for this card and the thickness is 1.6 mm.

Parasitic capacitance is important again for this method. Therefore, one needs to pay great deference to the distribution of ground loading and the capacitive loads on the card. The design itself, the shapes of the electrodes and the traces shall be able to decrease the level of parasitic capacitance. When Cx increases, SNR decreases. Therefore, one is expected to ensure that high frequency signals and ground loadings are far from the electrodes and the traces. The ground loadings on the card shall be stable. To this end, it will be beneficial, if the ground loadings are connected to the Vss pin on the processor. This is a kind of cleaner soil and it is relatively free from voltage spikes.

These types of sensors are connected to the MCU by means of conductive traces. These traces shall be as short and thin as possible. One is expected to ensure that the longest trace is of 150 mm. The traces on the PCB shall be away from ground loadings and foreign signals, because noise is couple and it leads to an increase with regard to the Cx. When one sensor is slide, the trace of the adjacent sensor shall be directed towards the ground. Therefore, two sensor traces shall be a bit far from each other. The distance between two traces shall refer to at least half or more of the PCB thickness. Furthermore, the RC time constant effect shall be examined during the design phase. The sensor traces on this card is of 0.3 thicknesses due to the PCB manufacturer.

X7R ceramic capacitor is used and the actual value of this capacitor is 4.9 nF. However, this value may change according to the test results. Again 1 k Ω is used as series resistor. 7805 regulator IC is preferred for a better voltage supply. There are buzzers and led for each sensors to warn the user by informing whether the RS232 integrity is touched or not.

Series resistor is important for both mutual type sensors and for the types described herein. The HF emission is going to decrease, especially when the pulse edges are slowed down by this resistor. Another advantage of this resistor is that it limits the flow going towards the pin against the ESD. However, one should always monitor the RC time constant effect, when this type of resistor is used.

Again there is no front panel of glass for this design. PCB serves as a front panel. All circuit components and the sensors are located on a single layer. Most of the sensitivity equations described in the mutual capacitance chapter are also valid for this chapter.

3.3.3 Microcontroller

Self-capacitive sensing card use the same IC as mutual capacitive sensing card. All the features of this IC explained in the previous chapter.

3.4 Software Design

3.4.1 QTouch library

The last version of QTouch Library 4.3 is used for the self capacitive sensing card. This last release prefers "libavr5g1-16qt-k-4rs.a" for ATmega 329P (WEB_2, 2010).

As in QMatrix, there is no excessive constraint in this library in terms of software. The most important part is to determine to which pins the sensors are to be connected. The pin connections shall be determined at beforehand before the schematic diagram of the card is drawn. The "AVR QTouch Studio" program is used in order to detect which sensors are to be connected to the relevant ports and to determine which ports are to be connected to the existing pins. Appendix D illustrates the pin connection and the schematic diagram within this context. Another limitation is on the slider sensor. The slider sensor includes 3 channels at most and these channels are expected to consist of the same ports or the same port pairs under an adjacent order. For instance, some slider combinations are like (0,1,2), (1,2,3), (2,3,4) (Atmel, 2010).

Most of the sensor parameters and functions described in QMatrix are valid for QTouch. The configurations of these libraries depend on the processor series and the acquisition method. Besides the sensor parameters described in the previous chapter, there are two drift mechanisms for QTouch.

   - Differential Drift
   - Common Mode Drift

As explained in the previous chapter, the differential drift method is described as the change of $\pm 1/secs.$ of the reference value according to the measured signals. As the conditions change slowly, the sensors are to calibrate themselves one by one thanks to this mechanism.

Sometimes the ambient conditions may change too fast under the common drift method and these conditions may not be easily tracked when the differential drift is not fast enough. When all channels display positive offset at the end of each acquisition, the reference values of all channels shall decrease by -1. If the channels display a negative offset, the reference values of all channels shall increase by +1. This method is 6 times faster than the differential drift method. This method also copes with the unexpected thermal changes (Atmel, 2010).

3.4.2 Software Process

The software architecture of the self-capacitive sensing card is of the same as the software architecture for mutual capacitive sensing card. The only difference is related to the function of READ_SENSOR (). The previous chapter clarified that this function included functions related to the frequency hopping. Since this design does not include any frequency hopping, these functions are not available.

Figure 3.11 illustrates the function and the flowchart diagram of the READ_SENSOR ( ) on a self-capacitive software on condition that the software architecture remains the same. Furthermore, as seen from this flowchart, the slew-rate limiter, the L-point running average and the oversampling filters remained the same. The software parameters did not change. Same parameters and size of filters are used in order to obtain good and objective results during the developing.
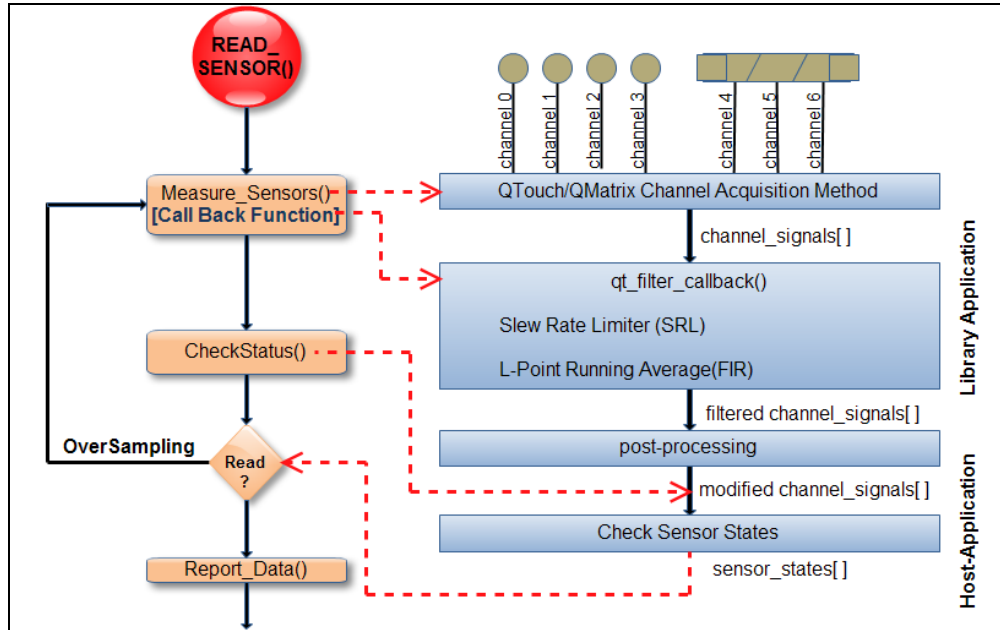
Figure 3.11 Flowchart diagram of the READ_SENSOR () function in the self-capacitive software

3.4.3 Frequency of Operation

An external crystal that is 8 MHz is used as a processor clock without a frequency hopping. The clock source of the processor core (MCU core) is determined by the CKSEL register. Normally, these processors are produced after having selected the Internal RC taking the default clock source as reference. When 1111-0000 is selected for the CKSEL register, the External Crystal/Ceramic Resonator is also selected. Figure 3.12 illustrates the structure of this clock, while table 3.2 explains the CKSEL options for the clock (Atmel, 2009).

Table 3.2 Device clocking options (Atmel, 2009)

Device Clocking Option	CKSEL3..0
External Crystal/Ceramic Resonator	1111-1000
External Low-frequency Crystal	0111-0110
Calibrated Internal RC Oscillator	0110
External Clock	0000
Reserved	0011, 0001, 0101, 0100
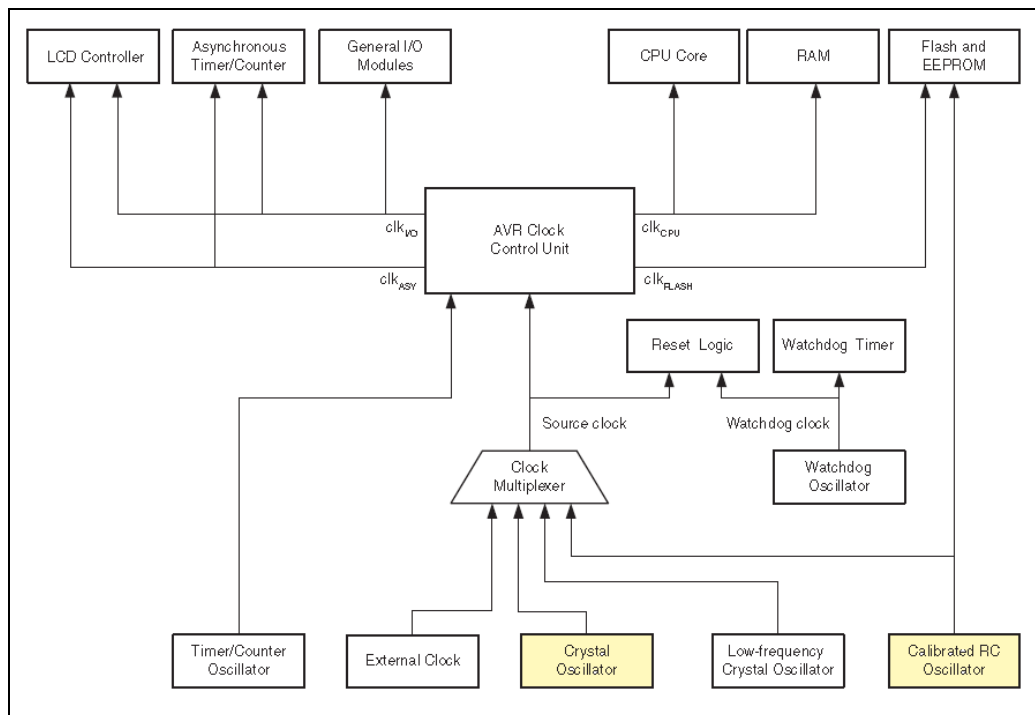
Figure 3.12 Clock distribution (Atmel, 2009)

3.4.4 Programs & Tools

AVR QTouch Studio is used to assign sensor channels in addition to the program and tools that are used during the developing of mutual capacitive card.

CHAPTER FOUR

EXPERIMENTAL RESULTS AND EVALUATION

4.1 Introduction

In this chapter, the basic problems in capacitive sensors and the causes of these problems are examined. Also the basic differences between capacitive and mechanical sensors are explained. The immunity of capacitive sensors, which are designed by two different methods, to the changing environmental conditions and EMC tests are being tested and compared.

Mechanical sensors are realized with a circuit that connected to the microcontroller's port. This port has two states, logic high or logic low. Each port gives user a single bit digital data at each reading. This data is debounced and it is decided if the button is pressed. If the operating environment is too noisy, debounce time is increased and noise is filtered.

Capacitive sensors are a kind of analog sensors. They do not have states like in mechanical buttons. While mechanical buttons are realized by just reading a microcontroller's pin, for capacitive sensors, additional modules in microcontrollers are needed in e.g. timer, ADC, compare etc… Every read value is filtered with different kinds of digital filters and debounce algorithms, and compared with the one read previously. In capacitive sensors, pressing or not pressing a button is a relative subject. If signals that are get changes in a consistent way, there is a touch. Also capacitive sensors drift according to ambient conditions, but in digital buttons there is not such a thing.

The difference between digital and analog results can also be seen in Figure 4.1. The push button is always in one of three states: high, low, or ringing from a recent transition. The capacitive touch sensor does not perform in the same way due to its analog result. Instead, it is able to drift and move. When noise is injected on the

sensor, it affects the quality of the readings, not just the time required to make a state transition (Davison, B., 2010).
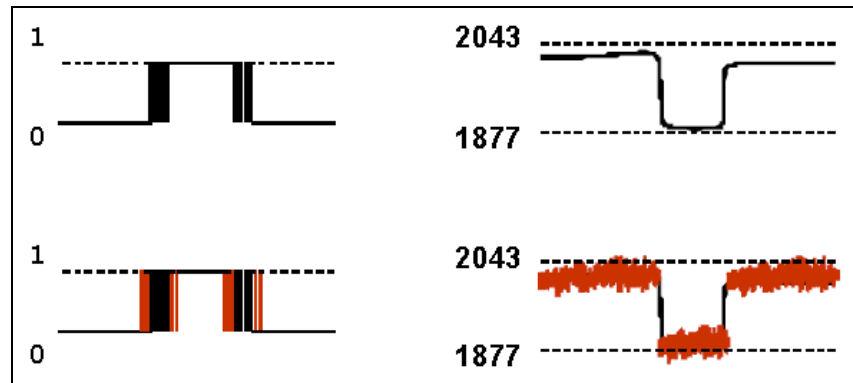

Figure 4.1 Mechanical buttons vs. capacitive touch sensor signal noise behavior

4.2 Temperature and Humidity

In a research about material discrimination using capacitive features of materials, the effects of temperature and humidity to touch sensors are explained like this: The capacitance of the capacitive touch sensor will change proportionally to the dielectric constant of a material because the lines of electric force pass through the inside of the material. Moreover, the capacitance will change with the temperature and the humidity, because the dielectric constant depends on the temperature, and the moisture in the air has the large dielectric constant. Therefore, the sensor always has to maintain the optimum sensing condition of the sensor for discrimination of material properties…. To measure the capacitance value accurately, we used relatively low frequency range because the capacitance value in high frequency was very small (Yuji, J., Yamaguchi, H., & Shida, K., 2004, pp. 2652 - 2655).

First, the effect of ambient temperature to both two cards is examined. When ambient temperature changes, the dielectric constant of materials(ε_r) changes. Depending on the change of ε_r, sensitivity factor ($S = \varepsilon_r / t$) changes. As seen in Figure 4.2, an increase in ambient temperature and humidity increases the dielectric constant of fr4 PCB as well. Therefore, depending on the temperature and humidity, an increase in sensitivity factor and the sensitivity of touch sensors is expected.
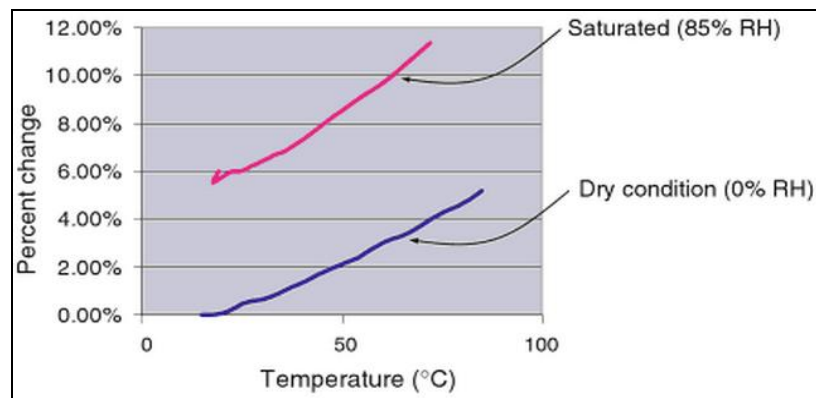
Figure 4.2 Change in FR4 dielectric constant due to temperature and humidity. The dielectric constant increases with temperature and with moisture concentration (Lu, D., & Wong, C. P., 2009, pp. 299-300).

Since the operating interval of microcontroller (Atmega329P) used on the designed cards is -40°C to 105°C, the signals are examined after heating the cards up to 105°C. Figure 4.3 is the measurement results of the sensors of mutual capacitive sensing card due to temperature, and Figure 4.4 is for the sensors of self capacitive sensing card.

Increased ambient temperature increases the dielectric constant of fr4 PCB. So the electric field starts to propagate better in PCB. Now each pulse makes the sampling capacitor charge more. In second graphs of figures, difference of signals that are acquired at -5 °C and +105 °C for each channel and the percentage change of these differences are displayed (See in Figure 4.3).
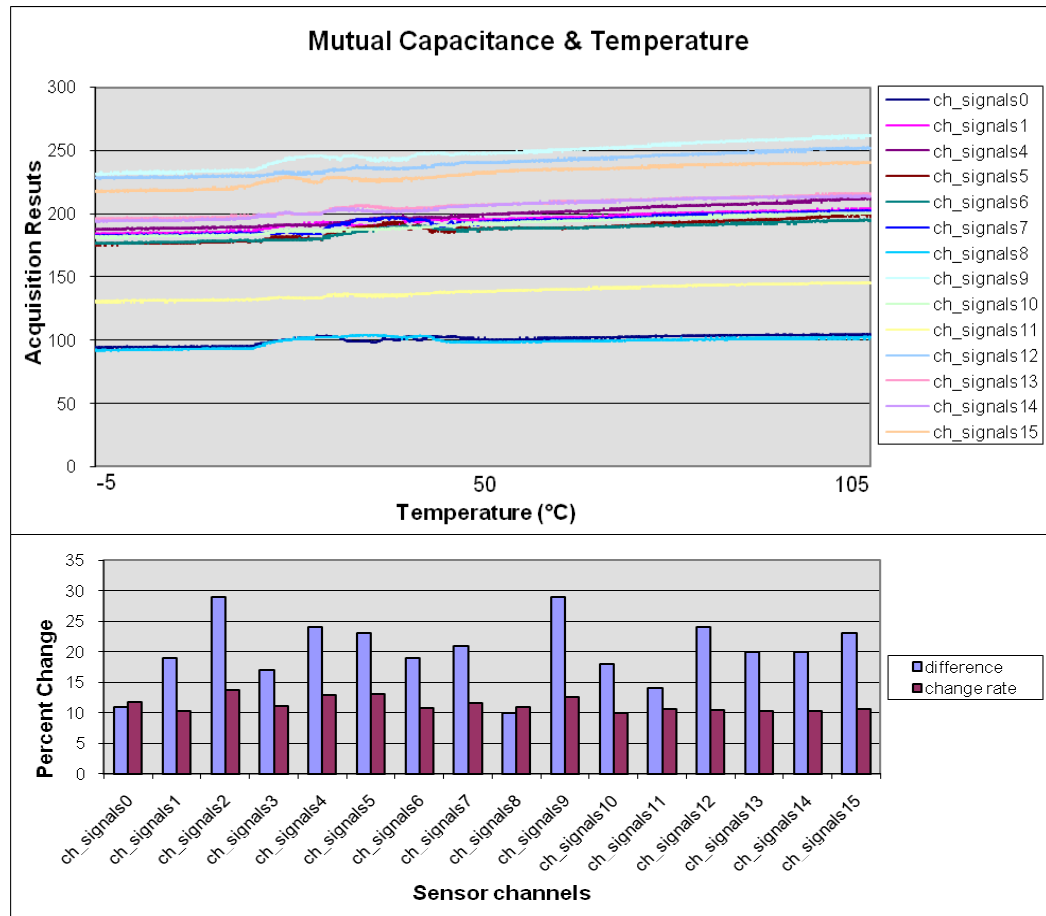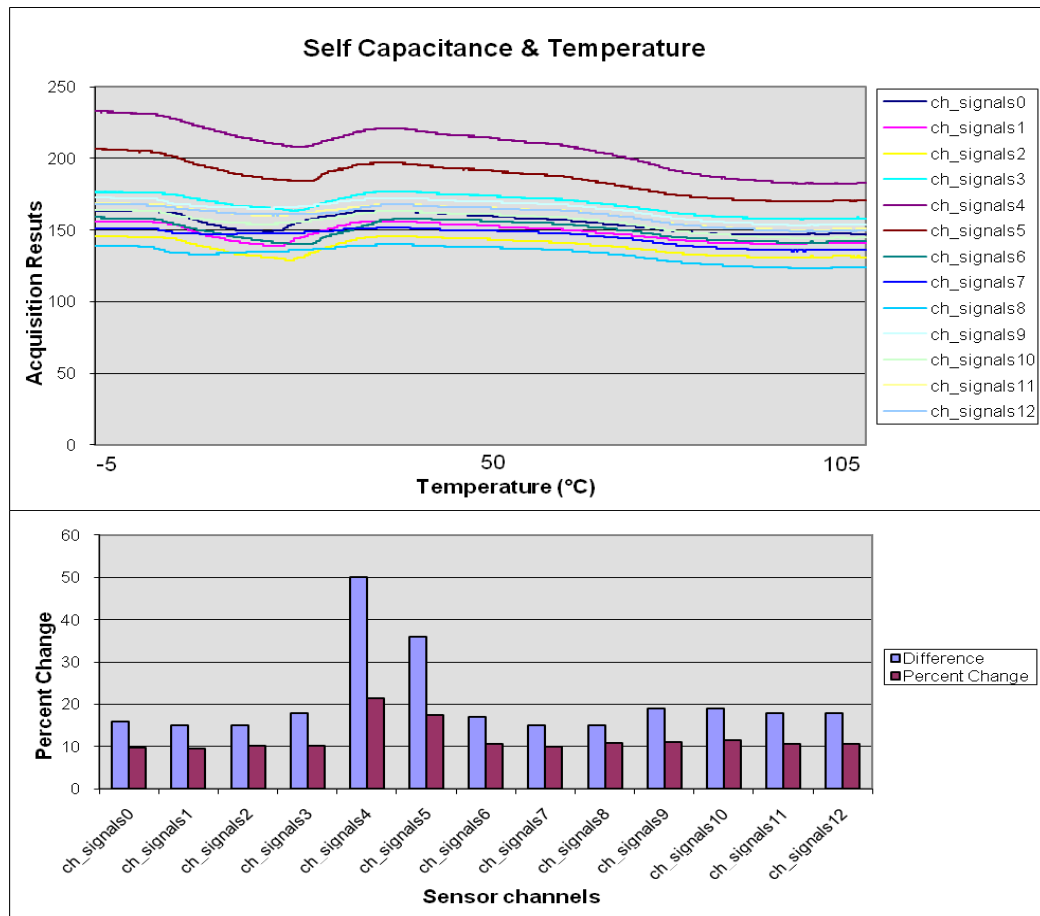
Figure 4.3 Channel signal values in the mutual-capacitive sensing card due to temperature changing from -5 °C to +105 °C. While the ambient temperature increasing, all signal values increase. The burst length in the test is 40 for all channels.

In Figure 4.4, temperature change for self capacitive sensing card is shown. In the upper graphic, the signal values that are acquired while temperature is increasing are displayed. In the below graphic, difference of signals that are acquired at -5 °C and +105 °C and the change of this signals according to signals at -5 °C are displayed. When the temperature increases, dielectric constant increases and so the sampling capacitor reaches to threshold voltage with fewer numbers of pulses.

Figure 4.4 Channel signal values in the self-capacitive sensing card due to temperature changing from -5 °C to +105 °C. While the ambient temperature increasing, the sampling capacitor is quickly charged, therefore, all signal values decrease.

QMatrix method is dual slope conversion. Thus, it is more stable to the changes in temperature. Also change will be less since the measurement of mutual capacitance is done in a small local area. This can also be seen in graphics. In second graphic of Figure 4.3, the change ratio is at most 13. 74 %, while in graphics for self capacitive cards of Figure 4.4, this ratio is at most 21. 45 %. Signal changes do not decrease properly, in graphics for signals in Figure 4.4. It can be concluded that mutual capacitive sensors are more stable to temperature changes than self capacitive sensors.

One of the important problems in capacitive sensors is moisture and water films. As the ambient moisture increases, the dielectric constant of ambient will increase and the signal values read from sensors will change. If this change is just caused by

ambient humidity, it will be compensated with drift algorithms that are available both on two cards. If this change is so fast, drift algorithms cannot detect this and false detection occurs. The only way to overcome this problem is to increase the drift mechanism. Although very fast drift mechanism overcomes this problem, when we bring our finger closer to sensor, sensor that drifts very fast according to our finger will not sense our finger.

Since humidity usually changes slowly, it can be tracked and sensors can change their reference values slowly according to values they read. In this part the water film effect is examined on both buttons and slider for two cards.

The most important effect of water films is causing false detection. Because water contains dissolved ionic molecules and these allow electrical conduction. A conductive water film acts like a finger and transports electric field occurred on sensor by absorbing it. This results in a false detection.

In Figure 4.5, the water film test is seen which is done on the slider of mutual capacitive sensing card. The slider sensor is covered with silicon and water is injected into it. All signal values decrease at every slider channel. Because slider channels are side by side and when a pulse is sent to a channel, other channels are grounded. The electric field that propagates from one channel goes through the ground of other channels over water. So less charge reaches to Y receiving electrode of pulse given channel.
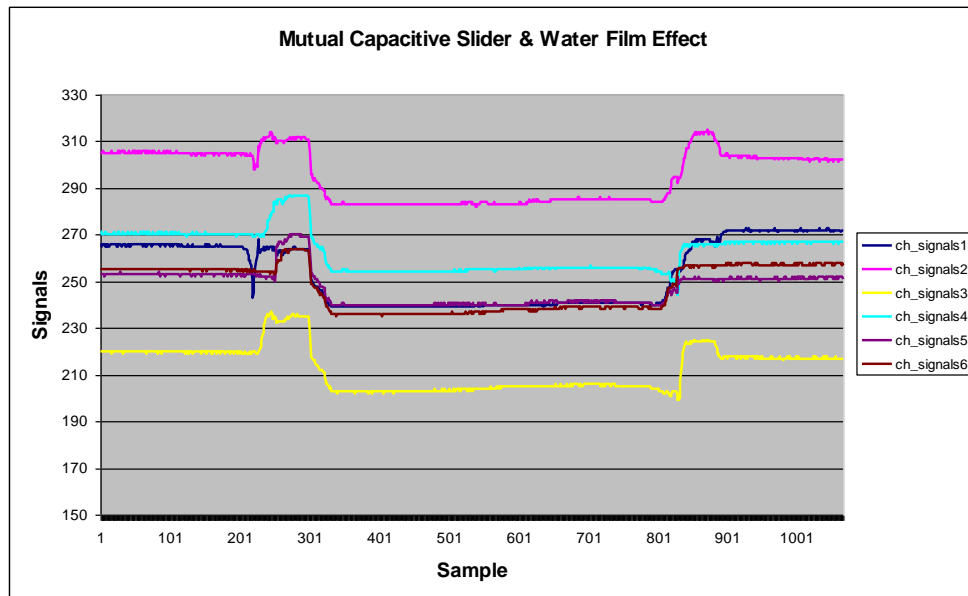
Figure 4.5 Slider channels in the mutual-capacitive sensing card. The moisture spreads far enough on the slider channels. It absorbs and transports the electric field away from a key to GND. This causes false detection.

In Figure 4.6, the effect of water drops that are injected only to the 10th channel is seen. 10 water drops are injected to this channel. Each water drop increases the mutual capacitance between X and Y electrodes and coupled electric field increases. So the acquired signal values increase. This does not cause false detection because human finger decreases the signal levels by absorbing some of the charge. This increases signal level effecting in an opposite direction. This attribute shows that the mutual capacitive sensors have naturally moisture suppression feature. At first 5 water drops, signal level increases but after fifth since water film spreads enough, electric field runs away from sensor to other areas. It is also seen on the graphic that the reference value of sensor drifts by following the signal at certain intervals.

Figure 4.6 Water test on the 10th channel. The water droplets induce only a slight increase in signal coupling. Since touch induces adecrease in signal, the contributions to signal coupling caused by moisture are in the 'wrong' direction and thus do not cause false detections.

Signal value decreases, if water drop is injected between sensor and ground not just onto the sensor (See Figure 4.7). To overcome this type of problem, the sent pulse width needs to be as narrow as possible. Because sent narrow charge pulses will not couple to GND over water. Here water film will act like a natural low pass filter. If pulse width is made too narrow, this time because of the RC constant, sensitivity will decrease. RC constant must be observed at all phase of design. In graphic, the process of negative drift mechanism can also be seen.

Figure 4.7 9th channel in the mutual capacitive sensing card. If the moisture also spreads far enough to couple field away to GND then this pushes the sensor back towards touch.

Self-capacitive sensors are constituted by an open circuit electrode. It senses the change in capacitance of the electrode's coupling back to the micro through any return path. Therefore, any extra coupling path, such a water film or droplet, tend to push the sensor towards touch. The moisture is directly on the key, that also bridges across to any neighboring region that is proximate to GND will potentially cause a false detection. Figure 4.8 shows this situation.
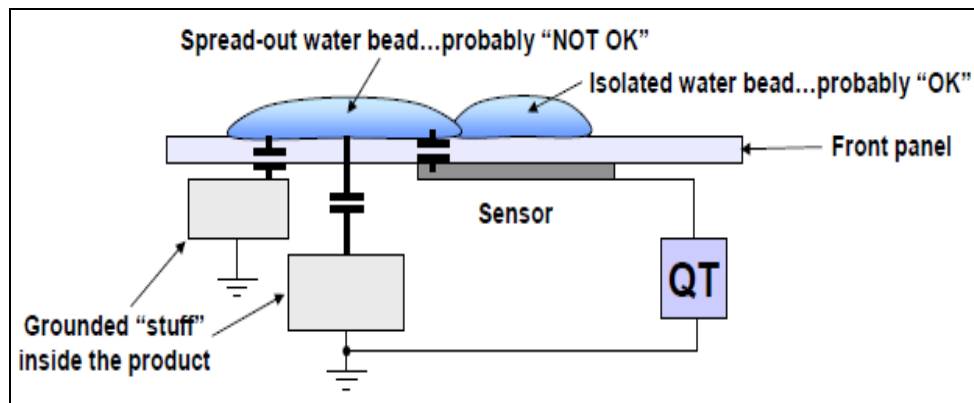

Figure 4.8 Water film directly on the channel or bridges across to any neighboring region that is proximate to GND (QRG, n.d., pp. 41).

In Figure 4.9, the water film test is seen which is done on the slider of the self capacitive sensing card. In this card, slider is composed of three channels. While driving any one of the channels, others are grounded. Since slider channels are side by side, the electric field that propagates from one channel goes through the ground of other channels. That means water increases Cx capacitance between electrode and GND. Thus, as expressed in equation 3-2 and 3-3, sampling capacitor reaches Vih with fewer numbers of pulses. This may result with a false detection.
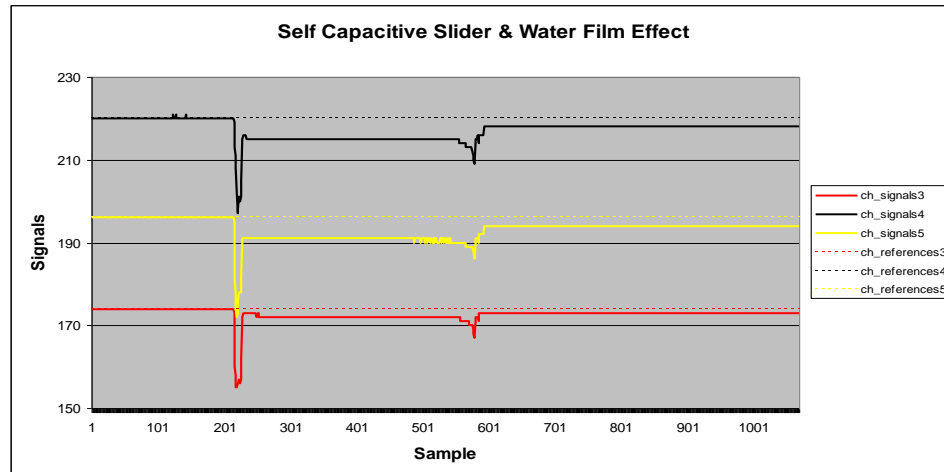
Figure 4.9 Slider channels in the self-capacitive sensing card. The moisture absorbs and transports the electric field away from a key to GND.

In Figure 4.10, the effect of water drops that is injected to 10th channel of self capacitive sensing card is seen. Each water drop increases the capacitance of electrode to the earth. Thus, it causes sampling capacitor to charge with fewer numbers of pulses. Normally, these signals are very stable. As seen in the graphics, every change in signals occurs with injected water drops. These water drops while sometimes reducing the signal levels, sometimes make just an instant change. This graphic is zoomed in.
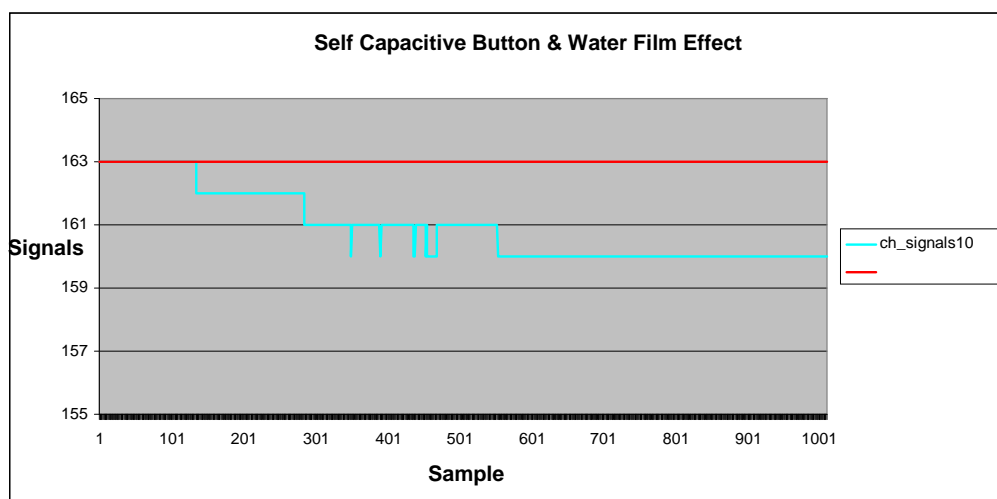
Figure 4.10 Water test on the 10th channel. Here, the moisture is extra capacitance to the earth and increases the electrode capacitance.

This result may be concluded from the water film tests. Mutual capacitive sensors that are composed of single channel, are advantageous than self capacitive sensors. Because water makes adverse effect according to finger by increasing the signal levels on these type of sensors. But generally, self capacitive sensors are more stable to water drops and signal change very little. To show this change, drift mechanism is prohibited during the tests. One reason of the self capacitive sensors to be more stable, that sensors are composed of one electrode and there isn't any ground line around them.

4.3 Touching Performance

In this part, the signals and performance of mutual capacitive and self capacitive sensors are examined with same software parameters. How the signals read from sensors are stable, crosstalk and response time features are compared.

In mutual capacitive sensing card, sensors are composed of 8x2 matrixes. While two sensors exist on each X line, 8 sensors exist on each Y line. Therefore sensors may affect each other when coupling occurs via lines. In self capacitive card, since each sensor has its own sampling capacitor and independent lines, there is no such an effect.

In Figure 4.11, signals of channels that are on same X line (X 7 line) are shown. These sensors are channel-7 that is on Y0 line and channel-15 that is on Y1 line. Although they are far from each other on the card, since they are on the same X line, affect each other.
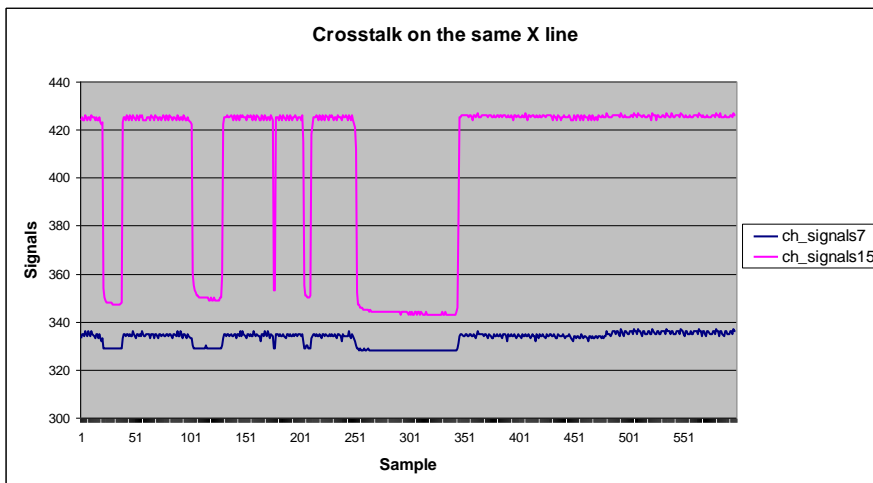
Figure 4.11 Crosstalk effect on two sensors which are on the 7th X transmitting line.

In Figure 4.12, signals that are obtained from 10th channel of both cards are seen. Actually response time is a relative concept. Because if burst length in software of mutual capacitive sensors is increased the response time increases.
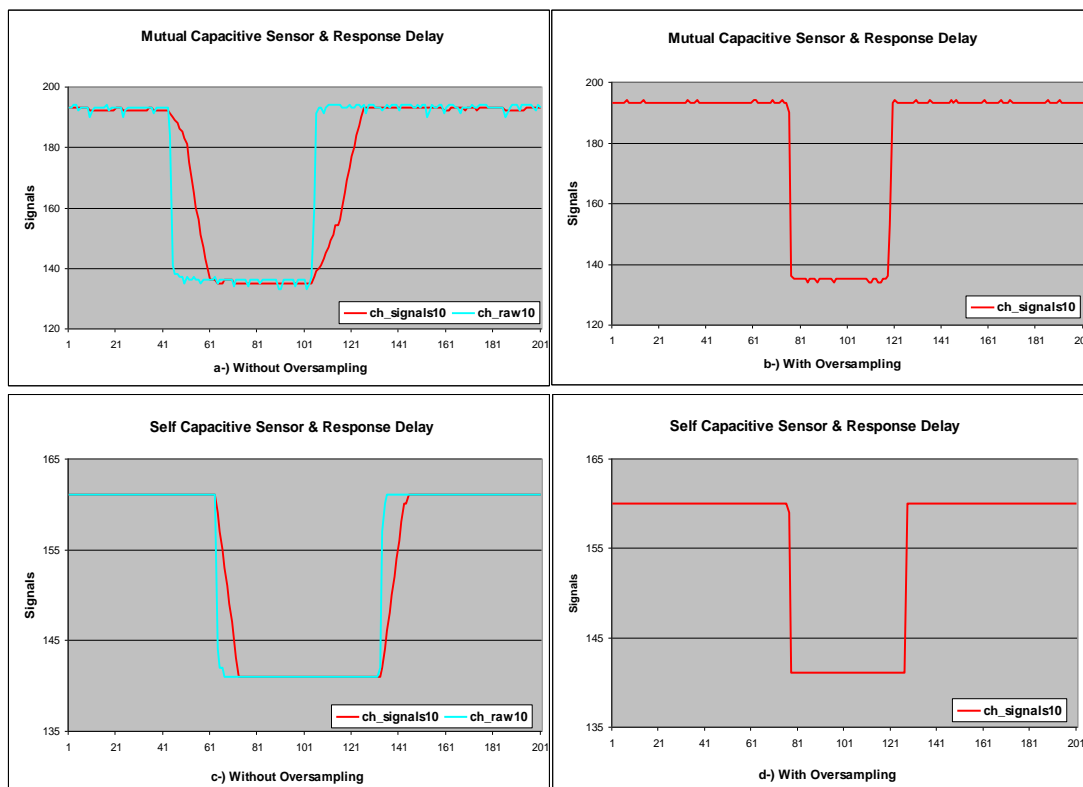
Figure 4.12 Response delay with and without oversampling filters in two types of sensor.

In Figure 4.13 and 4.14, signals of sensors on both cards are seen. Signals of self capacitive sensors are more stable and proper. This is because the sensors are not in matrix, sensor structure is simple and each sensor has its own sampling capacitor.
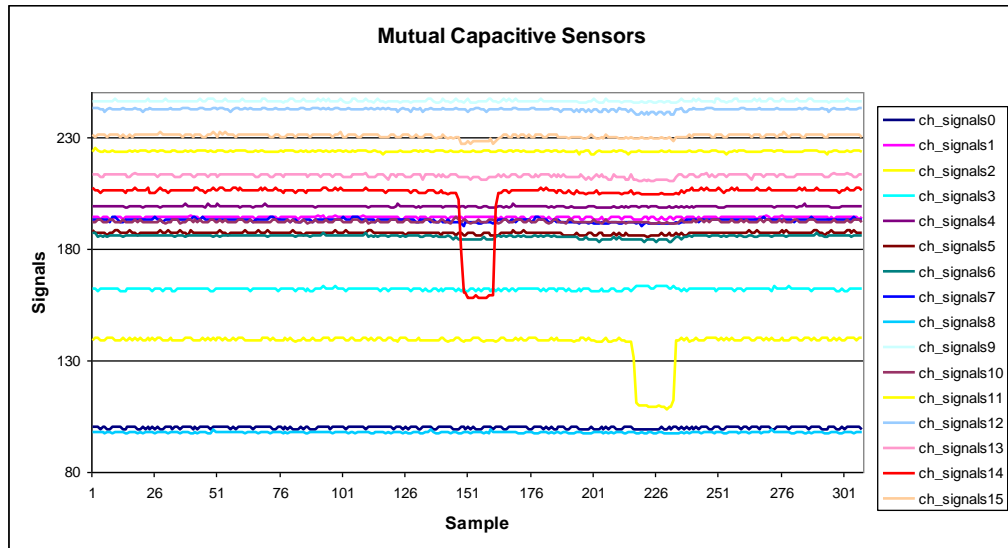
Figure 4.13 Signal of the channels in the mutual capacitive sensor. Noise coupling and crosstalk are seen on all the channels.
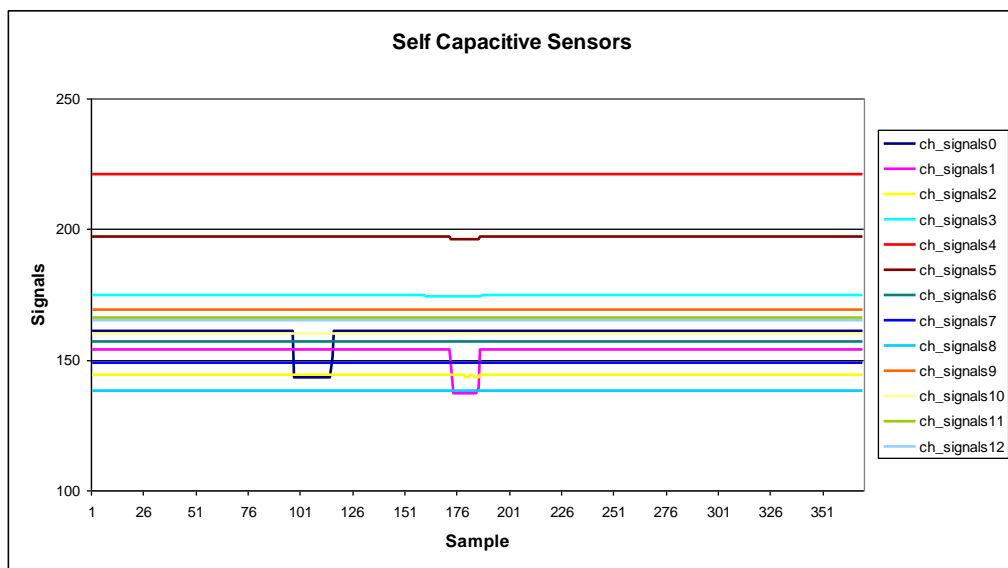
Figure 4.14 Signal of the channels in the self capacitive sensor. These sensors are more stable.

By looking at these graphics, the crosstalk and noise coupling effect is lesser on self capacitive sensor result is obtained. Although response time is a relative

concept, it is an advantage on mutual capacitive sensors for being changed with software parameters on run time.

4.4 Electromagnetic Immunity(EMC)

EMC (electromagnetic compatibility) is the ability of electrical or electronic equipment to operate without creating interference for other equipment in the vicinity, or to operate together with other electrical or electronic apparatus in an interference environment. EMC means that a device is compatible with (i.e., no interference is caused by) its electromagnetic (EM) environment and it does not emit levels of EM energy that cause electromagnetic interference (EMI) in other devices in the vicinity.

EMC has two sectors, immunity and emission. Emission is the ability of electrical or electronic equipment to operate without creating interference. Immunity is the ability of electrical or electronic equipment to operate together with other electrical or electronic apparatus in an interference environment (Döner, H., 2006, pp. 1-6).

In this thesis, how both types of sensors show immunity to electromagnetically noisy environment is considered. EMC problems will always exist since unwanted electromagnetic (EM) energy effects systems. To live with this, international expert organizations prepare the required EMC standards, and specify the radiated and immunity limits. Standards specify the required conditions for a device to perform the expected performance together with other devices. These conditions may be summarized as the maximum unwanted radiated levels and minimum immunity levels. Limit values states which threshold levels on how far to devices are allowed.

EMC tests are done on real operating environment of device and while the device is working. Since the operating condition is defined on a wide interval, test and measurement condition is created of some sense. The Mains is the most trouble interference source. Devices are always connected to mains in homes, offices, streets etc., from the mains to each other. The Mains is the most important EM coupling way that reaches each other the unwanted effects devices created. EM noise that is

created by a laundry machine working in neighbor or a drill working on next apartment may affect all other devices working on the mains.

Immunity tests are divided into two as conducted and radiated immunity. Both injected noise type creates instability on capacitive sensors. Conducted noise occurs on devices more that are powered from the mains. Radiated noise is the noise that propagates form devices working in high frequencies such as mobile phones or high-power communication lines.

There are several reasons that these types of noise are seen on capacitive sensors. First is that the capacitive sensors are analog. When reading a digital sensor, pin of microcontroller is in high or low state. But there is no such a thing in analog sensors. When the ambient conditions change, obtained values change. This problem is dealt with drift algorithms.

Another reason is when user touches sensors; it becomes a part of sensor circuit. Here user acts as ground. This is different from ground which the sensors reference from. At this time sensors have two different ground reference and they may interpret this as an injected noise.

In Figure 4.15, a sensor is on two different frequencies f1 and f2, signal values are obtained respectively (See Figure 4.15 a). Then sensor signals are saved by injecting noise just at f2 frequency (See Figure 4.15 b). As it can be seen, although the signals at f2 frequency are disrupted, signals at f1, which are obtained at the same time, are not. Later, while continuing to inject noise, sensor is touched (See Figure 4.15 c). With the effect of finger, while a proper decrease at noiseless frequency, disruption on noisy frequency increases. This is because, as mentioned above, that system has two different ground references.
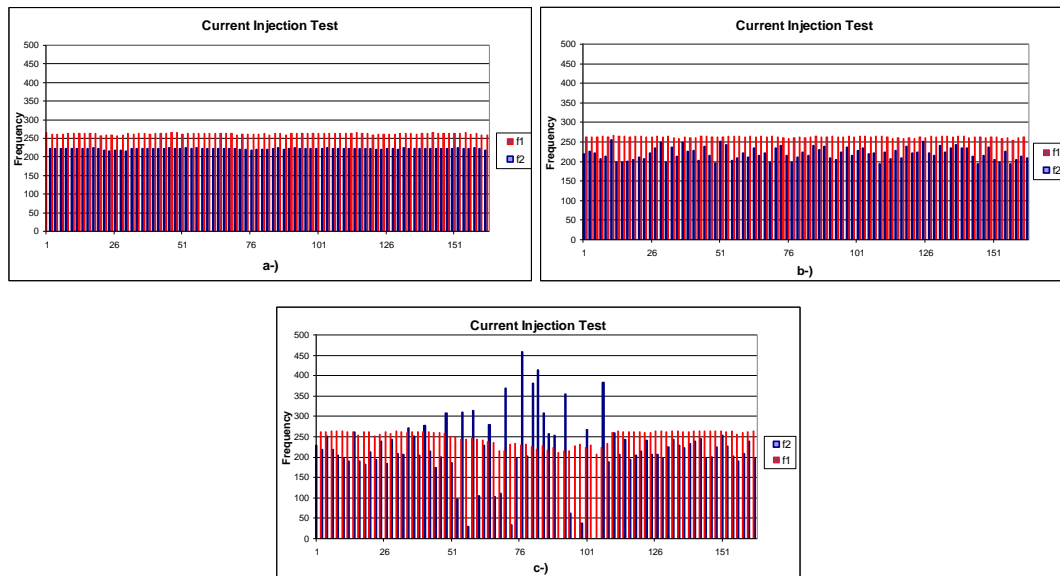
Figure 4.15 Effect of injected noise on a capacitive sensor. **a-)** without the injected noise **b-)** with the injected noise at f2 frequency **c-)** touching on sensor while injecting noise at f2 frequency.

"CE" mark (European Conformity) is looked for on products sold in many places around the world, especially European countries. The products that carry this mark are EMC compatible and comply with the limits stated in standards. EMC standard and limits defined by expert organizations varies from product to product.

No power supply card is designed in this study for designed cards. Some of the EMC tests are in interest of power supply cards. They test the immunity of power supply to noise given to mains and voltage changes on mains. Instead of a power supply, an EMC approved, CE mark carrying 9V adapter is used during the tests.

Since the cards are designed for test purposes, only some of the EMC tests are applied to both these cards. Used test laboratory is certified by international test organizations. With taking into account that the certificates laboratory owes, tests and standards that will be applied to cards are:

- EN 55022: Information tech. equipment. Radio disturbance characteristics;
- EN 55024: Information tech. equipment. Immunity characteristics;
- EN 61000-4-3-2002: Immunity to radio frequency fields;
- EN 61000-4-4-2004: Electrical fast transients / burst immunity tests;

- EN 61000-4-6-2007: Immunity to conducted disturbances, induced by radio frequency fields;

4.4.1 EN 61000-4-3-2002

Most electronic equipment is, in some manner, affected by electromagnetic radiation. This radiation is frequently generated by such sources as the small hand-held transceivers that are used by operating, maintenance and security personnel, fixed station radio and television transmitters, vehicle radio transmitters, and various industrial electromagnetic sources.

This standard is applicable to the immunity of electrical and electronic equipment to radiated electromagnetic energy. It establishes test levels and the required test procedures. The object of this standard is to establish a common reference for evaluating the immunity of electrical and electronic equipment when subjected to radiated, radio-frequency electromagnetic fields (EN 61000-4-3, 2002).

This test is done according to limits that are stated in EN 55024 standard. Because the cards are not owed by a product, and are just for test purposes, they are accepted as information technology equipment (ITE) product.

Some test parameters are;

Polarization of antenna: Horizontal and vertical
Distance of antenna - EuT: 3m
Frequency range: 80 MHz – 1000 MHz (AM)
Field strength: 6 V/m (CE requires 3 V/m)
Modulation: AM, 80 %, 1 kHz
Frequency step: 1 % / 3 sec.
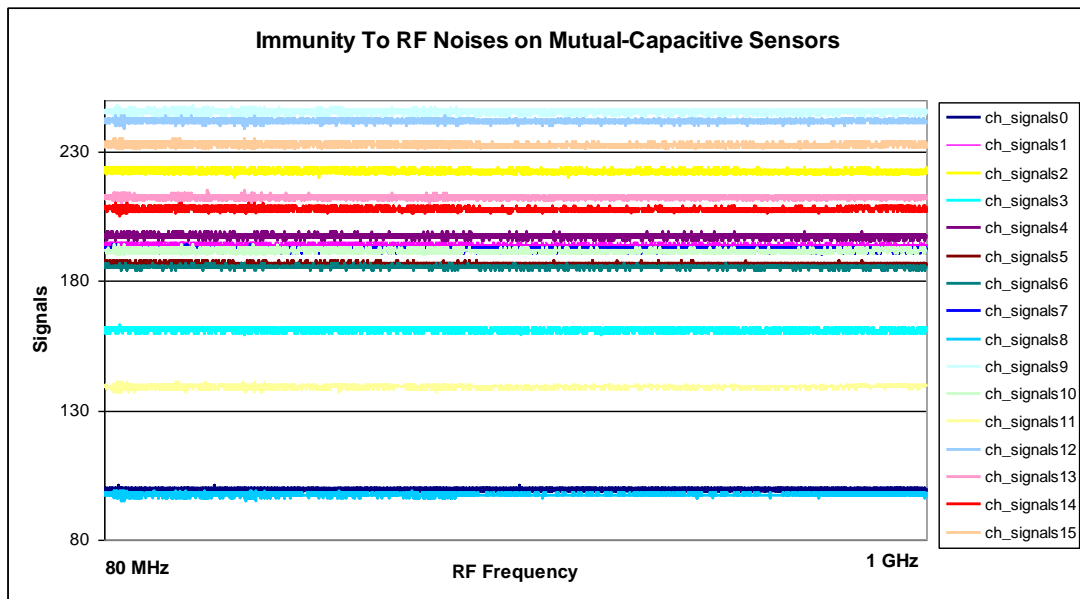
Figure 4.16 Radiated immunity test to radiated, radio-frequency and electromagnetic fields for horizontal polarization of the antenna in semi anechoic chamber
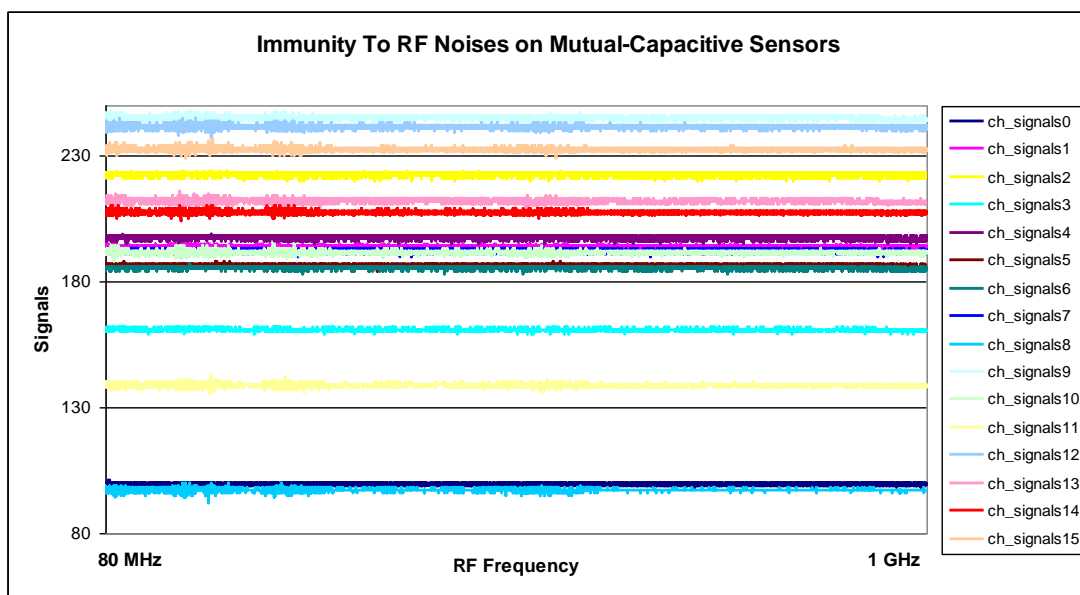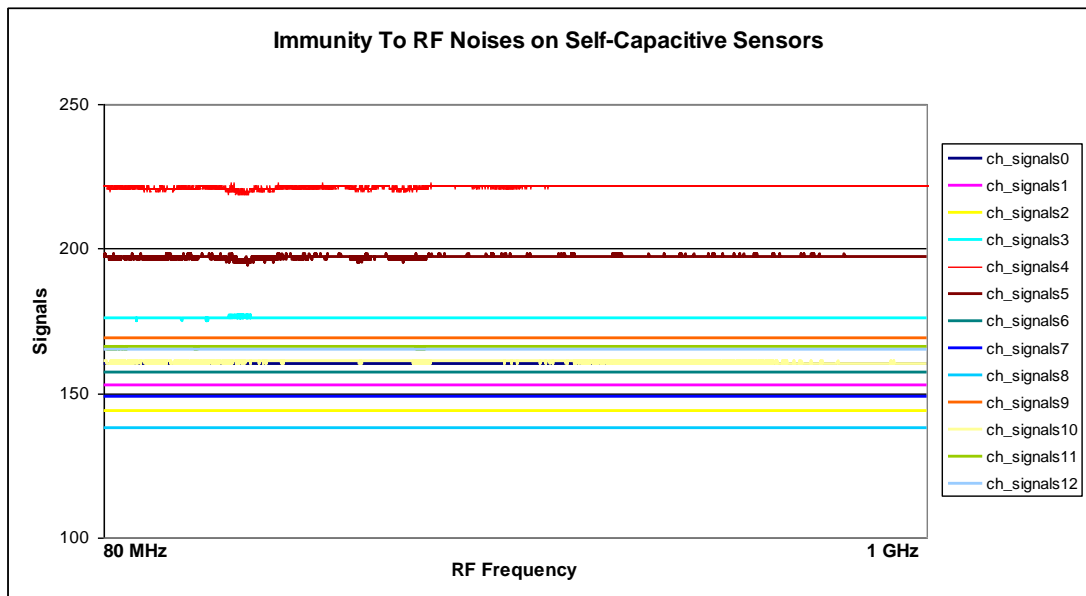

Figure 4.17 Test is repeated for vertical polarization of the antenna in the radiated immunity test
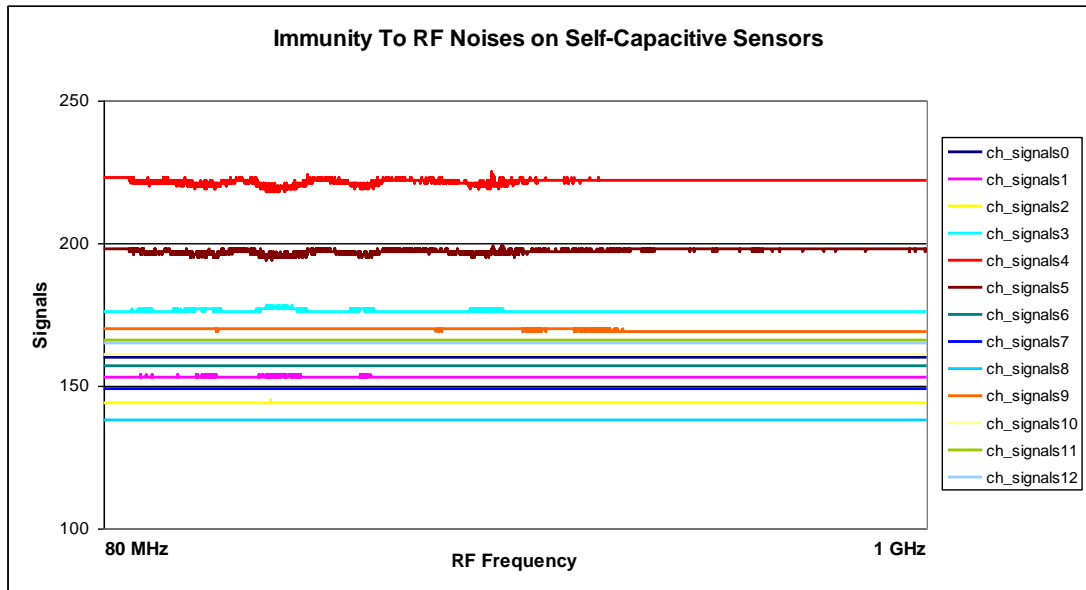
Figure 4.18 Radiated immunity test to radiated, radio-frequency and electromagnetic fields for horizontal polarization of the antenna in semi anechoic chamber

Figure 4.19 Test is repeated for vertical polarization of the antenna in the radiated immunity test

4.4.2 EN 61000-4-4-2004

This standard relates to the immunity of electrical and electronic equipment to repetitive electrical fast transient. It gives immunity requirements and test procedures related to electrical fast transients/bursts.

The repetitive fast transient test is a test with burst consisting of a number of fast transients, coupled into power supply, signal and earth ports of electrical and electronic equipment. Significant for the test are the high amplitude, the short rise time, the high repetition rate and the low energy of the transients (EN 61000-4-4, 2004).

Some test parameters are;

Pulse amplitude: 1 kV
Burst duration: 15 ms
Burst frequency: 5 kHz
Coupling time: 60 sec
Polarity: Negative and positive

Since noise with high amplitude and frequency is get from mains in this test, not only the touch sense cards are affected but also the Hawkeye tool and computer that is connected to these cards. Normally while a signal value of a sensor is limited to 4096, during noise very high values are obtained in the computer. This also shows that the obtained signals are not transmitted to computer properly.

The main purpose of this test is no interruption of any function and no detection of any sensor. Both cards are observed during the test and none of them has made any detections. Because the test values saved on excel file does not give clear information, test graphics from the computer screen is added.
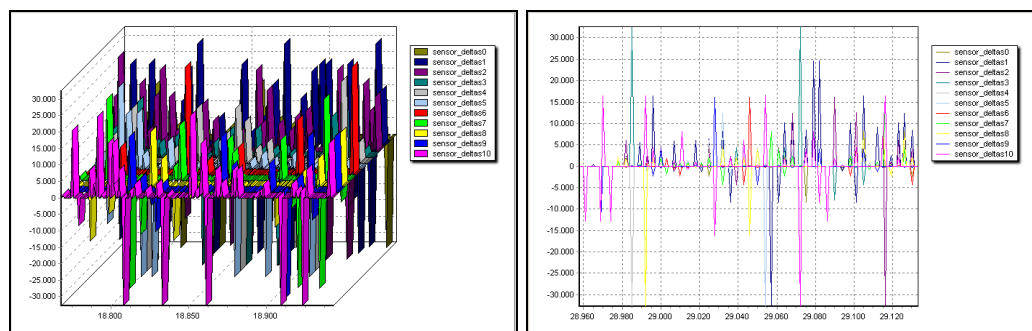
Figure 4.20 Burst immunity test to electrical fast transients and the switching noises on mutual-capacitive sensors for positive polarization of the burst pulses.
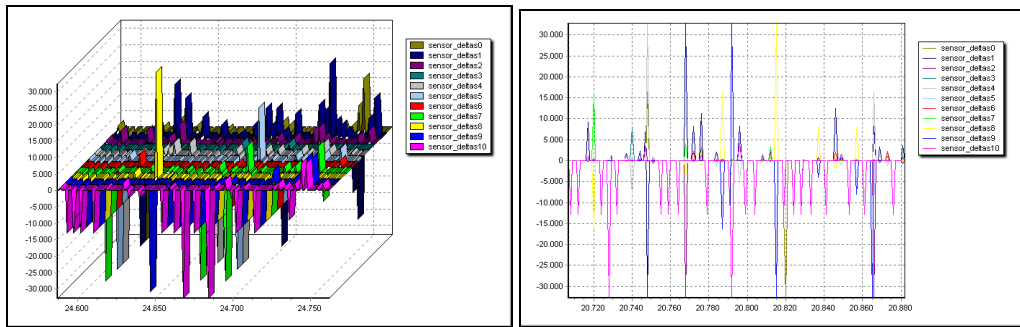
Figure 4.21 Test is repeated for negative polarization of the burst pulse in burst immunity test
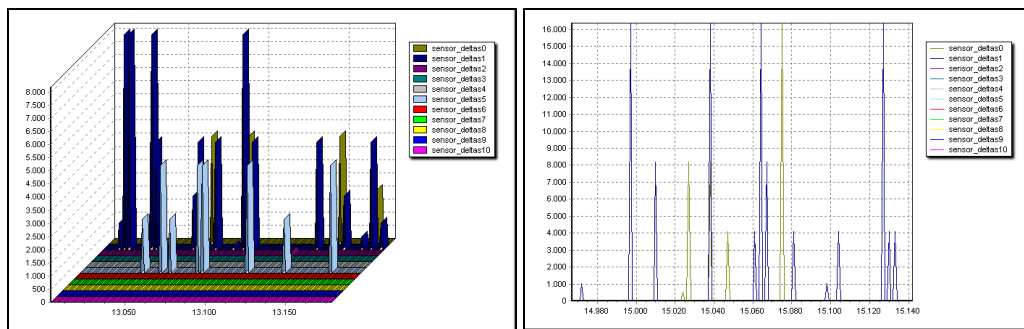

Figure 4.22 Burst immunity test to electrical fast transients and the switching noises on self-capacitive sensors for positive polarization of the burst pulses.
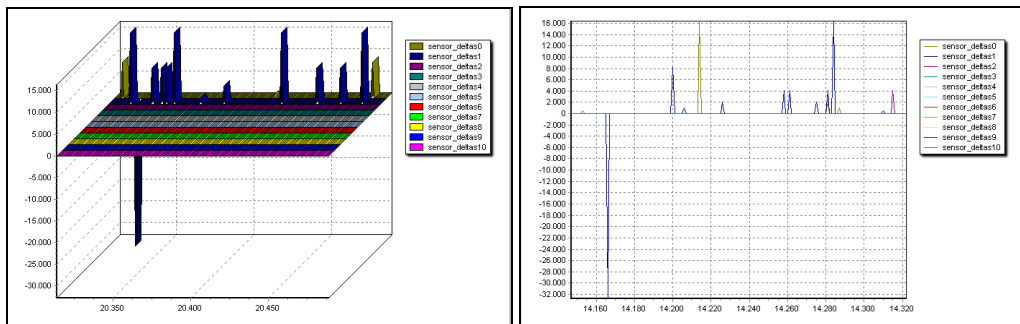

Figure 4.23Test is repeated for negative polarization of the burst in burst immunity test

As can be seen on these graphics, deltas of self capacitive sensors are more stable compared to mutual capacitive sensors in both test polarity. But as a result, no touching state occurred on both of the cards. The effect of slew-rate filters is important during these tests.

4.4.3 EN 61000-4-6-2007

This standard relates to the conducted immunity requirement of electrical and electronic equipment to electromagnetic disturbances coming from intended radio-frequency (RF) transmitters in the frequency range 9 kHz up to 80 MHz. Equipment no having at least one conducting cable (such as mains supply, signal line or earth connection) which can couple the equipment to the disturbing RF fields is excluded.

Main goal of this test is to measure immunity for electronic components inside the product against electromagnetic interference conducting from the cables and the effects of RF interference on cables (EN 61000-4-46, 2007).

Some test parameters are;

Frequency range: 150 kHz – 80 MHz

Voltage level (EMF): 6V

Modulation: 80% (AM)

Modulation frequency: 1 kHz

Frequency step: 1% / 3sec

The effect of the test on mutual capacitive sensors is seen on Figure 4.24. Driving frequency of sensor is 158 kHz and frequency hopping is forbidden. When driving frequency of sensor or its harmonics overlaps with the frequency of noisy signal, sensors are defected. This effect is decreasingly ongoing on high harmonics of driving frequency. Since any sensor is not touched with finger during this test, noise ratio is low. Below graphics show noise ratio versus disturbing frequency while above graphics shows deltas of sensors.
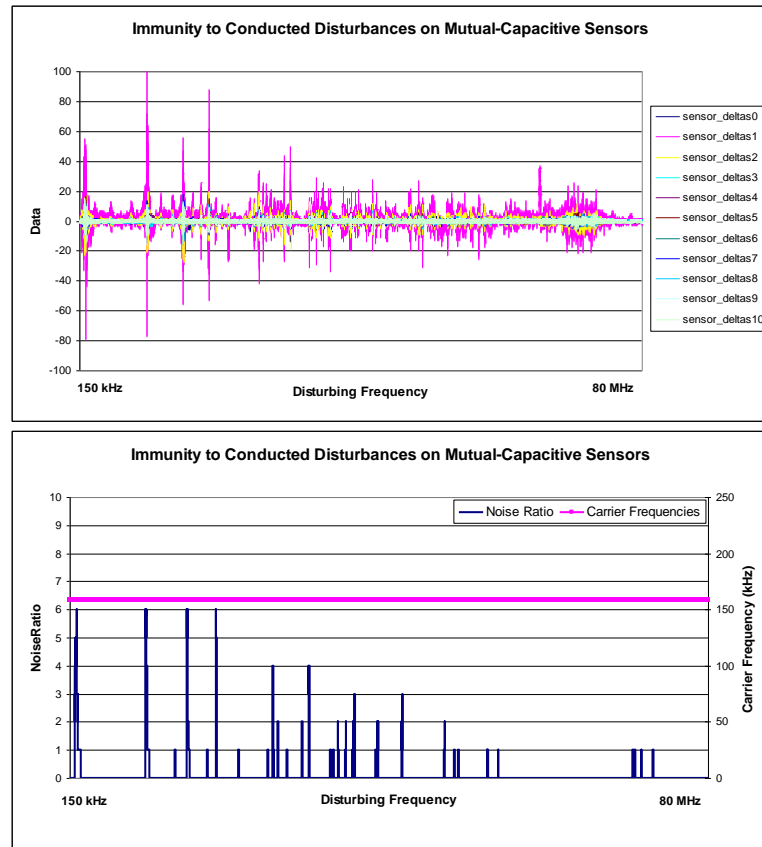
Figure 4.24 Conducted immunity test. In the test case, frequency
hopping is prohibited and the carrier frequency is at 158 kHz.

This test is done again with using frequency hopping algorithm. Results are in
Figure 4.25. Below graphic shows noise ratio and driving frequency while upper
shows deltas of sensors. Second graphics has two different axis and scaled in
different ratios. In the second graphic, both noise ratio and carrier frequency is seen.
When noise ratio reaches 3, driving frequency of sensors changes and noise
decreases. As seen on the right axis of graphics, driving frequency of sensors
changes when noise occurs at between 3 different frequencies.
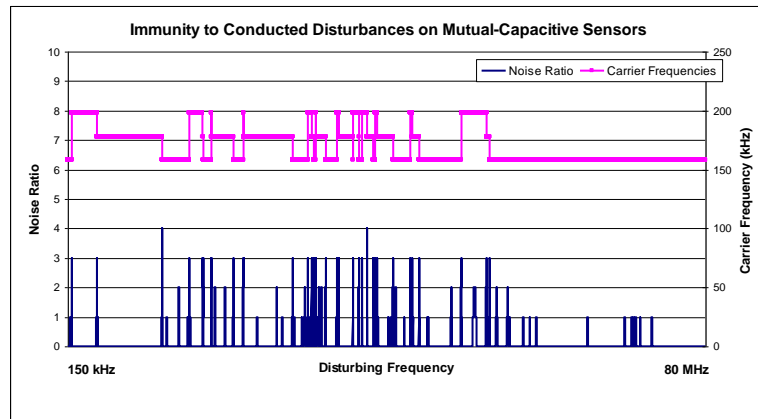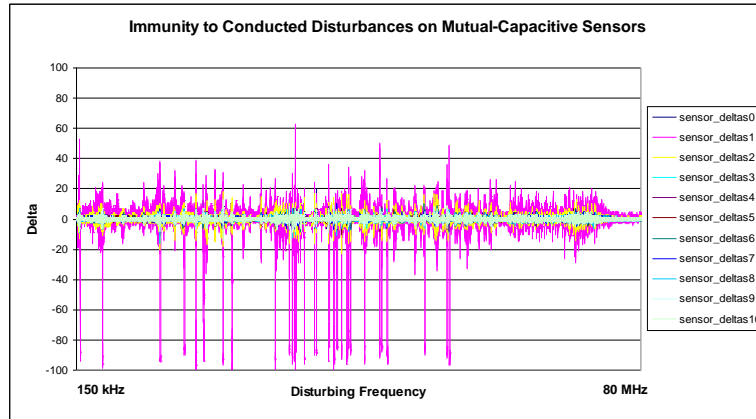
Figure 4.25 Frequency hopping is used and the carrier frequency varied between 158 kHz and 198 kHz when noise ratio reaches 3 and over.
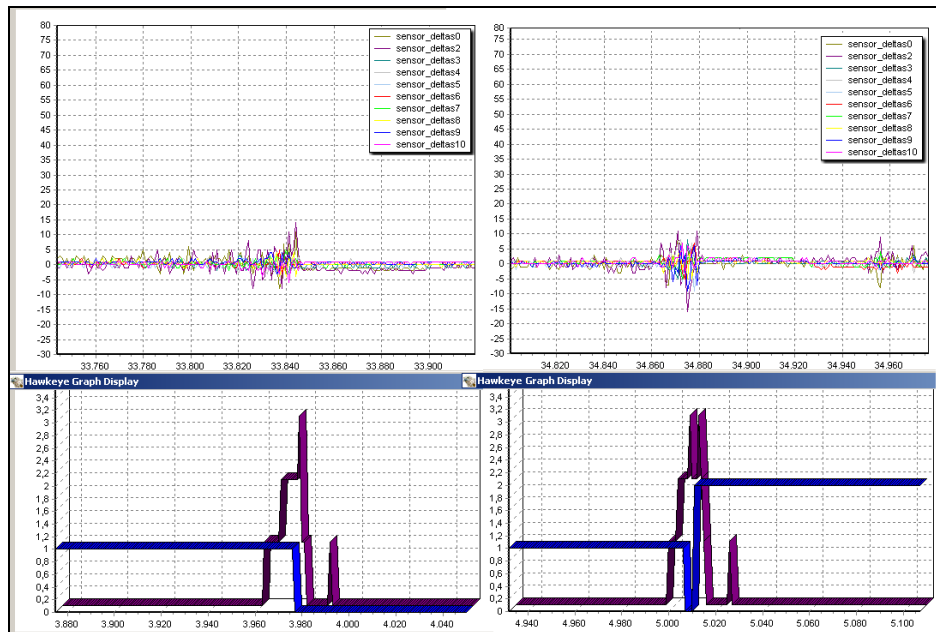

Figure 4.26 Frequency hopping. Blue line shows the carrier frequency of sensors. '0' means 158 kHz, '1' means 178 kHz and '2' means 198 kHz.

Figure 4.26 shows the clearer state and effect of frequency hopping. These graphics are taken from Figure 4.25 and zoomed in. As can be seen on these graphics, when driving frequency of sensors change noise is prevented and deltas of sensor recover. Also noise ratio drops down immediately. If noise ratio does not drop down when frequency is changed, frequency is switched again.

Another test case is the state of driving frequency of sensors and disturbing frequency to be same (See Figure 4.27). These tests are done by changing the voltage levels of noise signal. As voltage level of noise increases, sensors are defected more. During these test frequency hopping is forbidden.
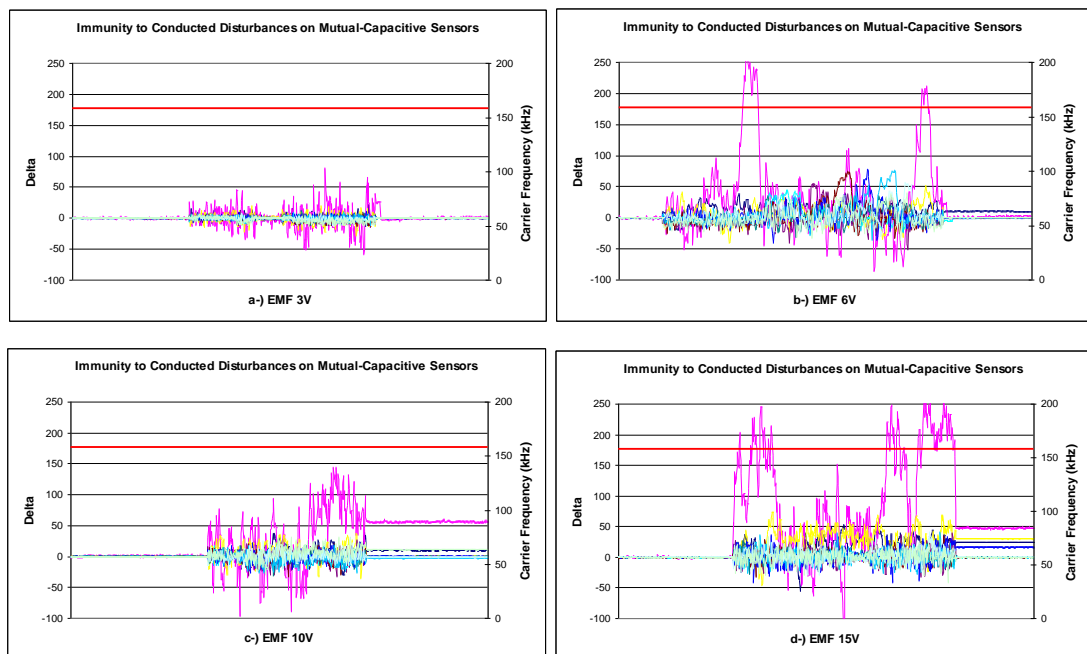
Figure 4.27 Disturbing and the carrier frequency are the same, at 158 kHz. This is worst case for all capacitive sensors. Voltage levels of disturbing signal are **a-)** 3V, **b-)** 6V **c-)** 10V and **d-)** 15V.

Self-capacitive sensors are less affected from conducted immunity test. Noise ratio graphics are not added since it is always zero. In Figure 4.28, effect of this test on self capacitive sensors is seen. Change on deltas of sensor is very low, and the most one is at slider sensor.
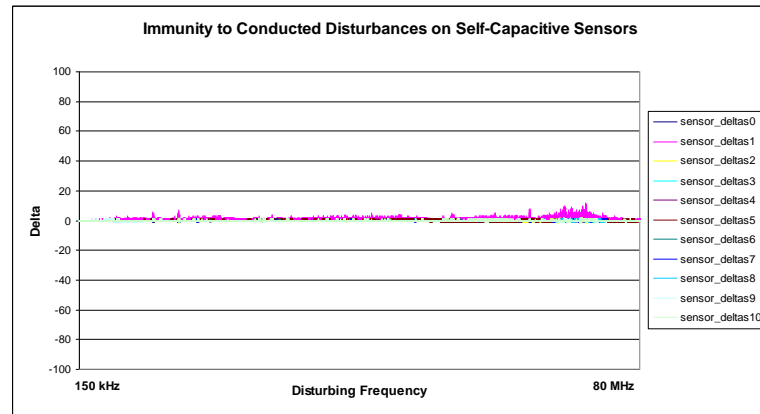
Figure 4.28 Conducted immunity test on self-capacitive sensors. The sensors are much less affected during the test.

Conducted immunity test starts from 150 kHz. Driving frequency of self capacitive sensors is 112.5 kHz. Because of this, the states of sensors are examined by injecting noise at a constant frequency, which is 225 kHz. These tests are done for different voltage values of noise signal. In Figure 4.29, the effect of these tests to self capacitive sensors is seen.
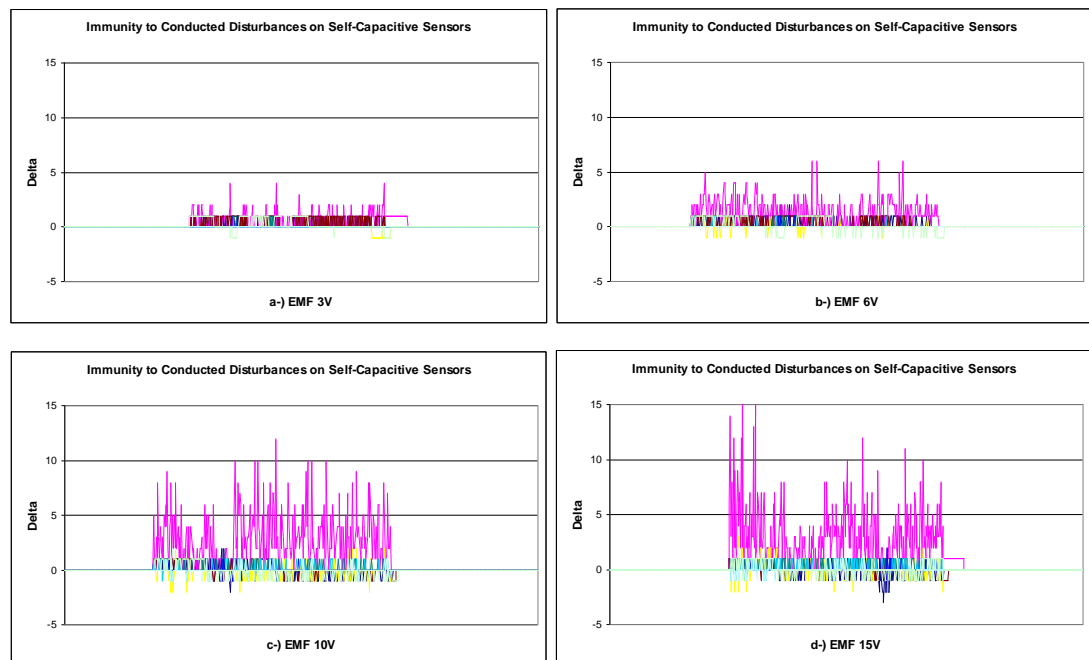

Figure 4.29 Harmonic of carrier frequency and disturbing frequency are the same, at 225 kHz. Voltage levels of disturbing signal are **a-)** 3V, **b-)** 6V **c-)** 10V and **d-)** 15V.

Self-capacitive sensors show greater immunity to EMC test. There are some reasons but first of all, the effects of electromagnetic mainly depend on the layout on the printed circuit board, and on the wiring between the electrode and the microcontroller. The first reason is that self-capacitive sensors have their own sampling capacitors and are driven independently from each other. Therefore, measurements circuits do not interact with each other. The second reason is direct capacitance-to-digital conversion without any external circuit or component, resistor. It means that the tracks of sensor are directly connected a microcontroller. So, its susceptibility to electromagnetic interference should be lower. The simple electrode shapes may be another reason.

Direct capacitance-to-digital conversion in mutual capacitive sensors relies on voltage comparison and timing and this is based on the charging and the discharging time of an sampling capacitor for 8 channels. The interface circuit includes a resistor outside microcontroller. This resistor can be affected by electromagnetic disturbance during both the capacitance-to-voltage conversion and the voltage-to-timing conversion. The 8 channels which exist on the same Y line are connected to each other. Therefore each channel can be affected by other one. The complex interdigitated electrode design may affect both its stability and its performans.

Table 4.1 Design and measurement results to evaluate advantages and disadvantages of each method

	Mutual Capacitive sensors	Self Capacitive Sensors
Plus	- Needs fewer pin - Better water film effect - Naturally moisture suppression - Short burst - lower power consumption - More localized touch-sensitive area	- Simple electrode design - Smaller code size - Fewer chip resource used - Don't need to any reference point - Stable, no crosstalk, more immune to EMC
Minus	- More complex electrode design - Larger code size - More chip resources used - Noise-sensitive - Unstable, crosstalk, EMC disturbance - Needs a reference point	- Needs more pin - Longer burst time - More sensitive to temperature

CHAPTER FIVE

CONCLUSION

Main contribution of this study is to design two types of touch sensing cards by using two different "charge transfer" capacitive acquisition methods and comparing these cards under several test conditions, so as to determine experimentally what type of capacitive sensor shows greater immunity to ambient conditions. In addition, another contribution is to apply the frequency hopping method, which is a new approach to overcome the above mentioned EMC problems on capacitive sensors. This method guarantees for the capacitive sensors to operate safely under noisy environments.

Capacitive values measured at capacitive sensors are usually in the pF range, and sometimes even below. Since the measured signal levels are too low, they can easily be disrupted.

To make the tests to be more comparable experimentally, two identical cards are designed just with different sensors. Used components, their layout on PCB, used processor, software architecture and sensor library are all the same.

Procedure and working principles for both hardware and software design is explained step by step. Mutual-capacitive design is much more complex than the self-capacitive design. Because of this, most details of the design is explained further when designing the mutual-capacitive sensors. When designing the self-capacitive sensors, only the different parts are explained. Frequency hopping algorithm is added to mutual-capacitive sensor software in addition to digital software filter and the effects of this to sensors are shown in graphics while explaining the working principles of this algorithm in details.

Self capacitive sensors can be implemented on lots of processors. Because they do not use any chip resource like timers, ADC, DAC or comparator. Also the code sizes

they use are small and they have simple sensor layout rules. But despite these; they use two pins of processor for each channel. Their burst lengths are long and this increases both the response time and power consumption. Since mutual capacitive sensors can be generated in matrix form, they use less pin for the same number of channels. This type of sensors has shorter burst lengths, and therefore their response time and power consumption is both low. Touch sensitive areas are more localized with their interdigitated sensor structure. Their disadvantages to self-capacitive sensors are complex electrode design, larger code size and using more chip resources.

In temperature and water film tests, it is seen that the mutual capacitive sensors much less changed. Because of using dual slope conversion method, these sensors are insensitive to changes in V_{dd} and Cs. This means the signal values change less with temperature. In water drop test, self capacitive sensors show greater immunity. For mutual capacitive sensors, the signal increases in the opposite direction to an effect of a finger. This shows the natural moisture suppression feature of it and it is much more advantageous than the self capacitive sensors in this aspect too.

Self-capacitive sensors show greater immunity to EMC test. Also the signal levels are more stable in noiseless environment and no crosstalk is detected. This is because each sensor has its own sampling capacitor and is driven independently of each other. Both tracks of sensor or measurement circuits do not interact with each other and their sensor structure has a very simple layout.

Frequency hopping approach is successfully applied to mutual-capacitive sensors. When noise frequency overlaps with driving frequency or its harmonics, resonance occurs and sensors are affected. Noise detection algorithm detects this noise and changes the driving frequency of the sensors. So they can be driven in a clearer frequency. But this approach is not enough for mutual capacitive sensors to show the immunity to EMC tests as self-capacitive sensors does. Test results and effects about this are experimentally revealed.

As a result, both cards are tested under several conditions, where self-capacitive sensors are more immune to EMC and crosstalk tests, the mutual capacitive sensors are more immune to temperature and water tests. Tests results are shown in graphical on the basis of the previous experimental result chapters.

For future work, studies should be done for both shortening the design duration and increasing the SNR. Capacitive sensors generally have lots of parameters. Most of parameters cannot be changed on run time. Also the capacitors and resistors used in measurement circuits have also constant values. These values are being determined for each different sensor design by testing and this also extends the design duration. Additionally many parameters like finger threshold, changes according to where sensors are used. There should be a software algorithm that calibrates the parameters automatically and changes these parameters on run-time by monitoring the SNR always. Also instead of a fixed resistor and capacitor, there should be ones that can be adjusted by processor outside. If processor supports, these components may be inside the chip. Thus a much higher signal levels can be obtained. Also driving frequency of the sensors should be on a wider frequency interval, such spread spectrum, not a fixed one.

REFERENCES

Ashby, D., Baker, B., & Stuart, S., (2008). *Circuit Design: Know It All*. USA: Elsevier. 489-494

Atmel Corporation (2008). Technical Reference AVR055, *Using a 32 kHz XTAL for run-time calibration of the internal RC*, Retrieved January 22, 2011 from http://www.atmel.com/dyn/resources/prod_documents/doc8002.pdf

Atmel Corporation (2009). Technical Reference, *ATmega329P/V* (rev.8021E), Retrieved January 11, 2011
from http://www.atmel.com/dyn/resources/prod_documents/doc8021.pdf

Atmel Corporation (2009). Technical Reference, *Touch sensor design guide*, Retrieved April 20, 2011,
from http://www.atmel.com/dyn/resources/prod_documents/doc10620.pdf

Atmel Corporation (2010). Technical Reference, *Atmel QTouch Library* (vers. 4.3), Retrieved February 11, 2011,
from http://www.atmel.com/dyn/resources/prod_documents/doc8207.pdf

Brasseur, G. (2002). *How to build reliable capacitive sensors for an industrial environment,* Instrumentation and Measurement Technology Conference, 2002. IMTC/2002. Proceedings of the 19th IEEE, Volume 1, May 2002, 141-144

Brasseur, G. (2003). *Design rules for robust capacitive sensors,* Instrumentation and Measurement, IEEE Transactions on Vol. 52, Is. 4, September 2003, 1261-1265

Carey J. (2009). *Getting in touch with capacitance sensor algorithm.* Retrieved March 20, 2011, from http://www.banktech.com/articles/219500393

CENELEC. (2002). BS EN 61000-4-3:2002 – *Electromagnetic compatibility (EMC) – Part 4-3: Testing and measurement techniques – Radiated, radio-frequency, electromagnetic field immunity test.*

CENELEC. (2004). BS EN 61000-4-4:2004 – *Electromagnetic compatibility (EMC) – Part 4-4: Testing and measurement techniques –Electrical fast transient/burst immunity test.*

CENELEC. (2007). BS EN 61000-4-6:2007 – *Electromagnetic compatibility (EMC) – Part 4-6: Testing and measurement techniques – Immunity to conducted disturbances, induced by radio-frequency field.*

Chatterjee, R., & Matsuno, F. (2008). *Capacitive touch sensor based user-interface : Generic design considerations and development of an wearable input device.* SICE Annual Conference, 2008, October 2008, pp. 2299-2304

Chou, W.C., Hsu, Y.C., & Liao, L.P. (2006). *Modulation / Demodulation System for Capacitive Sensors,* Microsystems, Packaging, Assembly Conference Taiwan, 2006. IMPACT 2006. International, February 2007, pp. 1-4

Davison B. (2010). Microchip Technology Inc. Technical Reference AN1334, *Techniques for Robust Touch Sensing Design*, Retrieved April 10, 2011, from http://www.newark.com/pdfs/techarticles/microchip/01334A.pdf

Dietz, P.H., Leigh, D., & Yerazunis, W.S. (2002). *Wireless liquid level sensing for restaurant applications,* Sensors, 2002. Proceedings of IEEE, Vol.1 , November 2002, pp: 715-720

Döner, H. (2006). *Radiated Emission EMC Testing using Full Anechonic Chamber*, DEÜ Electrical and Electronics Eng. Final Project Supervisor: Asst. Prof. Dr. Y. Yüksel, pp. 1-6

Gaitan-Pitre, J.E., Gasulla, M., & Pallas-Areny, R. (2007). *Direct interface for capacitive sensors based on the charge transfer method.* Instrumentation and Measurement Technology Conference Proceedings, 2007. IMTC 2007. IEEE, June 2007, pp: 1-5

Gerphiede, G., & Layton M. (1996). *Capacitance-Based Proximity Sensor With Interference Rejection Apparatus and Methods*. Published under the Patent Cooperation Treaty (PCT), Classification: G08C 21/00, Patent Num: 5565658 Publication Num: WO 96/18179.

Kero, N., Nachtnebel, H., Pommer, H., & Sauter, T. (2002). *Fault tolerant carrier frequency tracking for closed loop measurement systems,* Instrumentation and Measurement Technology Conference, 2002. IMTC/2002. Proceedings of the 19th IEEE, Vol. 2, August 2002, pp: 1529-1532

Kuo, S.M., Lee, B.H, & Tian, W. (2006). *Real-time digital signal processing: implementations and applications* (2nd ed.), 127-130, Great Britain: Antony Rowe Ltd. Chippenham, Wiltshire

Ling, Q., Li, T., & Ding, Z. (2007). *A Novel Concept: Message Driven Frequency Hopping (MDFH),* Communications, 2007. ICC '07. IEEE International Conference on, August 2007, pp: 5496- 5501

Lu, D., & Wong, C. P. (Eds.). (2009). *Materials for Advanced Packaging , 299-300.*

Morrison, R. (2007). Voltage and Capacitance In *Grounding and shielding: circuits and interference* (6th ed.), 10-18, USA: IEEE Press.

Nam, C., Pu, Y.G., & Lee, K. Y. (2009). 12×12 *Capacitive matrix touch sensing unit for SoC application in 0.18um CMOS process,* SoC Design Conference (ISOCC), 2009 International, March 2010, pp: 305-308

O'Dowd, J., Callanan, A., & Banarie, G. (2005). *Capacitive sensor interfacing using sigma-delta techniques,* Sensors, 2005 IEEE, March 2006, pp. 951-954

Quantum Research Group (2006). *QMatrix™ Technology White Paper*, Retrieved April 3, 2011, from http://www.atmel.com/dyn/resources/prod_documents/qmatrix_white_paper_100.pdf

Quantum Research Group (n.d.). *Quantum Research Group Training: QRGT-201/1, QRGT-200/1 and QRGT-203/1* Retrieved April 01, 2011, from Atmel

Reverter, F., Gasulla, M., & Pallas-Areny, R.(2004). *A low-cost microcontroller interface for low-value capacitive sensors*. Instrumentation and Measurement Technology Conference, 2004. IMTC 04. Proceedings of the 21st IEEE, Volume 3, November 2004, pp: 1771-1775

Robertson, R.C.(2008). *Fundamental Electrical and Electronic Principles* (3rd ed.), pp: 49-54, Slovenia: Elsevier.

Salas, M., & Marcos, A. (n.d). *How to design capacitive touch & proximity sensing technology into your application.* Retrieved March 28, 2011, from http://low-powerdesign.com/PDF/How-to-Design-Capacitive-Touch-and-Proximity-Sensing-Technology-into-Your-Application.pdf.

Sauter, T., & Nachtnebel, H. (2003). *A feasible noise estimation algorithm for resource-limited sensor systems,* Instrumentation and Measurement, IEEE Transactions on, Volume 52, Issue 6, November 2003, pp. 1854 – 1858

Sheu, M.L., Lai, C.K., Hsu, W.H., & Yang, H. M. (2005). *A Novel Capacitive Sensing Scheme for Fingerprint Acquisition*. Electron Devices and Solid-State Circuits, 2005 IEEE Conference on, July 2006, pp: 627-630

Stenmark F. (2008). *Design of a touch screen interface for a mobile position aware instant messaging client*, Master's Thesis in Umea University Department of Computing Science, Retrieved March 13, 2011, from *http://www8.cs.umu.se/education/examina/Rapporter/FiaStenmark.pdf*

Toumazou, C., Hughes, J.B., & Battersby, N.C. (Eds.) (1993). *Switched-currents: an analogue technique for digital technology, pp.* 13-14 UK: Short Run Press Ltd.

WEB_1. (n.d). *The working principle of capacitive touch screen* Retrieved March 26, 2011, from   http://www.onetouch.com.tw/en/images/tech/Eng-Capacitive.pdf

WEB_2, (2010). Technical Reference, *QTouch Library (revision 4.3)*, Retrieved September 10, 2010, from http://www.atmel.com/dyn/products/tools_card.asp?tool_id=4627&source=redirect

Wikimedia Foundation Inc. (2011). *Touch screen.* Retrieved March 25, 2011, from http://en.wikipedia.org/wiki/Touchscreen

Winder, S. (1997). Filter integrated circuits. In *The Analog and digital filter design* (2nd ed.), 339-343. United States of America: Elsevier Science.

Yuji, J., Yamaguchi, H., & Shida, K. (2004). *Temperature and humidity sensing functions of a capacitive touch sensor for material discrimination.* SICE Annual Conference, Volume 3, August 2004, pp: 2652 - 2655

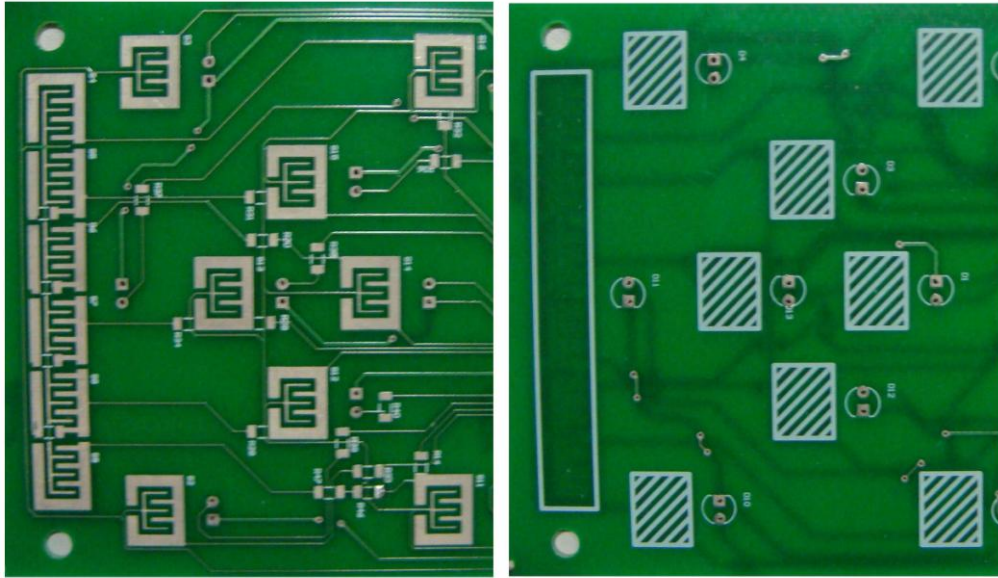Zheng, Q. (n.d.). *Touch Screen Sensor*. Retrieved March 13, 2011, from http://www.scribd.com/doc/50497109/Touch-screen-sensor-1

APPENDICES

APPENDIX A: Real PCB apperance type of mutual capacitive sensors.

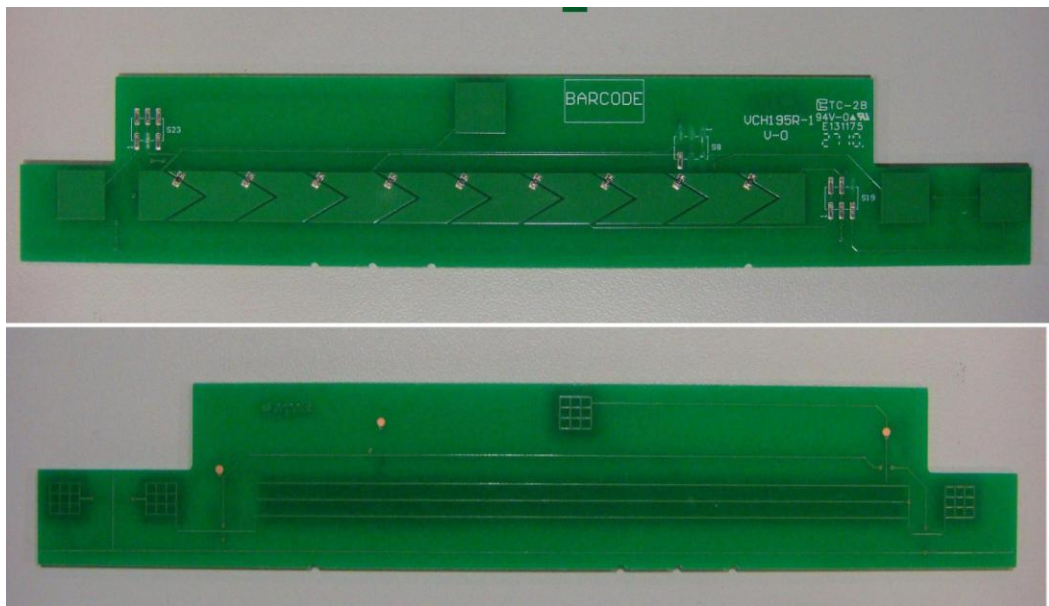Figure A.1 Mutual capacitive button and slider sensors apperance on planar construction

Figure A.2 Mutual capacitive button and slider sensors apperance on non-planar construction

APPENDIX B: Dielectric Constants

Table B.2 Relative Dielectric Constants for Materials (Atmel, 2009)

Material	Dielectric Constant
Vacuum	1 (by definition)
Air	1.00059
Glass	3.7 to 10
Sapphire Glass	9 to 11
Mica	4 to 8
Nylon	3
Silicon	11 to 12
Silicone Rubber	3.2 to 9.8
Silicone Moulding Compound	3.7
Paper	2
Plexiglass	3.4
Polycarbonate	2.9 to 3.0
Polyethylene	2.2 to 2.4
Polystyrene	2.56
PET (Polyethylene Terephthalate)	3
Pyrex Glass	4.3 to 5.0
Quartz	4.2 to 4.4
Rubber	3
FR4 (Glass Fiber + Epoxy)	4.2
PMMA (Polymethyl Methacrylate)	2.6 to 4
Typical PSA (Pressure Sensitive Adhesive)	2.5 to 2.7

APPENDIX C: Real Appearance, Schematic, PCB and Layout of Mutual Capacitive Touch Sensing Card
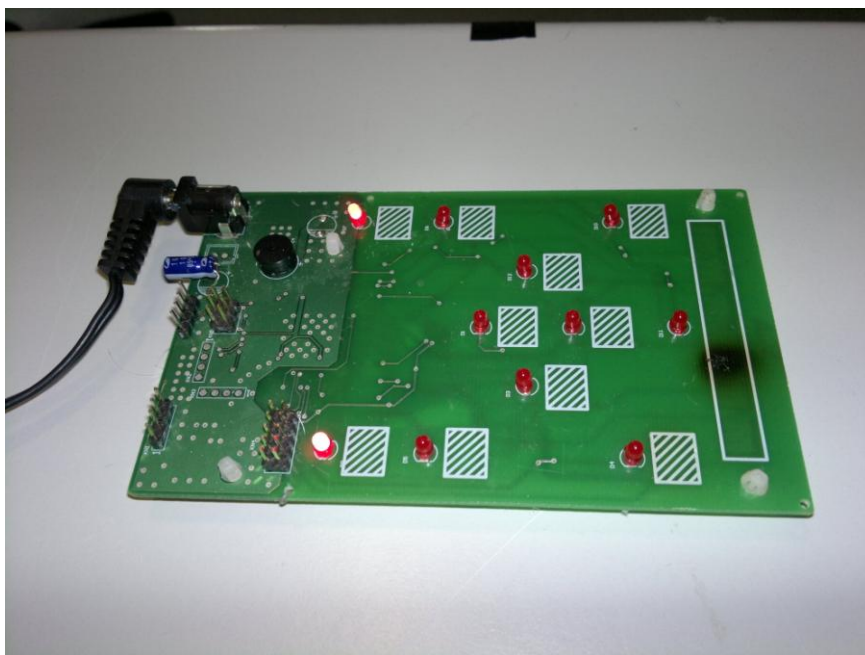
Figure C.1 Real Appearance of mutual capacitive touch sensing card
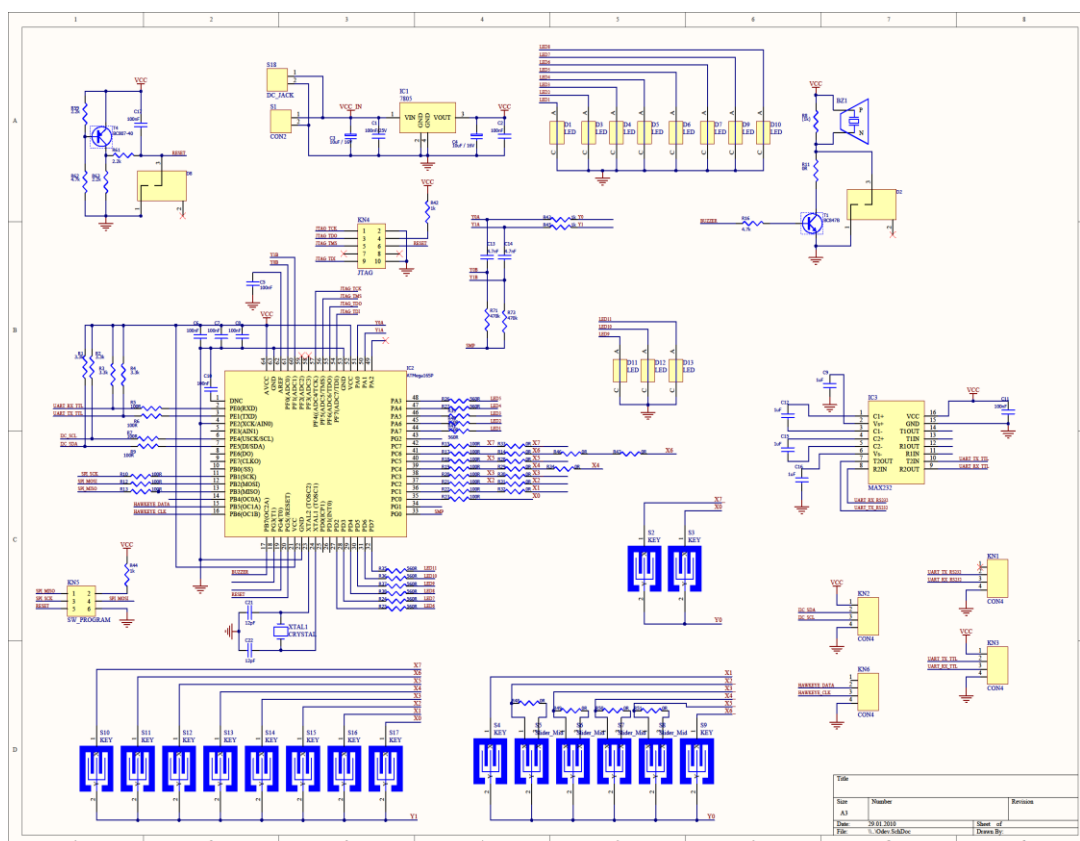
Figure C.2 Schematic diagram of mutual capacitive touch sensing card
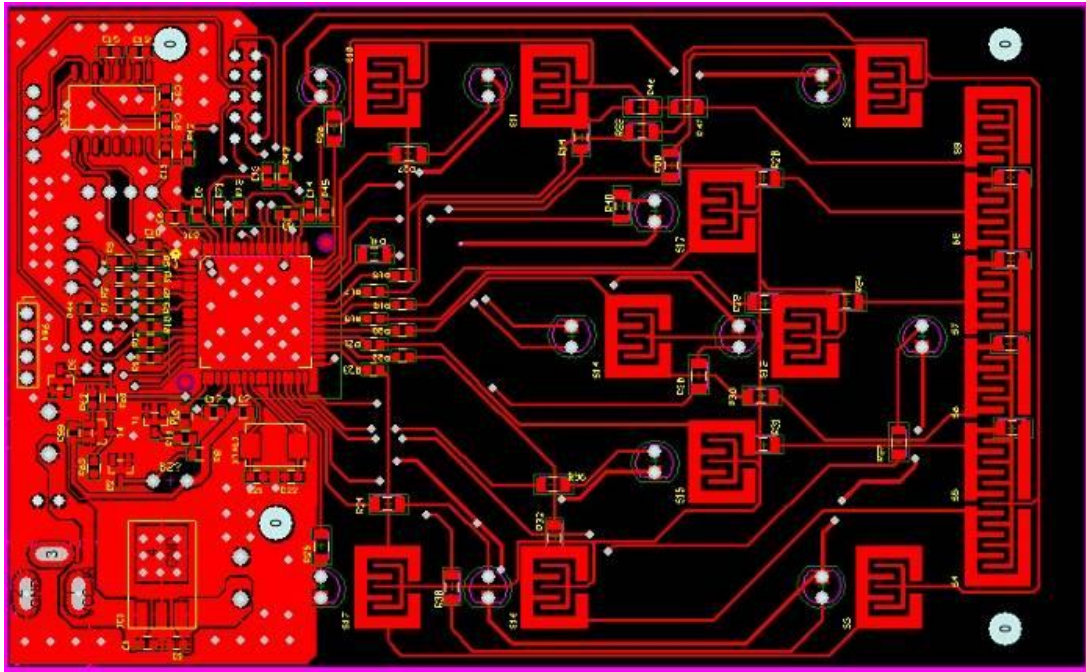
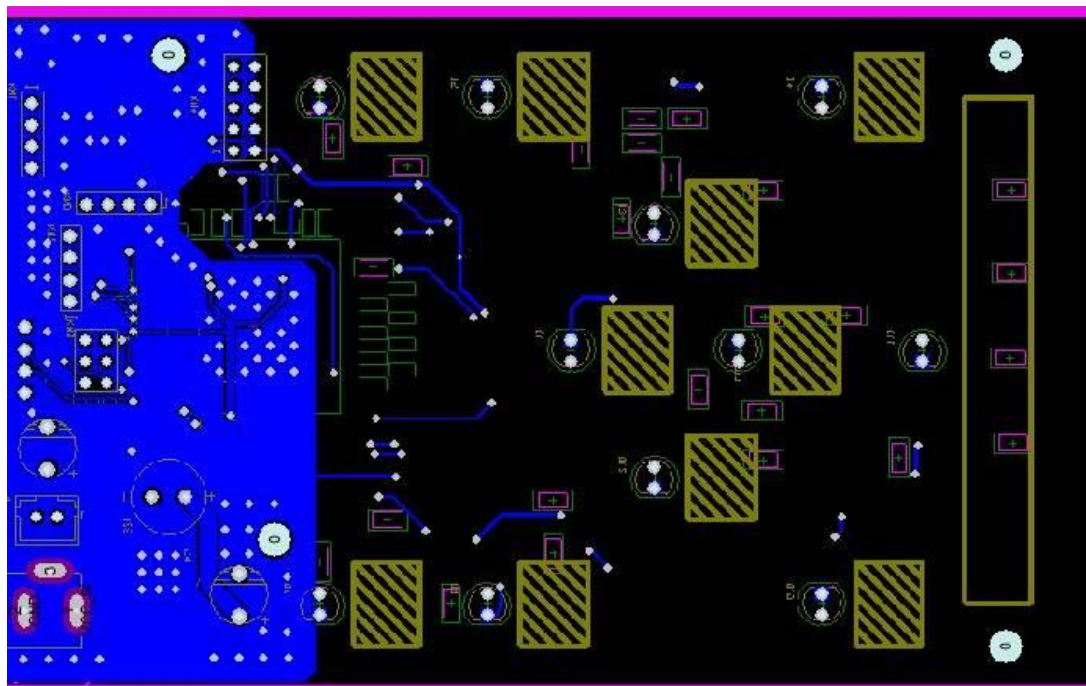Figure C.3 Top copper layer of mutual capacitive touch sensing card

Figure C.4 Bottom copper layer of mutual capacitive touch sensing card

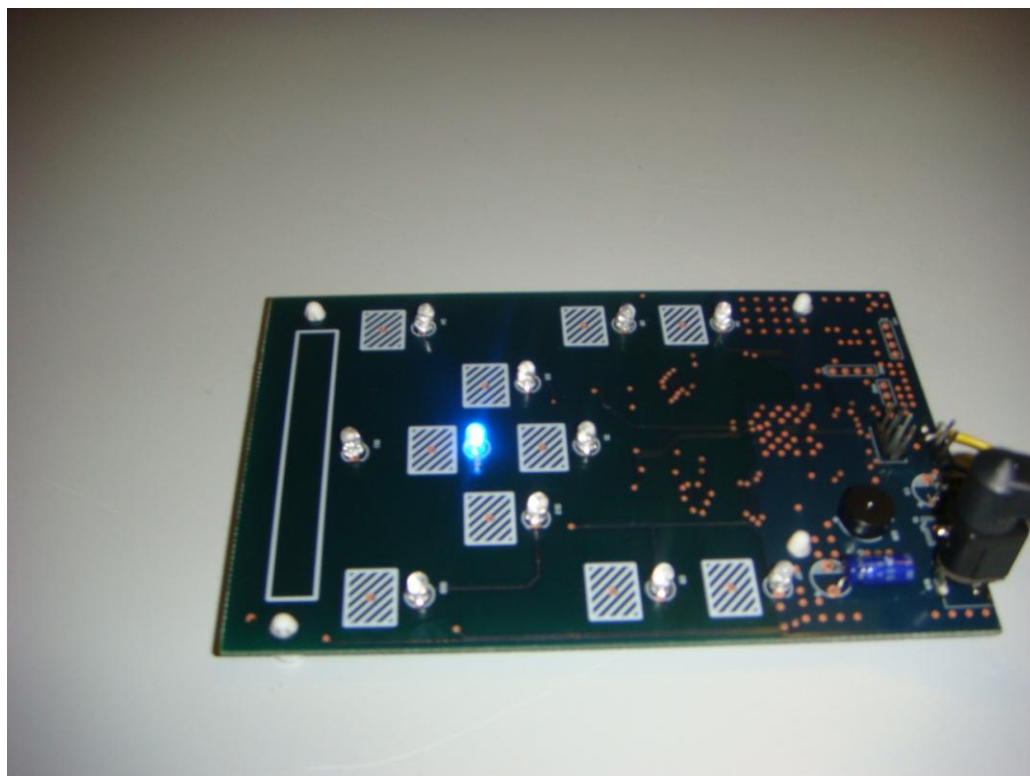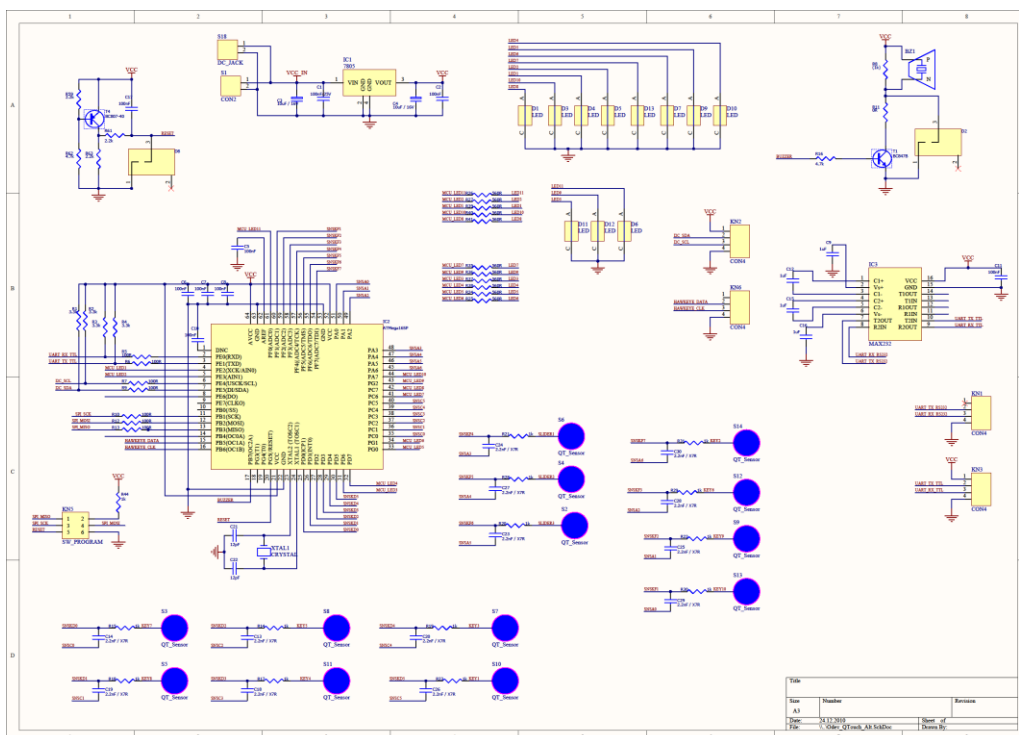**APPENDIX D:** Real Appearance, Schematic, PCB and Layout of Self Capacitive Touch Sensing Card

Figure D.1 Real Appearance of self capacitive touch sensing card

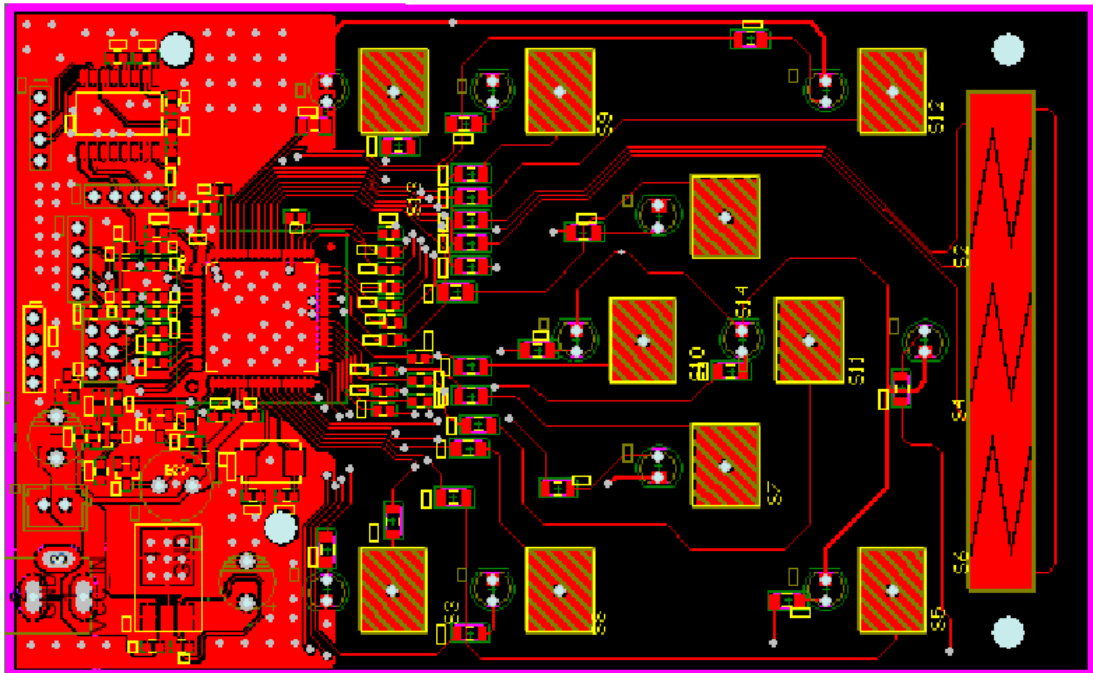Figure D.2 Schematic diagram of self capacitive touch sensing card

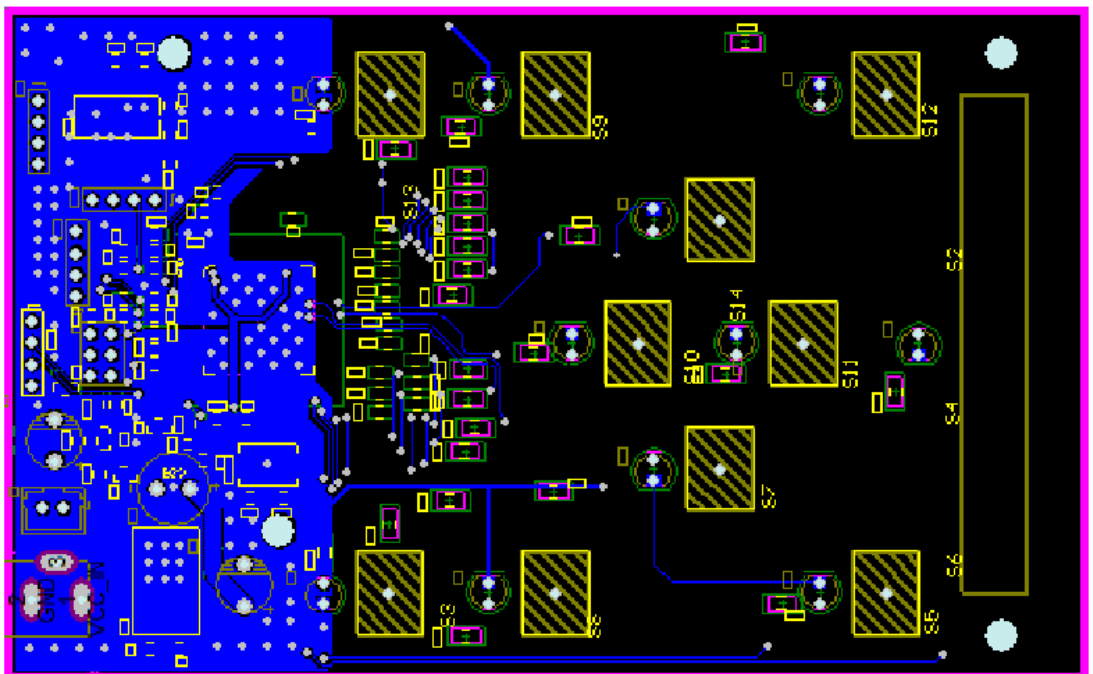Figure D.3 Top copper layer self capacitive touch sensing card

Figure D.4 Bottom copper layer of self capacitive touch sensing card

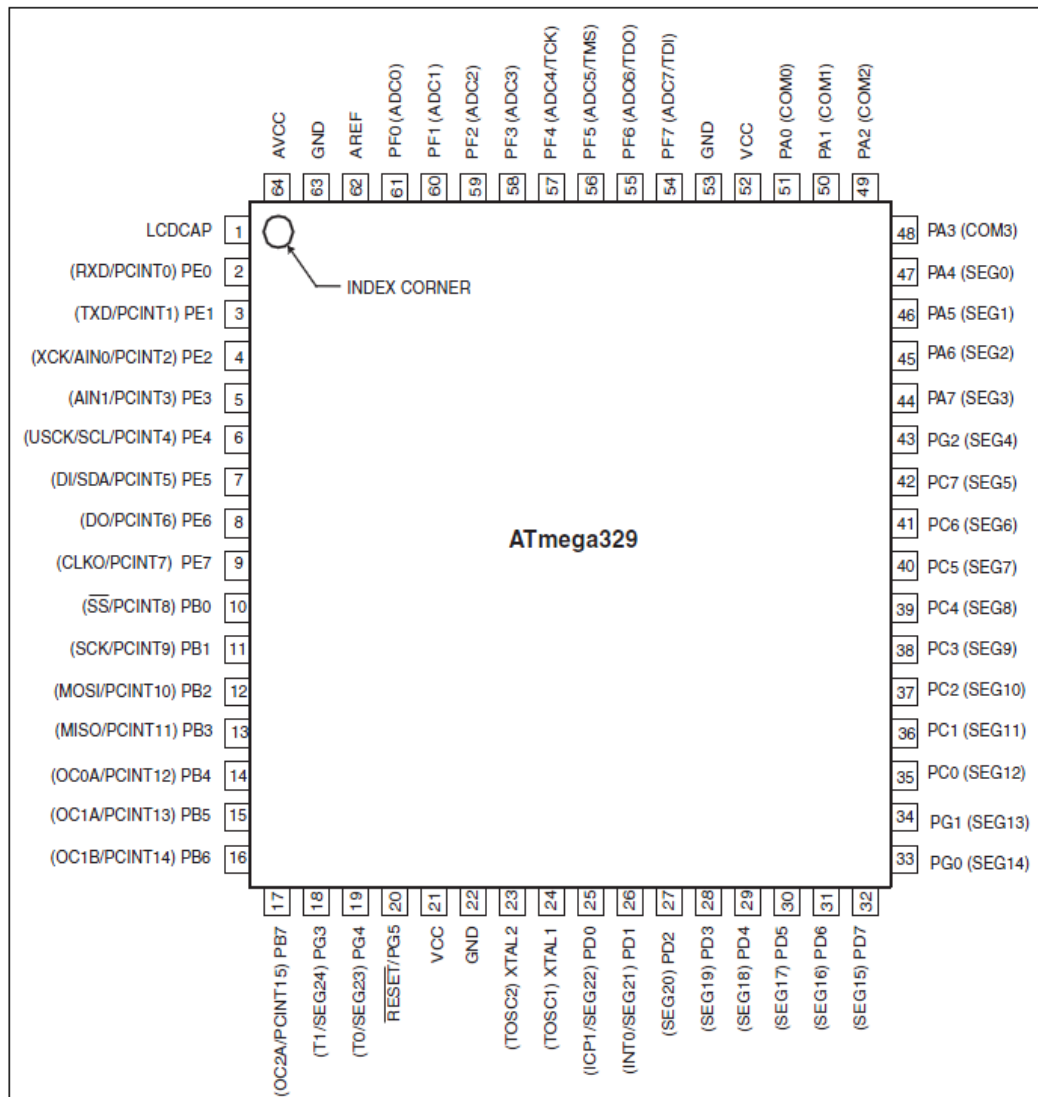**APPENDIX E:** Pin Diagram of ATmega329P

Figure E.1 Pin diagram of ATmega329P that is 64-pin in TQFP package (Atmel, 2009)